**Evaluating Axial Compressive Capacity of Helical Piles Installed in Clay Tills**

by
Brent Hay

A Thesis Submitted to the Faculty of Graduate Studies of The University of Manitoba
in partial fulfillment of the requirements of the degree of
MASTER OF SCIENCE

Department of Civil Engineering
University of Manitoba
Winnipeg

December 14, 2022

## Abstract

To support power generation infrastructure in northern Manitoba, 1,100 helical piles with shaft diameters of 244 mm, lengths of 18 m to 21 m and helix diameters of 457 mm were installed into hard clay tills. Sixty-eight axial compressive load tests were completed during construction and fifty-seven were used for this study. Six of the tests were instrumented with strain gauges to evaluate the contribution from shaft adhesion.

Helical piles are becoming more common place in heavy civil construction and further analysis is required to better understand prediction of ultimate capacity and behavior under loading. Several theoretical methods to predict the ultimate capacity of helical piles have been adopted from common shallow or deep foundations formulas and are investigated. Empirical methods to predict capacity from torque measurements obtained during install are also common and used to compare to other capacities, predicted or measured. Pile load tests are often completed to refine estimates of capacity and numerous interpretation methods are available to estimate a failure load from the test results. Several methods are explored and the interpreted capacity is compared to theoretical and empirical methods.

Using the theoretical methods, the influence of bearing capacity factors and shear strength of the soil were seen to be the largest contributors with calculated capacities ranging from 1190 kN to 2660 kN using an bearing capacity factor, $N_{c,}$ of 8.11. Based on the ultimate capacity obtained from failure criteria, the theoretical methods over predicted capacity in every case. This is attributed to the selection of

unrepresentatively high shear strengths, high $N_c$ factors or a combination thereof. The selection of shear strengths is further scrutinized based on variability in testing data and it was found that an appropriate, cautious estimate could be as low as 60% of the mean. Torque relationships predicted capacities from 400 kN to 7,000 kN, owing to the large range of $K_T$ factors available. From site specific data, an average $K_T$ value of 11.9 was back-calculated.

Load tests can provide significant value to projects however many of the failure criterion available may not be applicable as they under-estimate capacity or simply aren't applicable if the pile isn't loaded to failure. This issue is compounded when a load testing program is completed on production piles, as the risk of over-stressing the underlying soils and taking piles to large deflections is not tenable due to potential risks with building performance afterwards.

Several failure criterion were reviewed and three were used to estimate capacity from load-deflection curves. From this exercise it was determined that methods which were applicable in most cases (5%D and Davisson) underestimated the capacity by an average of 7% to 10% when compared to the highest interpreted value. The method presented by Elkasabgy produced the highest capacity in most cases and was found to be applicable in 9 instances. Based on the De Beer failure criteria, a modified method, denoted the Creep limit, was developed which utilizes graphical and mathematical approaches to interpret a failure load. The Creep limit was found to be applicable in 14 cases and resulted in capacities near plunging failure and within 0.6% to 6.4% of Elkasabgy.

## Table of Contents

## List of Tables

## List of Figures

## List of Copyright Material

Aerial Imagery. Bing Maps. 2021.

**Acknowledgements**

I'd like to thank Mortensen Canada for permission of the use of the load test data, particularly Heather and Mike. This thesis would not have been possible without the support of Gil at Dyregrov Robinson Inc. Thanks for the occasional poke about getting this completed and the technical insight during the project. The data would not have been obtained without the hard work of TREK employees who braved the northern Manitoba winters, it was a pleasure working with you. The same goes to the piling crew with a special tip of the hat to Roy. I would also like to thank Dr. Marolo Alfaro for his patience and advice throughout the thesis writing process. The partners at TREK, especially Kent Bannister, for their technical guidance and overall support throughout the years. Also, to mom and dad for your support with my education throughout the years. Lastly and mostly importantly, I would like to acknowledge my wife for her enduring support while undertaking this thesis, you and the kids make it all worth while.

## Dedication

**This thesis is dedicated to my Grandfather.**

## Notations

Pile Depth (H)

Helix Spacing (S)

Helix Diameter (D)

Pile Diameter (d)

Helix Pitch (p)

Bearing Capacity Factors (Nc, $N_\gamma$, $N_q$)

Undrained shear strength ($s_u$)

Unit weight of soil ($\gamma$)

Embedded area of helix ($A_h$)

Effective length over which $Q_s$ is calculated ($H_{eff}$)

Adhesion coefficient ($\alpha$)

Inter-helix Spacing to Helix Diameter Ratio (S/D)

Embedment Depth to Helix Diameter Ratio (H/D)

Capacity derived from pile shaft ($Q_s$)

Capacity derived from pile helix ($Q_b$)

Ultimate Capacity ($Q_u$)

Ultimate Capacity Calculated from Theoretical Methods ($Q_{uc}$)

Ultimate Capacity Calculated from CTC Methods ($Q_{ut}$)

Ultimate Capacity Calculated Interpreted from Failure Criterion ($Q_{ui}$)

Empirical Torque Factor ($K_T$)

Installation Torque (T)

.

## Glossary of Terms

Capacity to Torque Correlations (CTC)

Individual Bearing Method (IBM)

Cylindrical Shear Method (CSM)

Ultimate Limit State (ULS)

Service Limit State (SLS)

.

# Chapter 1: Introduction

## 1.0 Introduction

Helical piles consist of a single or multiple helical shaped bearing plates attached to a central shaft. The piles come in many configurations with varying shaft shape, size, length, number of helices, helical plate size and pitch. Helical piles are manufactured from steel in prefabricated lengths and extensions are threaded, welded or bolted to lengthen the pile as required. Installation is usually completed using conventionally available heavy equipment outfitted with hydraulic drive heads to screw the pile into the ground. Helical piles derive their capacity by their individual helix, multiple helices, adhesion along the central shaft or a combination thereof. The resistance provided by the helices is mobilized either along the base of the helix or along the column of soil between multiple helices.

Helical piles have traditionally been used as foundation elements to resist lighter loads, particularly for loads in tension and thus have been extensively applied in areas such as towers, powerlines, gas lines and guy anchors where uplift is a governing load scenario. Recently, the use of helical piles has become for frequent to support compressive loads, as well as lateral and cyclic loads. The use of larger pile sizes, thicker pile sections, more powerful installation equipment together with a better understanding of pile behavior has contributed to this more frequent use, which have also allowed for larger capacity helical piles. Further, due to their ability to accommodate many load combinations, helical piles are increasingly becoming a viable foundation alternative for numerous types of infrastructure.

The capacity of helical piles depends on several factors such as the pile geometry, site conditions, installation procedures and installation depth. In this regard, the prediction of helical pile capacity is in turn heavily dependant on project specific parameters. There has been a significant amount of research regarding the design of helical piles over the last 30 years. For example, studies which evaluate the failure mode, influence of soil type, soil strength, pile sizes, pile geometry and loading condition (e.g., axial compression, tension or lateral) have been completed and offer significant insight and progress to the use of helical piles.

Despite the significant amount of work that has been done to date, there is a common theme in recent literature that suggests additional research is required to further the design and understanding of helical piles. For example, Perko (2009) indicates this should focus on refining theoretical predictions using load test data, Elsherbiny and El Naggar (2013) indicate that more rigorous design approaches are required due to the increased need for more complex and efficient designs, Lanyi-Bennet (2018) states that helical pile engineering behavior has not been well defined in literature specifically as it relates to helical pile groups, and more generally Mohajerani et al (2016) states that further research is essential to ensure helical piles evolve and become common place in the engineering community.

This study is based on the work completed at the Keewatinohk Converter Station in Northern Manitoba, approximately 100 km southwest of the Hudson's Bay and the mouth of the Nelson River, as shown in **Error! Reference source not found.**. In Manitoba, the use of helical piles is increasing, and several local contractors offer

helical pile installation, however they are still largely considered only for anchors and as foundations for lightly loaded structures.


**Figure 1.1 - Location Plan**

Throughout 2015 and 2016, thousands of helical piles were installed to support the Converter Building and Transformer Building that are part of the AC-DC Converter Station that feeds into the hydro-power network of the Province. A test pile program was completed prior to production piling which included 4 fully instrumented

compressive load tests. Following selection of helical piles as the preferred foundation option, over 1,100 helical piles were installed, and 68 axial compressive load tests were completed as part of the quality control program. Of the 68 tests, 57 were included in the analysis for this paper.

Based on the results of these tests, this paper attempts to refine theoretical predictions of helical pile capacities in compression. The load test data is also used to interpret ultimate capacity using established failure criterion and presents an updated failure criterion for large diameter, heavily loaded helical piles that are intended for production (i.e. it will be part of a foundation system).

## 1.1 Research Hypotheses

1) The accuracy of commonly used theoretical methods to predict helical pile capacity can be improved by comparing calculated capacities to failure loads obtained from load test data.

2) The validity of Capacity to Torque Correlations should be confirmed on a project by project basis to assess their validity in estimating pile capacity.

3) Interpretation of load test data using established failure criteria may not be appropriate for production piles and an analysis of multiple load tests may provide an updated criteria.

The prediction of helical pile capacity using theoretical methods is often separated into two failure modes – Cylindrical Shear Method (CSM) and Individual Bearing Method (IBM). Both methods are adapted from commonly used design approaches for other foundation types. Empirical predictions such as Capacity to Torque Correlation (CTC) methods are also commonly employed. Examining the theoretical and empirical capacities and comparing them to load test data may provide an improvement to the prediction of helical pile capacity. A specific focus is directed towards the selection of shear strength and bearing capacity factors in theoretical methods as it relates to common engineering practice.

Additionally, numerous failure criteria exist to determine the ultimate capacity of piles from load test data. Some methods are known to underpredict capacity while others require large deflections that are not practical for a load test program on production piles. Evaluating how failure criteria may be applied to production pile load tests without requiring excessive deflections can add an additional method of interpretation to the practicing engineer for this load test scenario.

### *1.1.1 Thesis Objectives*

The objectives of this thesis are to improve the understanding of the design and performance of helical piles as follows:

- Investigate and refine theoretical and empirical predictions for heavily loaded helical piles installed into clay tills.

- Investigate and refine the interpretation of load test data to predict ultimate capacity for helical piles installed as production piles.

## 1.2 Helical Piles and Foundation Alternatives in Manitoba

As helical piles gain popularity for use in Manitoba a brief discussion of various foundation options typically used in the Province is warranted to serve as a comparison. Several local companies offer helical pile installations and provide guidelines for allowable capacities based on soil conditions and helical pile sizes on their websites. For example, Postech Screw Piles provide axial compressive, Service Limit State Capacities (SLS) ranging from 4 kN to 49 kN for 200 mm to 255 mm single helices bearing in soft clay to dense sand, respectively (Postech, 2021). Goliathtech piles provide allowable compressive capacities (in working stress design terms, which is generally comparable with the SLS capacity) of 44 kN to 1,067 kN for various pile sizes and assuming a maximum torque is achieved during installation (Goliathtech, 2021). EBS Geostructural (EBS, 2021) provides SLS compressive capacities of 115 to 680 kN for various pile sizes in cohesive and non-cohesive soils. It is important to note that these capacities are provided for guidance only and require evaluation for project specific conditions. Hoyt and Clemence (1989) note that pile capacities from 89 to 444 kN are more typical (in uplift). Based on these examples, there is clearly a wide range of applicable loads where helical piles may be employed.

Commonly used deep foundation types in Manitoba include Cast in Place Concrete (CIPC) piles (either friction or end bearing), driven precast prestressed hexagonal concrete (PPCH) piles, driven steel pipe or driven steel H-piles. Timber piles have been used extensively in the past however based on the authors professional experience over the past dozen years, are becoming less common. In general, CIPC friction piles are towards the lower range of capacity for the deep foundations mentioned above, with capacities generally increasing in order of CIPC end bearing piles, driven PPCH piles and steel H-piles, respectively. The approximate range of capacities for these pile types is presented in Table 1.1 - Typical Deep Foundation Capacities in Winnipeg, summarized from relevant, local literature.

**Table 1.1 - Typical Deep Foundation Capacities in Winnipeg**

| Pile Type | Approximate SLS Capacity Range |
|---|---|
| CIPC Friction Piles | 90 kN to 460 kN (1) |
| CIPC End Bearing Piles | 220 kN to 6700 kN (1) |
| Driven PPCH Piles | 580 kN to 1040 kN (2) |
| Driven Steel H-Piles | 836 kN to 2324 kN (3) |

*Notes:*
*1 – adapted from Baracos et al (1983) using recommended shaft adhesion values of 11 to 20 kPa, typical pile diameters of 350 to 600 mm and common depths of 7.6 m to 12.2 m.*
*2 – Skaftfeld (2018).*
*3 – average ULS capacities for HP200x54 to HP360x132 sections as reported by Belbas (2013).*

Based on the range of loads presented by helical pile suppliers and those shown above, there is a large overlap between helical pile capacity and other foundations alternatives used locally. In his paper which discussed the design and analysis of helical piles, Pack (2000) says helical screw piles are a viable and accepted deep

foundation alternative for heavily loaded structures and should be considered anytime deep foundation options are being developed. This is clearly possible for foundations in Manitoba based on the loads presented.

## 1.3 Thesis Organization

Chapter 1 provides an introduction to the use of helical piles, a brief project background, the hypothesis, the thesis objective, an overview of helical piles, other foundation alternatives in Manitoba and the thesis organization. Chapter 2 provides a review of existing literature relative to the prediction of helical pile capacity and the interpretation of load test data. Chapter 3 provides the project background, site soil conditions, soils laboratory testing results, pile installation methodology and load testing procedure. Chapter 4 presents the results of the theoretical and empirical predictions of pile capacity. Chapter 5 describes the results of the load tests; the various failure criterion used and compares calculated ultimate capacity to interpreted ones. Chapter 6 summarizes the thesis results and provides recommendations for further research.

## 1.4 Chapter 1 Discussion

Helical piles have been in use for many years and their design and performance is becoming better understood with on-going research. There is a continued need for further study to better define the numerous parameters which govern helical pile performance. Helical piles can offer advantages over traditional foundation alternatives, and their ability to support the requisite loads is possible.

Based on 57 axial compressive load tests completed during the installation of over 1,100 helical piles, existing methods to predict helical pile capacity will be compared to load test data. This research and discussion within the engineering community will allow for a more robust selection of potential foundation alternatives in Manitoba and beyond, ultimately benefiting designers, owners and end users of the structures on which they are founded.

# Chapter 2: Literature Review

## 2.0 Literature Review

A review of existing literature was undertaken to summarize the current standard of practice and general understanding of helical pile design. The effect of various properties such as helical pile geometry, construction methods, installation depth and soil types on pile capacity are discussed. Methods of predicting ultimate capacity from load test data using failure criterion is also presented.

## 2.1 Introduction to Helical Piles

Helical piles, also commonly referred to as screw piles or anchors, have been in use for nearly 200 years, with the earliest documented uses being at the Maplin Sands Light House by Alexander Mitchel in the Thames Estuary in 1838. Helical piles were originally used mostly as anchors to support tensile loads for transmission towers and buried pipelines (Mohajerani, 2016). Their use came out of popularity when the steam engine was developed and pile driving equipment replaced human-powered installation. With the advent of hydraulically powered equipment, helical piles have again become more popular.

The analysis of screw piles was first established in literature in 1965 by Trofimenkov and Maruiposhii who developed the Individual Bearing Method (IBM) concept of analysis for single helix piles, with further research in the 1970's and 80's developing methods of analysis for multi-helix piles (Mohajerani, 2016). Mitch and Clemence (1985) and Mooney et al (1985) then introduced the concept of the Cylindrical Shear

Method (CSM). Several studies which aim to improve on the IBM and CSM are further discussed below.

Helical piles have gained popularity for use in not only smaller structures requiring tensile support, but also for larger foundations due to several advantages they offer. Mohajerani (2016) describes these advantages as being easy to install, requiring minimal equipment, generally no dewatering is needed within the pile shaft, piles may be re-used and they are relatively quick to install. Pack (2000) indicates that it has been shown 10 helical piles can be installed to 12 m depth in the same time it takes to drill one cased shaft, not including concrete placement. Further advantages include that loading can be applied immediately after install (e.g. as opposed to concrete piles that require curing or driven PPCH piles that may require a re-strike), they are suitable for small access areas, they are capable of high tensile and compressive loadings, they can be installed into slopes and minimal noise and vibration are produced during installation compared to conventional pile driving equipment.

Disadvantages of helical piles include potentially lower capacity compared to other options (i.e. driven steel H-piles), they may be difficult to install in very dense soils or soils with cobbles and boulders, although Pack (2000) states installation in soils with Standard Penetration Tests (SPT) -N values greater than 90 are possible. Installation in dense soils will also be affected by capacity of driving equipment and ability of the pile to handle the driving stresses. Helical piles may also be more expensive (i.e. on a dollar per kN of resistance basis) than other pile options such as CIPC or PPCH piles,

however are becoming more economical. The availability of specialized contractors, especially for higher capacity piles may make helical piles less economical for smaller projects.

### *2.1.1 **Pile Geometry***

Helical pile geometry varies significantly in lengths, shaft diameters, shapes, helix sizes and helix arrangements depending on the supplier or project specific needs. It is common for helices to be 2 to 3 times the pile diameter (Rao et al, 1991). Shaft diameters (d) can vary from as small as 73 mm to upwards of nearly 1 m with corresponding helices diameters (D) from 150 mm to 1.2 m. With the varying geometries, it is useful to define some additional, common parameters used in helical piles design:

- The distance from the bottom helix to the ground surface is known as the embedment depth (H).
- The distance from the leading edge of the helix to the top of the flight is known as the helix pitch (p).
- For piles with multiple helices, the distance between helices is known as the inter-helix spacing (S).

Of these properties, the helix diameter, number of helices, helix embedment and inter-helix spacing play a large role in determining pile capacity with other factors

such as helix pitch playing less of a role. Figure 2.1 illustrates the general arrangement of a helical pile.

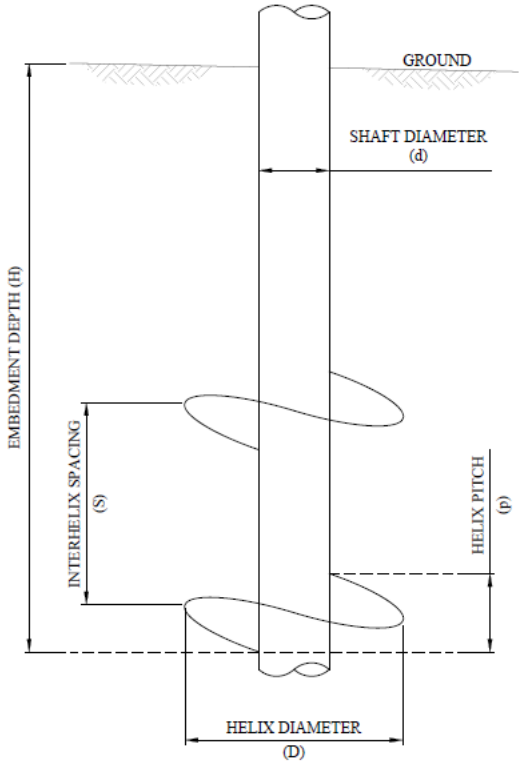


**Figure 2.1 - General Helical Pile Arrangement**

Given the discussion above, some general comments on helical pile geometry and their affect are summarized as follows:

- Helix Diameter (D): The theoretical predictions, which are discussed in more detail below, all incorporate the helix diameter in predicting the pile capacity. Simply put, larger diameter helices result in higher capacity piles. Although larger diameter helices produce higher capacity piles, they also produce disadvantages such as

requiring more powerful equipment to install. The increase in capacity may not scale directly with the increase in helix size.

- Number of Helices: In general, an increase in the number of helices will result in an increase in pile capacity, although there are diminishing returns as more helices are added. Piles with single helices will always act in IBM.

- Shaft Diameter (s): An increased shaft diameter will increase the area available to generate shaft adhesion above the helices. However, an increase in shaft diameter may also reduce the bearing area of piles acting in IBM.

- Helix Pitch (p): Ghally and Hanna (1991) found that torque increases with an increase in helix pitch. This does not necessarily mean an increase in capacity.

- Inter-helix Spacing to Helix Diameter Ratio (S/D): This spacing is critical in determining whether the pile should be analyzed using CSM or IBM (for multi-helix piles only). More tightly spaced helices will result in piles trending towards a CSM behavior whereas broader spacing will result in piles trending towards IBM behavior. Numerous studies have been conducted which explore this ratio relative to IBM or CSM behavior. Generally, a S/D ratio of 3 or greater is considered sufficient to develop IBM, where a tighter spacing will result in CSM, however this can vary depending on soil conditions and pile geometry. As this study focuses on single helix piles, a detailed discussion of S/D ratios is not provided however an excellent summary is provided in Mohajerani et al (2016).

- Embedment Depth (H): an increase in embedment depth will generally result in an increase in pile capacity, particularly for piles behaving in IBM and soils acting in a drained condition.

- Embedment Depth to Helix Diameter Ratio (H/D): This ratio controls the failure mode of the pile in both tension and compression. Piles in compression with H/D ratios of less than 5 are classified as shallow foundations while those with ratios of greater than 5 are classified as deep foundations (Mohajerani et al, 2016). The capacity also increases as this ratio increases. For example, Zhang et al (1998) found an increase in capacity from 13 to 31% with embedment ratios from 4.79 to 10.7.

### *2.1.2 **Soil Properties***

The main soil parameter controlling helical pile capacity is the shear strength. Properties which influence shear strength, such as soil type (cohesive or non-cohesive) and moisture content (as well as the elevation of the groundwater table) are therefore also of interest. Helical pile design as it relates to soil type can be split into cohesive and non-cohesive models. For cohesive soils, pile capacity will increase with the undrained shear strength ($s_u$), which is generally interpreted from in-situ soil data such as unconfined compressive tests, shear vanes, SPTs or empirical correlations. Elsherbiny and El Naggar (2013) found that an increase in clay strength resulted in an increase in pile capacity. In non-cohesive soils, pile capacity will increase with the friction angle of the soil, which is dependant on factors such as density, gradation and particle angularity. An increase in elevation of the water table

will generally result in a decrease in capacity for non-cohesive soils and depends on the method of analysis (i.e. total stress or effective stress) when considering clay soils. As most methods use total stress parameters when predicting capacity for cohesive soils, the water table elevation won't have a direct influence on the calculation, although some methods do include a term for effective stress at the installation depth.

Generally, an increase in moisture content results in a reduction in undrained shear strength. Rao et al. (1991) found that a reduction in the moisture content of clays significantly increases capacity and to the contrary found an almost 50% reduction in the ultimate capacity with an increase in moisture content from 40 to 50%. Establishing soil index properties such as Atterberg limits and the Liquidity Index may be valuable in explaining variation in pile capacity for similar sites. As the moisture content increases and approaches the liquid limit, higher Liquidity Indices may be a predictor or lower shear strengths and thus lower pile capacity. The capacity of piles in granular soils will generally also be higher than cohesive soils, although high capacities can still be realized in cohesive soils, for example in hard clay tills.

### *2.1.3 Installation Conditions*

Helical piles are installed by rotation and applying a downward force on the pile shaft using a drive head attached to hydraulicly powered equipment. This downward force is commonly referred to as crowd. The drive head can be fastened to the pile with a bolted connection, or pile tops that are fitted to match the drive head, much like a

socket and bolt, while crowd is applied. The rotation and downward pressure are resisted by the soil, creating torque, which is commonly measured during installation and used as a quality control measurement as it is relates to the driving force required to advance the pile. The helix should pass cleanly through the soil without augering it which requires the crowd be applied sufficiently and pile rotated at a rate such that the pile advances at one helix pitch per rotation. Although Perko (2009) indicates that a rate of a least 80% of the helix pitch per rotation is adequate. When the rotation exceeds one revolution per pitch, the soil is overly disturbed, or churned, as the pile is advanced. This churning of the soil results in remoulding of fine-grained soils and can impact the pile capacity. The degree of remoulding is dependant largely on the installation conditions, such as the pile advancement matching one pitch per rotation. Weech and Howie (2012) and Lanyi (2017) both mention that the remoulding will more significantly affect piles acting in CSM versus IBM, as the soil surrounding the helices is partially remoulded as the pile advances, while the soil below the pile (or lead helix) is largely unchanged. The resulting shear strength of the remoulded soil will be somewhere between the intact strength and remoulded strength.

There is a tendency for increased crowd (i.e. downward pressure) from the operator as driving conditions become more difficult. This is done to facilitate advancement of the pile and reduce the likelihood of auguring/disturbing the soils (Harnish, 2015). Ghallay and Hanna (1991) noted from an experiment where they installed 5 piles with varying geometrical arrangements in compacted sand and loaded under laboratory conditions that the installation process causes densification of adjacent soil due to

downward force applied and lateral movement of the soil. The amount of compaction depends on initial soil density, applied downward pressure and relative depth ratio of the anchor. The study shows that dense sands have higher pullout capacity than medium and loose sands, although it is not explicit that the densification of sands during installation results in higher capacity.

Shaft resistance, particularly above the upper helix, may be more heavily influenced by installation disturbance. The concept of the effective length ($H_{eff}$) has been introduced to account for this, which is the length of shaft over which shaft resistance can be accounted for. For example, Mohajerani et al (2016) suggests that this length is the embedment depth minus one helix diameter. Mohajerani also notes that unless the shaft is embedded at least 3D, then shaft contribution should not be considered. Results from tests in compression by (Zhang et. al, 1998) show a decrease in shaft adhesion for roughly 5 helix diameters for clay soils and 2.5 helix diameters for sandy soils (immediately above the upper helix). The Canadian Foundation Engineering Manual (CFEM) also states that the shaft adhesion is generally not considered for diameters less than 100 mm (CFEM, 2006).

In cohesive soils, the driving process may temporarily result in increased pore pressures and thus a reduction in shear strength (ergo, pile capacity). Lanyi (2017) noticed that no reduction in strength was observed due to installation effects on piles that exhibit IBM in fine grained soils. This was accomplished by measuring pore pressure response with vibrating wires close to the installation depth, slightly above the helix. Similar results were observed by Weech and Howie (2012), although they

did note in their study that pile installation significantly affected the adjacent soil (i.e. piles acting in CSM, as noted above), but the soil below the bottom helix essentially remained intact. Lutenegger and Tsusha (2015) found a reduction in shear strength from install disturbance was negligible in stiff clays but was significant in soft, sensitive clays. Similar results were noted by Elkasabgy and El Naggar (2015) for shaft resistance where the mobilized shear resistance of cohesive soils was found to be 20% to 40% of the intact strength, although this recovered over time to about 65%.

Predrilling to facilitate pile installation may also affect pile capacity as noted by Sakr (2011) and should be considered when evaluating capacity. The predrill can both reduce the shaft capacity, for example by up to 50% in the study by Sakr (2011) and in the IBM depending on how far below the prebore the helix is advanced.

## 2.2 Ultimate Capacity from Theoretical Correlations

As discussed earlier, the capacity of a helical pile depends on numerous factors such as the shaft size, shaft shape, helix size, installation depth, groundwater level, soil type and strength, time from install to loading and installation conditions. The various IBM and CSM address some of these factors and several authors have proposed variations in the models. Perko (2009) developed a relationship between SPT and settlement behavior but only for piles up to 274 mm diameter and regression coefficients ranged between 0.48 to 0.51. SPT results from the current field work were generally all taken to refusal (i.e. they all equal 100) and thus would likely produce a less meaningful correlation than observed by Perko.

The CSM assumes the pile capacity develops along the cylindrical plane between the upper most and lowest helical plates (shown in Figure 2.2). The IBM assumes the capacity is developed below each of the individual helices (shown in Figure 2.2). Both of these methods may or may not include contribution from shaft adhesion above the helix, provided the pile is deep enough (Sakr, 2009). If the shaft adhesion is included, the effective length ($H_{eff}$) should be accounted for.

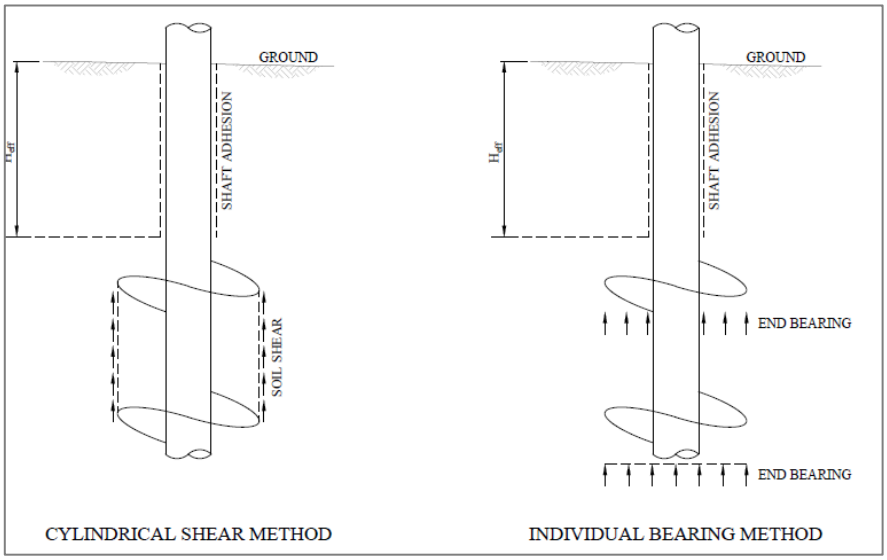


**Figure 2.2 - CSM and IBM Illustration**

The following sections discuss some of the theoretical methods used to predict pile capacity in both IBM and CSM. CSM will only be discussed briefly as this study focuses on single helix piles in which CSM is not applicable.

### *2.2.1 Individual Bearing Method*

The CFEM (2006) provides helical pile capacity as the bearing capacity of each individual bearing plate (helix) plus the shaft adhesion, in the following equation:

$$R = Q_t + Q_f \qquad \text{(Equation 2.1)}$$

where $R$ is the ultimate helical pile capacity, $Q_t$ is the sum of the individual helical bearing capacities ($Q_h$) and $Q_f$ is the resistance along the shaft, if applicable. The individual helical bearing capacity and shaft resistance are defined as:

$$Q_h = A_h\left(s_u N_c + \gamma D_h N_q + 0.5\gamma B N_\gamma\right) \quad \text{(Equation 2.2)}$$

$$Q_f = \sum(\pi d f_s \Delta L_s) \quad \text{(Equation 2.3)}$$

where $A_h$ is the area of the individual helix, $s_u$ is the undrained shear strength of the soil under the helix, $\gamma$ is the unit weight of the soil, $D_h$ (referred to as H in this thesis) is the depth to the helix (embedment depth), B (referred to as D in this paper) is the diameter of the helix and $N_c$, $N_q$ and $N_\gamma$ are the bearing capacity factors for the local shear conditions. For Equation 2.3, d is the diameter of the shaft, $f_s$ is the adhesion between the soil and shaft and $\Delta L_s$ is the incremental pile length over which $f_s$ is taken as constant, i.e. $H_{eff}$.

Equation 2.2 is an obvious adaptation of the general bearing capacity formula proposed by Terzaghi and then later adapted by Meyerhof and Vesic. Many of the other studies work to a further adaptation of Equation 2.2 and 2.3. For example, Tappenden and Sego (2007) proposed the following equation for helical piles in compression in cohesive soils where $Q_{ult}$ is the sum of Equations 2.4 and 2.5:

$$Q_b = \frac{\pi\left(D^2 - d^2\right)}{4}\left(N_c s_u + \gamma' H\right) \quad \text{(Equation 2.4)}$$

$$Q_s = \pi d H_{eff}\, s_u \alpha \quad \text{(Equation 2.5)}$$

where $Q_b$ and $Q_s$ are the capacity derived from the helix and shaft, respectively and α is the adhesion coefficient. These equations are essentially identical to Equations 2.2 and 2.3, with the term $N_q$ not being included as it is equal to 1 in a total stress (cohesive soil) analysis. The omission of $N_\gamma$ is due to the equation being used in cohesive soils as it is equal to zero. They note that *d* may be neglected for the lower most helix in Equation 2.4, indicating the bearing is developed by both the helix area and pipe/shaft area. It is important to consider that this assumes that the shaft is either closed ended or a sufficient plug has developed within the shaft to account for the full end bearing area of the pile.

Empirical relationships suggested by others, such as in Elkasabgy and El Naggar (2015) for end bearing piles in clay are similar to those presented above and is shown in Equation 2.6.

$$Q_{ult} = A_h s_u N_c + \pi d H_{eff} \alpha s_u \qquad \text{(Equation 2.6)}$$

The above equation has been adapted to account for only a single helix. Again, the $N_\gamma$ portion is not included as the study was completed in cohesive soils (i.e. $N_\gamma = 0$). The notable difference is that the depth of the helix term and unit weight is not included, as in Equation 2.2 and 2.4. In the same study Elkasabgy and El Naggar (2015) suggest another equation for end bearing of the lowest helix in clay soils which accounts for the embedment depth:

$$Q_{ult} = (A_h + A_t)(\, s_u N_c + \sigma'_{vo} N_q) \qquad \text{(Equation 2.7)}$$

This will produce a very similar result to Equation 2.4 as $N_q = 1$ for undrained analysis and the effective stress at the helix depth ($\sigma'_{ov}$) is essentially the same as $\gamma'H$ for a uniform soil deposit. Layni-Bennet and Deng (2018) have cited similar methods, which is an adaptation of the method presented in the CFEM for calculating the ultimate toe resistance of the deep foundation unit in cohesive soils as:

$$Q_b = N_t s_u A_b n + \alpha s_u (\pi d H_{eff}) \quad \text{(Equation 2.8)}$$

where $N_t$ is a bearing capacity coefficient, $A_b$ is the area of helical bearing area and n is the number of helices. The CFEM suggests that $N_t$ is equal to 6, 7 or 9 for bearing areas larger than 1 m, between 0.5 m and 1 m and less than 0.5 m, respectively. Overall, the bearing capacity factors have a large effect on the predicted capacity and therefor must be chosen carefully. For example, Layni-Bennet and Deng (2018) found $N_t$ ranged from 6.2 to 7.7 for 305 mm diameter helices compared to the value of 9 for the helix diameter suggested by the CFEM. He attributed this to the inclination of the helical plate to the bearing surface. Harnish (2015) recommends that shaft adhesion factors and bearing capacity factors be investigated for different soil types, especially those that may be subject to significant remoulding during installation. Gavin et al. (2014) notes from estimates of ultimate capacity that the results are very sensitive to $N_t$ factors and therefore must be chosen carefully to not severely over or underpredict actual values. The same conclusion is reached by Tappenden et al (2018).

From the theoretical relationships presented above, it can be seen that for a given project, many of the variables (e.g. helix area, soil unit weight and embedment depth) involved in computing theoretical capacity will be constant if the same pile type is used, leaving the undrained shear strength and bearing capacity factors as the main influence when using theoretical predictions.

### *2.2.2 Torque to Capacity Relationships*

Capacity to Torque to Correlations (CTC) have been in use since the 1970's. Hoyt and Clemence (1989) were the first to formally develop a CTC relationship to predict ultimate capacity. It is a reasonable assumption that the required install torque is related to pile capacity as the torque is a direct measurement of the shearing resistance provided by the soil as the pile is advanced. The initial relationship proposed by Hoyt and Clemence is fairly straightforward where the ultimate capacity is related to the measured install torque and an empirical torque factor. This initial CTC relationship is also provided in the CFEM (2006) for the ultimate capacity as:

$$Q_u = K_T \, x \, T \qquad \text{(Equation 2.9)}$$

Where $K_T$ is the empirical torque factor and T is the average installation torque. The torque is often recorded from a pressure meter gauge mounted to the installation equipment which measures the hydraulic pressure being applied during installation. The recorded pressure is then converted to a torque value using an established calibration factor for the equipment. Hoyt and Clemence (1989) suggests that T is taken as the average of the readings over the depth equal to 3 helix diameters from the

final embedment depth of the helix. Although the experimental results used to develop this initial equation were based on uplift capacity, it has been extended to axial compressive capacity as well and Perko (2009) notes that $K_T$ factors are higher for piles in compression than in tension. They also increase disproportionally to an increase in pile size, that is, there are diminishing returns as the helix size increases. A study completed by Ghaly and Hanna (1991) discusses the additional factors which should be taken into account such as helix diameter, pitch of the anchor, helix angle, diameter of the shaft, general configuration of the pile, thickness of the helix blades, the shape of the cutting edge, manufacturing (e.g. bolted assembly, welded, riveted, etc.), pile material/roughness and the helix end state (e.g. whether it is conical or flat). The effect of installation depth is also noted to be a factor, with an increase in torque with an increase in depth. Of these factors they indicate that the helix pitch to diameter (p/D) ratio, helix angle and general pile configuration are the most significant factors affecting performance and the remaining factors can mostly be eliminated by proper design and by fabricating the piles as one piece (e.g. welded, smooth edges).

The CFEM provides ranges of $K_T$ from 10/m to 33/m (where torque is measured in N-m), depending on shaft diameter. Several studies have been conducted which refine $K_T$ based on other factors such as soil conditions and pile dimensions. A summary of $K_T$ factors from various studies are presented in Table 2.1 - Torque to Capacity RelationshipsTable 2.1.

**Table 2.1 - Torque to Capacity Relationships**

| Source | $K_T$ ($m^{-1}$) | Notes |
|---|---|---|
| CFEM (2006) | 33<br>23<br>10 | Default value<br>shaft dia. = 90 mm<br>shaft dia. approaching 200 mm |
| Harnish (2015) | $27.64A_e^{-0.5}$ (2) | Function of embedded pile area |
| Perko (2009) | $1433D^{-0.92}$ (1) | Function of largest helix dia. |
| Lanyi (2017) | 20.4 to 24.0 | Homogeneous clay<br>($s_u$ from 60 to 100 kPa) |
| Tappenden (2007) | 9.2 to<br>16.9 | From linear regression in multiple soil types |

*Notes:*
*1 – From Perko (2009) where D is the helix diameter in mm.*
*2 – where $A_e$ is the total embedded area (i.e. helix and shaft).*

As can be seen from Table 2.1, there is a significant variation in the CTC relationships which is further varied when other factors such as helix diameter and soil strength are taken into account. In this regard, relying on CTC relationships should be done with caution and site-specific values, confirmed by load test results and detailed subsurface information is necessary if these correlations are to be used.

Harnish (2015) also presents a method to calculate installation torque, which is noted to be a 'direct' function of the embedded area and soil shear strength. These correlations likely don't apply to the current study due to the prebore activities where a majority of the shaft would not be in direct contact with soil during install.

Despite the correlations developed by Harnish, several papers note that a limitation of CTC relationships is they cannot be used prior to construction to determine capacity, rather they are used to confirm capacity following installation. Harnish also notes based on the work by Hoyt and Clemence (1989) that between IBM, CSM and CTC, CTC was the best predictor of ultimate capacity, however all three methods over-predicted capacity and a large factor of safety (or reduction of factors in limit states design) is warranted to account for this.

Harnish (2015) notes that the accuracy of CTC methods for large diameter helical piles is adversely affected by the inaccurate measurement of torque from employing hydraulic pressure torque indicators. This is often completed visually, under field conditions where weather or other environmental effects could further impact the accuracy of readings.

## 2.3 Load Transfer

When load is applied to a helical pile it is resisted by either the CSM or IBM and potentially via shaft adhesion. The proportion of load that is carried between the shaft and the helix depends on the magnitude of the load and deflection, pile length, helix diameter, shaft diameter, soil type and installation conditions. The magnitude of movement required to mobilize resistance along the shaft or helix is generally expressed as a percentage of the shaft or helix diameter. Fellenius (2006) states that ‘very small’ relative movement between the pile and soil is required to mobilize shaft resistance. These movements can be as little as a few millimeters.  Movements to

fully mobilize end bearing are often much greater but are more dependant on the method of installation (e.g. bored vs driven piles).

To determine the proportion of load between shaft and end bearing, strain gauges are often installed along pile shafts. Strain gauges are electronic devises that can accurately measure small amounts of strain, which can then in turn be used to calculate load using simple stress-strain relationships (the geometry and material properties of the pile). By analyzing the change in applied load at the pile head and at strain gauge locations, the contribution from adhesion can be estimated. The load along the shaft is not always equally distributed and therefore gauges are often installed at a few locations, generally with one near the bottom of the pile, such that the distribution of the load can be better understood.

Alternate methods to determine the contribution from shaft and end bearing include the use of an Osterberg cell (O-Cell) installed at the base of the pile. An O-Cell is a pressurized hydraulic loading device which is installed within a pile, usually near the pile toe and can be used to quantify shaft resistance and end bearing individually. Simply put, the difference between the load at the bottom and top of the pile is measured and the contribution from shaft resistance can be calculated from the difference.

Layni (2017) evaluated the load transfer along single and groups of 6.1 m long, double helix piles. The piles had 305 mm diameter helices with S/D ratios of 3 and 5. The study included 6 instrumented load tests in cohesive soils. He found that helical

bearing was mobilized at 5% to 6.6% of the helix diameter, where the shaft was fully mobilized at 3% to 5.5% of the shaft diameter.

Elkasabgy and El Naggar (2015) completed a study on several instrumented piles using strain gauges between 6 m and 9 m in length. The piles had either single or double helices with 324 mm diameters and were installed into cohesive soils. A driven steel pipe pile was also instrumented for comparison. Shaft adhesion was fully mobilized at less than 1% of the shaft diameter and at 24 mm to 26 mm (~8%) and 30 mm to 33 mm (~10%) for the 6 m and 9 m piles, respectively.

Similar to the above tests, Weidong et al (2017) found that shaft resistance was mobilized at a much greater rate (i.e. at lower displacements) than helical bearing. They found the shaft resistance was mobilized at 0.5% to 1.2% in clay and 1.0% to 2.8% in sand, whereas the helical base resistance was still increasing after 10%D in clay and 5% D in sand.

Aydin et al. (2011) installed a single helix and triple helix pile in high plastic lacustrine clay and completed two static axial load tests using an O-Cell. This work was completed at the same test site as Tappenden (2007), and the study found good agreement with empirical correlations and Tappenden's results. The use of the O-Cell allowed the researchers to also evaluate load transfer between the pile head and pile toe. They found shaft adhesion contributed 34% whereas end bearing contributed 64% at the ultimate capacity, as determined from the Birch-Hanson 80% Failure Criterion from the O-Cell load-displacement curve.

Elsherbiny and El Naggar (2013) completed full scale loads tests on helical piles in cohesionless and cohesive soils along with numerical modelling of the load tests to calibrate numerical results. They note the initial portion of the loading curve exhibited higher stiffness than the unload curve in dense soils. This may be explained by two factors: more shaft adhesion is gained as the pile moves downwards, but less so as it rebounds, and; permanent bending of the helical plate may occur as the pile is loaded. Similar to the other studies, they found as load increased the contribution from shaft decreased. Initially shaft resistance contributed around 45% however as the pile approached maximum loading it was closer to 20%. For clay soils they also found the theoretical capacity is much lower than numerical modelling produced. They attributed this to use of a low $N_c$ factor explaining that the $N_c$ factor is evaluated using a 2-dimensional failure surface that doesn't account for confining effects in 3 dimensions (contrary to load testing results when compared to theoretical capacities noted in the studies above). In this regard, they suggest increasing $N_c$ to 12 from the standard recommended value of 9 (for D <0.5m) and 6 (for D >1 m).

## 2.4 Ultimate Capacity from Failure Criteria

To reliably assess the performance of foundations, design loads can be confirmed by pile load tests, the most common of which is the static load test (Fellenius, 2006). The Quick Load Test Method described in ASTM D1143 – Standard Test Methods for Deep Foundation Elements Under Static Axial Compressive Load is frequently the selected test method. During this test, displacements and load at the pile head are measured as load is applied in pre-set time increments (the test procedure is described

in more detail below). The test proceeds until a predetermined load or displacement is reached or safety considerations dictate. Additional instrumentation to measure strain or load, such as the use of strain gauges or O-Cells as discussed above are often employed. Significant design and construction efficiencies can be realized by completing load tests as many design codes allow for higher reduction factors, meaning less piles are required (i.e. cost savings) or design risks are minimized.

Interpretation of the load test data is then completed by plotting the load versus displacement. Hirny and Kulhaway (1989) suggest that the curves generated from this data can be separated into three distinct regions:

1. An initial linear elastic region with a flat slope (i.e. a region of high stiffness).
2. A non-linear transition region where the displacements are largely disproportionate to the load increments, and:
3. A final linear region with a steep slope (i.e. a region of low stiffness).

These regions are shown graphically in Figure 2.3 from a load test at the project site.

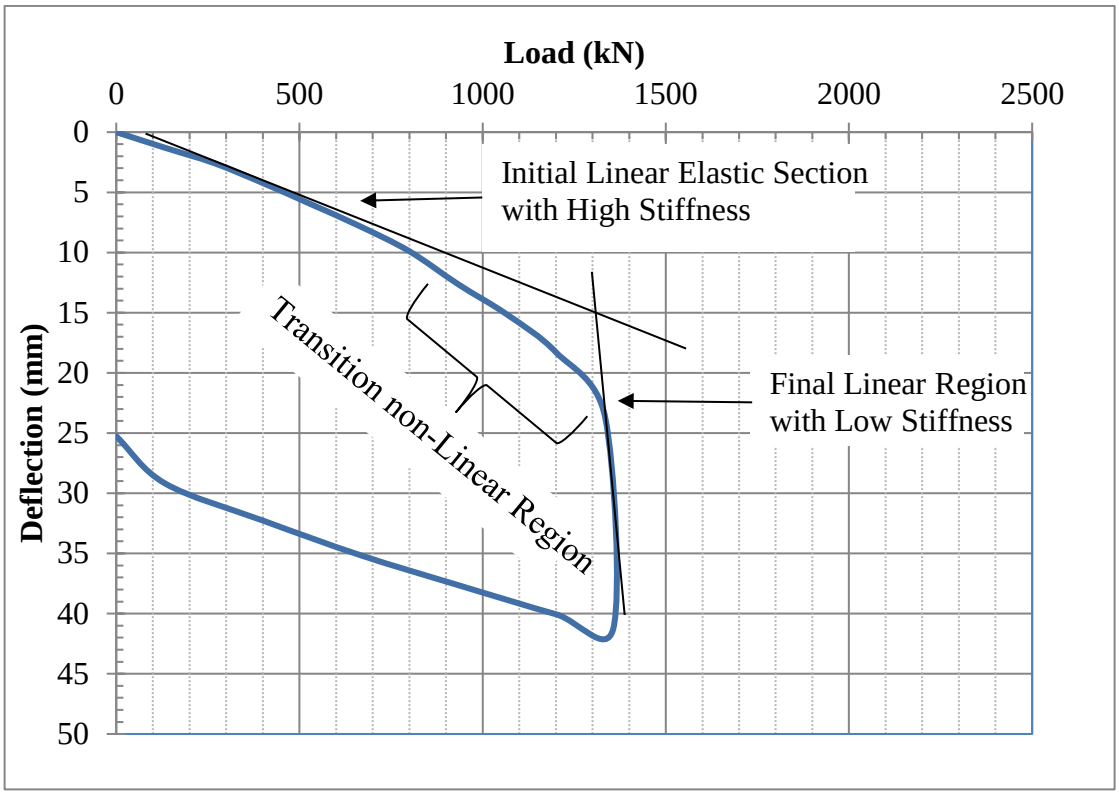


**Figure 2.3 - Load Deflection Curve Regions**

The large displacements experienced at plunging failure are often not appropriate for the structures on which they are intended to support. Further, the displacement within this region may be a function of the pile-soil interaction as much as human effects due to the rate of the applied load (i.e. the person at the load cell can arbitrarily control the rate of advancement). Ideally the factored ultimate capacity should be obtained before the final linear region, as creep displacements become significant at loads after this region, which can be seen in the plot above. However, the failure load from load test interpretation should be obtained within the final region of low stiffness, as this is the load which is also represented by theoretical capacities.

Many interpretations of load to displacement data have been developed which attempt to determine an ultimate capacity, commonly referred to as failure criterion. An early estimate of the ultimate capacity, generally credited to Terzaghi (Fellenius, 2006) is the load where the displacement is equivalent to 10% of the pile (or helix) diameter. For larger diameter piles (e.g. 457 mm diameter as used in this study), significant deflection in the load tests are required to meet this limit and simply isn't practical to load a pile to this magnitude if the pile is meant for production. Overstressing the soil at the pile toe could also result in cohesive soils reaching reduced strengths, further affecting the structure that production piles are meant to support. O'Neil and Reese (1999) suggest that a more appropriate criteria is 5% of the pile diameter (referred to as the 5%D criterion going forward), which was developed for bored piles. Methods based on simple ratios of pile geometry do not take into account the elastic compression of the pile, which may be significant for higher loads and longer piles.

Davisson presented an offset criterion to interpret load-displacement curves known as the Davisson Offset Limit. The offset criterion is defined as the load corresponding to a displacement of 4 mm plus the pile diameter divided by 120 including the elastic compression of the pile, as shown in Equation 2.10:

$$S_{ult} = (4 + \frac{D}{120}) + \frac{QL}{AE} \qquad \text{(Equation 2.10)}$$

Where $S_{ult}$ is the displacement (in mm) at the pile head which intersects the load-displacement curve at the ultimate capacity, $Q_u$, Q is the applied load, L is the pile length, A is the cross-sectional area of the pile and E is Young's Modulus of the pile.

The Davisson Offset Limit was developed by analyzing a number of load tests from driven, straight shaft piles and is therefor more appropriate for driven piles, as compared to bored or cast in place piles. The reason for this is the assumption that 4 mm plus D/120 is sufficient to fully develop resistance along the shaft and toe, respectively. For a driven pile, a compressed soil plug forms below the toe, whereas for a bored pile, additional movement would be required to mobilize the same resistance at the toe due to the uncompressed soil (NeSmith, et. al, 2009). Given this, modified versions of the Davisson Offset Limit have been presented. For example, Davisson recommends that the soil quake term (D/120) be multiplied by a factor of 2 to 6 for bored piles resulting in a range of D/20 to D/60.

Several similar methods to the Davisson Offset Limit have been discussed which maintain the elastic compression of the pile and adjust the relationship between the ratio of the pile diameter. Elkasabgy and El Naggar (2015) developed a site-specific method for calculating $Q_u$ based on helix diameter (610 mm diameter helices were used in the study) and the elastic compression of the pile (referred to as the Elkasabgy criteria going forward):

$$S_{ult} = 0.035D + \frac{QL}{AE} \qquad \text{(Equation 2.11)}$$

This produces a result very similar to the modified criteria recommended by Davisson above (i.e. D/30 is 0.033D compared to 0.035D above). Equation 2.11 was based on several full-scale axial load tests completed on single and double helix piles in cohesive soils. As part of the study they also looked at 4 load test failure criteria,

including the Davisson Offset Limit, Tangent Intersection Method, and those proposed by O'Neil and Reese (1999) and Livneh and El Naggar (2008). Based on the analysis, they indicate that none of the methods, with the exception of O'Neil and Reese (1999), are suitable for large capacity helical piles as they significantly under or over predicted the capacity, 'especially those with helices resting in very stiff to hard soils'.

Graphical methods which consider the slope of the load to displacement data have also been developed, such as the Brinch-Hanson 80% criterion, proposed by Brinch and Hanson (1961). This criterion assumes that the shape of the load to displacement curve is such that the movements, denoted as Δ, when plotted along the X-axis and with $\sqrt{\Delta}/Q$ plotted along the Y-axis, produces a straight line. The straight line has a slope of $C_1$ and y-intercept of $C_2$. From this curve, $Q_u$, for the displacement $\Delta_{ult}$, is the failure load, if the load at $0.8Q_u$ gave the movements $0.25\Delta$. This criterion is only applicable for tests which have experienced plunging failure and the point $0.8Q_u/0.25\Delta_u$ plots on the curve (CFEM 2006). Once the constants C1 and C2 are determined, the load at failure and displacement at failure can be calculated using equations 2.12 and 2.13.

$$Q_u = \frac{1}{2\sqrt{C_1 C_2}} \qquad \text{(Equation 2.12)}$$

$$\Delta_u = \frac{C_2}{C_1} \qquad \text{(Equation 2.13)}$$

Other graphical methods, such as the tangent intersection method provide the ultimate capacity as the intersection of two lines: tangent lines of the two linear sections of the load-displacement curve. Fuller and Hoy (1970) suggest that maximum proven design (i.e. the load at ULS) load is taken as 50% (i.e. a Factor of Safety of 2) of the ultimate bearing capacity as indicated by this method. Fellenius (2006) cautions against the use of graphical methods as they can be extremely dependant on the scale of the graph (i.e. change the scale and the ultimate capacity changes). The De Beer failure criterion is also a graphical method where the settlement is plotted versus the corresponding load on logarithmic scales. The plot produces two straight lines, and the intersection of these lines is the corresponding failure load. An example of the various failure criterion (with the exception of De Beer) are shown below in Figure 2.4. The Davisson, Elkasabgy and 5%D methods were selected given their variable applicability (i.e. developed separately for driven, helical and bored piles) in an effort to assess which might be most appropriate for helical piles in this study setting.

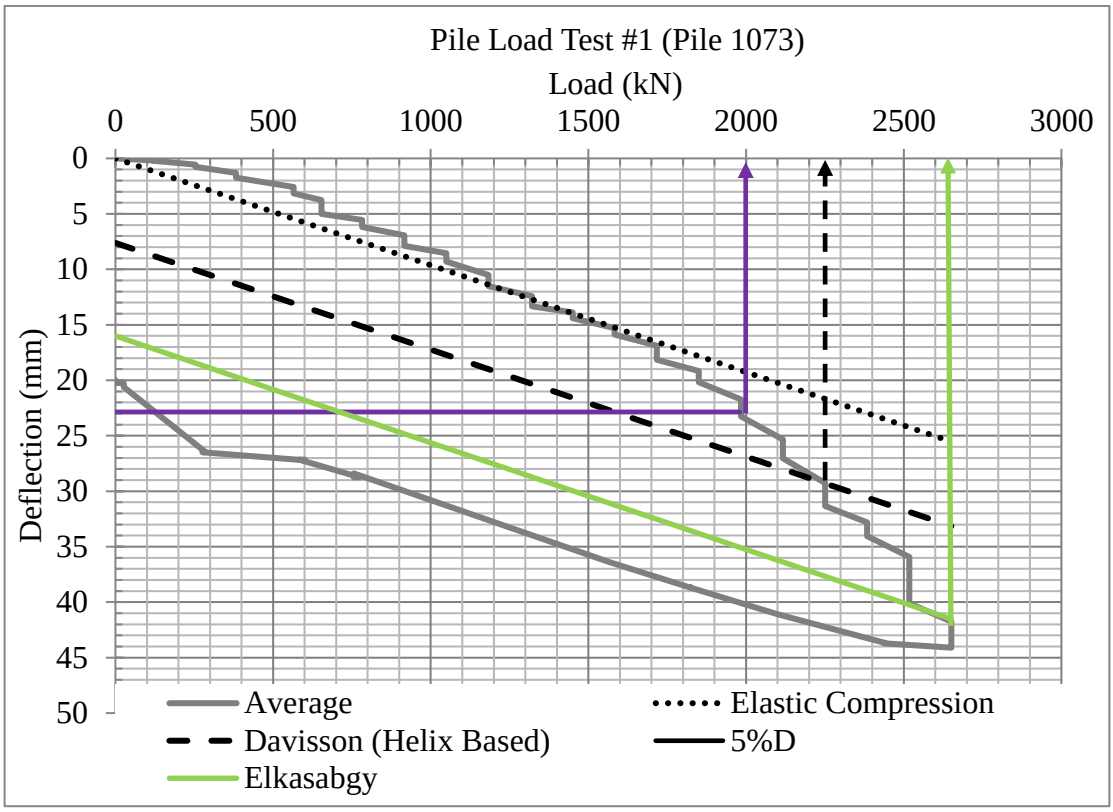


**Figure 2.4 - Example of Load Displacement Interpretation**

Figure 2.4 shows a wide range in the predicted capacity from roughly 2000 kN to just over 2600 kN. For the Tangent Intersection Method, the plunging failure is not well defined in this test. Should the test have been allowed to carry on to further develop the final region of low stiffness, it would result in the second tangent line being more vertical, and thus a higher capacity could be interpreted. A similar method to the De Beer criterion was presented by Kumar et al (2014) where they adopted a creep limit for piles founded on rock by plotting the 8 minute load step deflection and load on non-logarithmic scales.

Examples of the De Beer failure criterion and how the load test data from this study does not produce two straight lines are shown in Figure 2.5 and Figure 2.6. As Khan

(2018) notes, the De Beer failure criteria assumes that the pile was loaded to plunging failure. This trend is similar with the remaining tests completed for this study. It is likely that the piles were not sufficiently loaded to plunging failure to allow for a meaningful interpretation with the De Beer failure criterion.

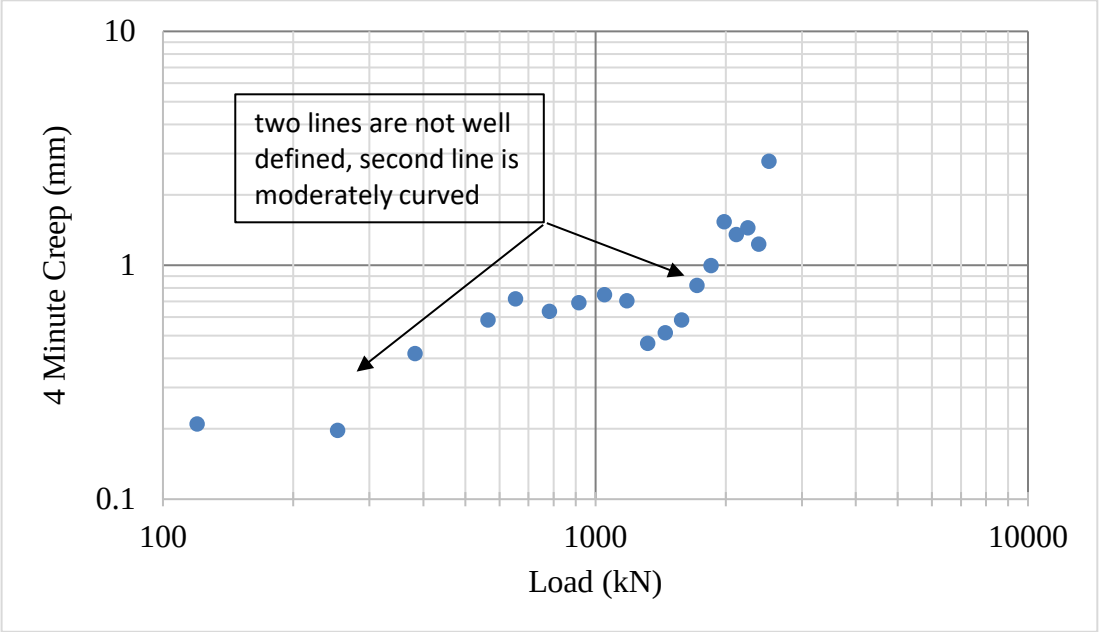


**Figure 2.5 - De Beer Failure Criterion Pile 1073**

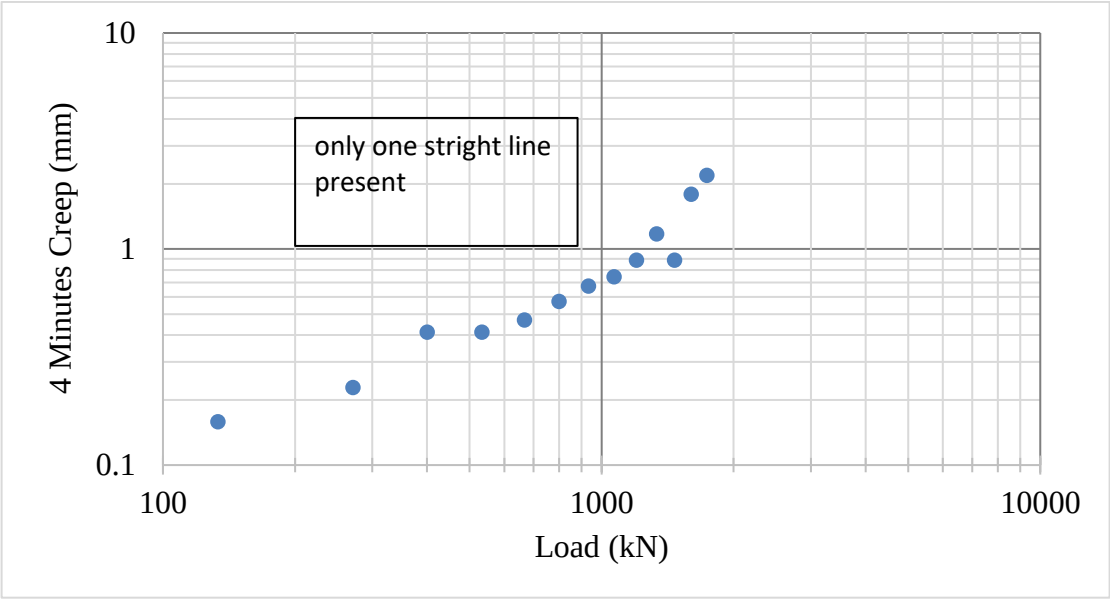


**Figure 2.6 - De beer Failure Criterion Pile 7010**

## 2.5 Predicted versus Measured Ultimate Capacities in Literature

The following section will focus on studies which have analyzed IBM modes of failures, as the CSM correlations are not relevant for the current study.

In the study discussed above where Elkasabgy and El Naggar (2015) analyzed 4 methods of interpreting load to displacement data, they found that the methods under or over predicted the capacity of the piles when compared to their proposed criterion, summarized as follows:

- Davisson Offset Limit – underestimated $Q_u$ by 18-34%
- Tangent intersection – underestimated $Q_u$ by 14-43%
- O'Neil and Reese, 5%D (1999) – over estimated $Q_u$ by 6-12%
- Livneh and El Naggar (2008) – over estimated $Q_u$ by 18-44%

Based on the values shown above, the 5%D criterion provides the closest approximation to the ultimate capacity predicted by Elkasabgy and El Naggar (2015). From this same study, measured settlements at design capacity (FS of 2) were less than 1% of D. Similarly, Elsherbiny Z.H. and El Naggar (2013) find that the 5%D criterion was consistently higher than the predicted capacity (by approximately 25 to 36%) from theoretical methods and always fell within the second linear region (which is considered an appropriate target).

Elkasabgy and El Naggar (2015) showed predicted vs measured capacities from +15.9% to -22.9% using Equation 2.6. Tappenden found that predicted capacities using Equation 2.4 and 2.5 for 26 helical piles tested, 21 fell within 20% of the measured capacities, while the remaining 5 underpredicted capacity. Layni et. al (2018) consistently overpredicted capacity using Equation 2.7, which they attributed to the high default value for $N_t$ of 9.

In a controlled laboratory study, Rao et al. (1991) fabricated 11 helical piles of relatively small diameter and tested them in prepared tanks in cohesive soils. The piles were equipped with 2 to 4 helices ranging from 75, 100 and 150 mm on 25, 44 and 60 mm shafts installed to 640 and 1000 mm depths. The tests were completed in cohesive soils (3 different clays with liquid limits of 38, 65 and 75) and the moisture content of the soils were changed in some tests, which indicated an almost 50% reduction in the ultimate capacity with an increase in moisture content from 40 to 50%. Their experimental values were always lower than those predicted by theoretical correlations, ranging from 69 to 99% of the theoretical value.

Hoyt and Clemence (1989) state that theoretical or empirical methods (i.e. IBM, CSM and CTC) tend to over predict capacity, indicating the need for high FS in deterministic design. They also found that torque correlations showed more consistent results when compared to the IBM and CSM models.

Harnish (2015) completed 6 axial compressive tests, 5 of which were instrumented in over consolidated glacial till where peak shear strengths ranged from approximately 300 kPa to 600 kPa and remoulded shear strengths between 250 kPa and 310 kPa. Using the average of these values he found that the IBM generally over predicted capacity. The over prediction may be attributed to the use of intact shear strengths in the predictive models. It is noted that it may be more appropriate to use a value somewhere between the remoulded and intact strengths.

## 2.6 Chapter 2 Discussion

Helical piles have several advantages as foundation options and come in numerous shapes and sizes. The configuration of the piles can affect the capacity as can soil conditions and installation factors. Methods to predict the ultimate capacity of helical piles have been adopted from common shallow or deep foundations methods, such as the general bearing capacity equation. Due to the varying nature of helical piles, several alterations to these equations have been proposed by researchers to refine predictive models. Generally, the predictive models overestimate capacity when compared to load test data and further work would be valuable to assess the applicability of these methods.

Pile loads tests are commonly used to refine estimates of ultimate capacities of piles. Load tests can provide significant value to projects however many of the failure criterion available may not be applicable to certain projects. Particularly when a load testing program is completed on production piles, as the risk of over-stressing the underlying soils and taking piles to large deflections is simply not tenable. Contrary to the theoretical equations, the failure criterion may over or under predict capacity.

# Chapter 3: Background Information

## 3.0 Background Information

The pile installation was part of Manitoba Hydro's Bipole III project which involved construction of a high current 500kV Direct Current (DC) transmission line to the southern part of the Province. The main pieces of infrastructure required at the project site to facilitate transmission are the Transformer and Converter Buildings, DC Yard and several ancillary support structures. Foundations on site consisted of cast in place concrete piles, shallow footings, driven steel pipe piles and helical piles. To support the Transformer Building and Converter Building 1,118 Helical piles (425 at the Transformer and 693 at the Converter) were installed, along with several test piles.

The project was completed by Mortenson Canada Corporation (Mortenson) and the geotechnical program was undertaken by Dyregrov Robinson Inc. (DRI) with support from TREK Geotechnical Inc (TREK). Pile installation was completed from November 2015 to October 2016 with production pile load testing completed throughout this time. The test piling program and load testing was completed in August to September 2015 under the supervision of TREK personnel with senior technical oversight from DRI and CH2M.

The structural design for the helical piles was based on an Ultimate Limit State (ULS) load of 1340 kN and a Serviceability Limit State (SLS) load of 1075 kN with a maximum head displacement of 25 mm for each pile. For piles corresponding to more lightly loaded foundation elements, the ULS and SLS capacities were 1021 kN and

817 kN, respectively. The capacities above are near the upper end of those noted in **Error! Reference source not found.** and Pack (2000) states 'heavily loaded structures' are in excess of 445 kN column loads, and in this respect the piles for the project are regarded as heavily loaded. Similarly, it can be seen from comparison with Table 1.1 that these capacities are towards the higher end of values for local pile types.

## 3.1 Geotechnical Field Program

Following initial site investigations by others, seven test holes were completed by TREK near pile locations to further define soil stratigraphy and soil properties. The test holes were completed using a track mounted CME-850 geotechnical soils rig operated by Paddock Drilling Ltd. under the supervision of TREK personnel, including the author. The test holes were advanced using HQ core barrel and core samples were obtained along with split spoon samples where SPTs were completed. Temperature measurements were also obtained using a handheld digital thermometer at regular intervals on both core and split spoon samples. A visual assessment of ice content was completed on both core and split spoon samples to evaluate the presence of potentially permafrost affected soils. Samples were retained and shipped to Winnipeg for further classification and testing (see Section 3.2.1).

The upper 12 to 14 m, roughly to elevation 79 m, above sea level (asl), of these test holes were not sampled or logged as the target bearing elevation was below this depth and the properties of these layers were already well established (TREK, 2015). These depths correspond to below 75 m, asl for the Transformer Building and below 75 m to

72.5 m depending on pile location for the Converter Building. Additionally, due to the pre-boring activities which will be discussed below, the contribution from shaft adhesion was considered to be minimal and thus further establishing sub-surface conditions within this zone was not considered necessary at this point in the project.

## 3.2 Site Stratigraphy

The surficial soils were deposited during the Holocene era by the deep Tyrell Sea and consists of offshore glaciomarine sediments (clay, silt and minor sand) often overlaid by peat (Matile, et al, 2006). These glaciomarine sediments are underlain by clay till followed by limestone bedrock. The limestone bedrock was not encountered during the work. The site is also located in the zone of extensive discontinuous permafrost (50 to 90% coverage by area) with low (<10%) to medium (10 to 20%) ground ice content (Canada, 1995).

Prior to site development, the ground cover varied, consisting of low-lying organic areas with layers of peat and other areas with grasses, shrubs and trees. For site development, the organic materials were stripped and a compacted granular pad, on average 3 m thick but up to 5 m thick was placed to create a working platform. The granular pad was sourced from a nearby esker and was placed without processing (i.e. screening), consisting of a well graded sand and gravel with trace to some fines, trace cobbles and trace boulders. The working platform has an approximate elevation of 90 to 92 m asl and allowed for a flat, level surface for construction traffic and site development. Upwards of 2 m to 3 m of organics were removed during site

preparation, resulting in a final working platform elevation at or slightly above the previous grade.

Test hole information from on-site indicates that the upper glaciomarine sediments vary from approximately 2 to 6 m thick. The sediments consist of alternating layers of sand, silt, silty sand and sandy clay with individual thicknesses ranging from 1 to 5 m, being moist to wet and having consistencies of loose to compact.

The clay till was generally encountered at approximately 6 m below pad elevation. In general, the clay till is silty, contains trace sand, trace gravel and trace cobbles, is damp, hard and of low to intermediate plasticity. A detailed discussion of soil properties is presented in Section 3.2.1.

Frozen and non-frozen soils were observed in select test holes with measured soil temperatures ranging from -0.7$^{o}$C to 4.9$^{o}$C. Within the frozen soils, visible ice was present either as a coating on soil particles (Vc), inclusions (Vx) or as lenses (Vs) up to 25 mm thick. Well bonded frozen soil was also observed which did not contain visible ice or excess moisture (Nbn). The visible ice did not extend beyond 16.3 m below pad elevation (approximately 75 m, asl).

As the measured temperatures were near 0$^{o}$C where visible ice was present, degradation of the permafrost was considered likely given the change in ground cover and installation of piles. Degradation of the permafrost will result in ground settlements where a volume reduction occurs either from the phase change of water from a solid to a liquid or reduction in pore space from expulsion of liquid water (i.e.

following melt). Due to this settlement, shaft resistance within this zone could not be accounted for in design and down drag loads were considered (the down drag load was subtracted from the pile capacity in design however is not important during evaluation of load test data). Most importantly, it was critical that the helix be embedded below this zone such that any degradation of the permafrost did not result in settlement of the pile toe. In this regard, a zone of thaw sensitive soils (TSS), that is soils that will undergo settlement when thawed, was established for the project. This elevation was above 75 m, asl for a most of the project area and 72.5 m in select areas where deeper TSS were potentially present. Below this depth, any degradation of permafrost was considered to not result in settlement due to the low moisture content and relatively high density of the soils and thus not impact pile performance. Piles were thus to be founded below this depth.

### *3.2.1 Summary of Soils Testing Results*

The soils laboratory testing program was focused on the clay till as this was the layer in which the helices would be founded. The field and laboratory testing consisted of:

- SPTs (ASTM D1586) - 31
- Moisture Content Determination (ASTM D2216-98) - 60
- Atterberg Limits (D4318) - 20
- Grain Size Determination -Hydrometer Method (ASTM D422) - 20
- Bulk Unit Weight (ASTM D7263-21) - 15

- Unconfined, Undrained Compressive Strength (ASTM D2166) – 33

The SPTs resulted in refusal in all 31 tests (i.e. the SPT blow count was 100 or higher for two consecutive sets within 150 mm). In this regard, the SPT results should not be seen as meaningful, suffice to say they indicate the clay till is hard in consistency. The remaining soils testing results are summarized in Table 3.1 and graphically in Figure 3.1.

**Table 3.1 - Summary of Lab Testing in Clay Till**

| Test | | Count | Min | Average | Max |
|---|---|---|---|---|---|
| Moisture Content (%) | | 60 | 6 | 15 | 10 |
| Bulk Unit Weight (kN/m$^3$) | | 15 | 22.6 | 23.2 | 23.7 |
| Undrained Shear Strength (kPa) | | 33 | 311 | 902 | 1632 |
| Atterberg Limit | Plastic Limit | 20 | 11 | 13 | 15 |
| | Liquid Limit | | 14 | 23 | 28 |
| Grain Size | % Clay | 20 | 15 | 29 | 39 |
| | % Silt | | 25 | 40 | 48 |
| | % Sand | | 19 | 27 | 45 |
| | % Gravel | | 0 | 4 | 14 |

The moisture content is near, and sometimes even below, the plastic limit. This is consistent with the relatively high undrained shear strength measured in the UUC tests, albeit there is significant scatter in the results, ranging from roughly 300 kPa to 1600 kPa. There does not appear to be a trend with location or depth in relation to strength, i.e. the variability of undrained shear strength is spatially random. Further, the results of the moisture content testing and Atterberg limits didn't show an area

with wetter soils where shear strengths could be expected to be less. This finding is not all that surprising, as tills in Manitoba are known to be quite variable.

Soils were classified in general accordance with the United Soil Classification System (USCS). Classified by percent weight, the clay till would be described as a clayey sand and silt with trace gravel. However, based on plasticity (i.e. behavior), the clay till is classified as a low (CL) to intermediate (CI) plasticity clay and this is the distinction which was used throughout the project.

The groundwater elevation varied significantly across the site from as shallow as 3 m to as deep as 20 m below ground surface. The difference is likely attributed to drilling conditions where surface water runoff was ponded between the granular pad and less permeable clay till at a shallow depth, causing seepage into the pile hole and therefor a relatively shallow, interpreted groundwater level. The deeper levels likely correspond to the regional piezometric groundwater levels present in the clay tills, potentially influenced by the underlying bedrock. These measurements are based on short term observations following pre-boring activities during pile installation or upon completion of test holes and are not reflective of stabilized groundwater conditions. Given the variability, the groundwater levels are likely a representative of more permeable, water bearing layers that were exposed during prebore activities (i.e. the pad as discussed above). The selection of groundwater levels and the effect on pile capacity are discussed in Chapter 5.

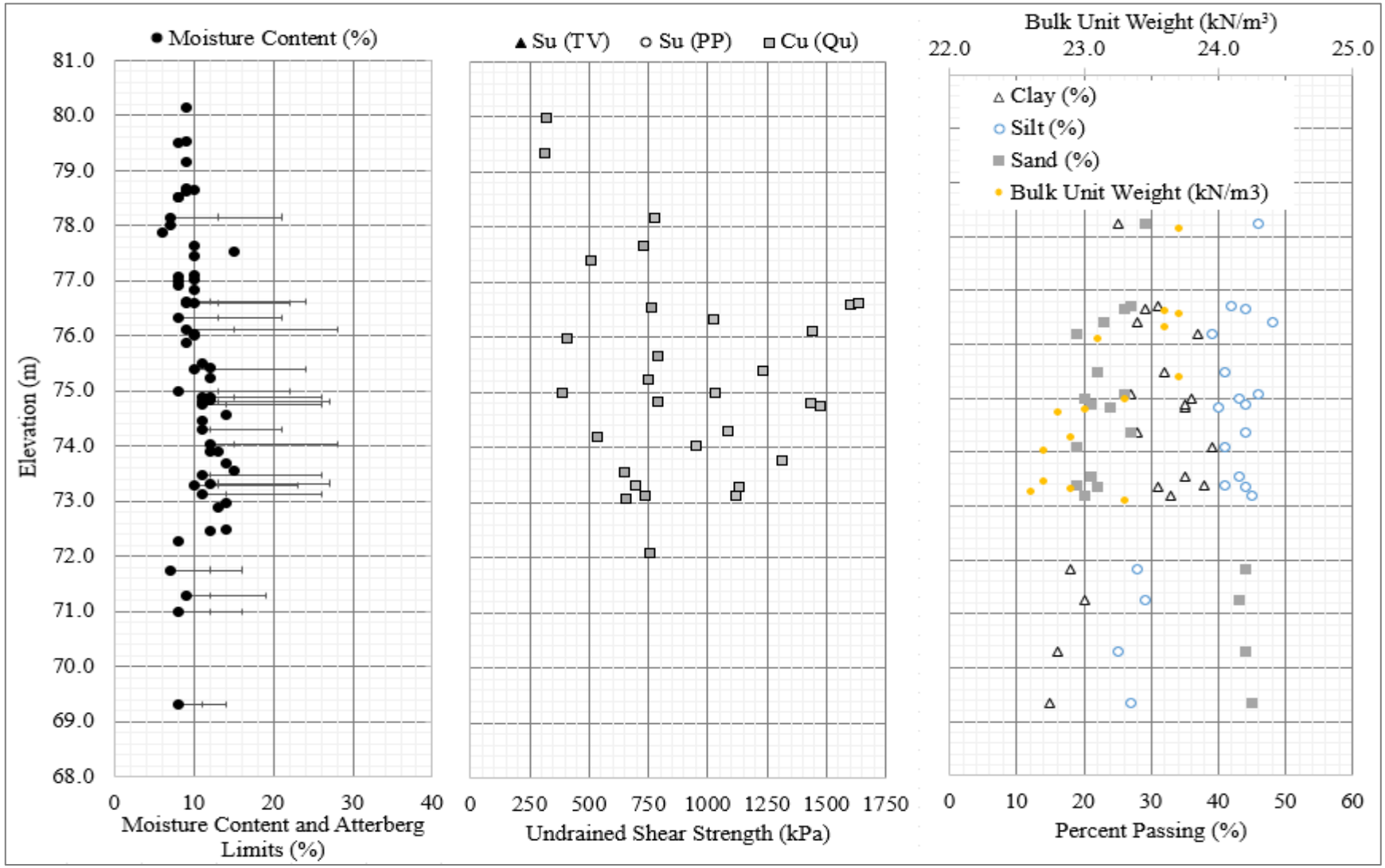


**Figure 3.1 - Soils Testing Summary**

## 3.3 Pile Installation

### *3.3.1 Helical Pile Description*

Piles consisted of an open-ended pipe with a 245 mm diameter shaft of nominal 13 mm wall thickness and a single 20 mm thick, 457 mm diameter helix with a 165 mm pitch. Pile sections were shipped in 6.1 m lengths and were pre-threaded such that they could be extended as required. Figure 3.2 illustrates the helical pile geometry.

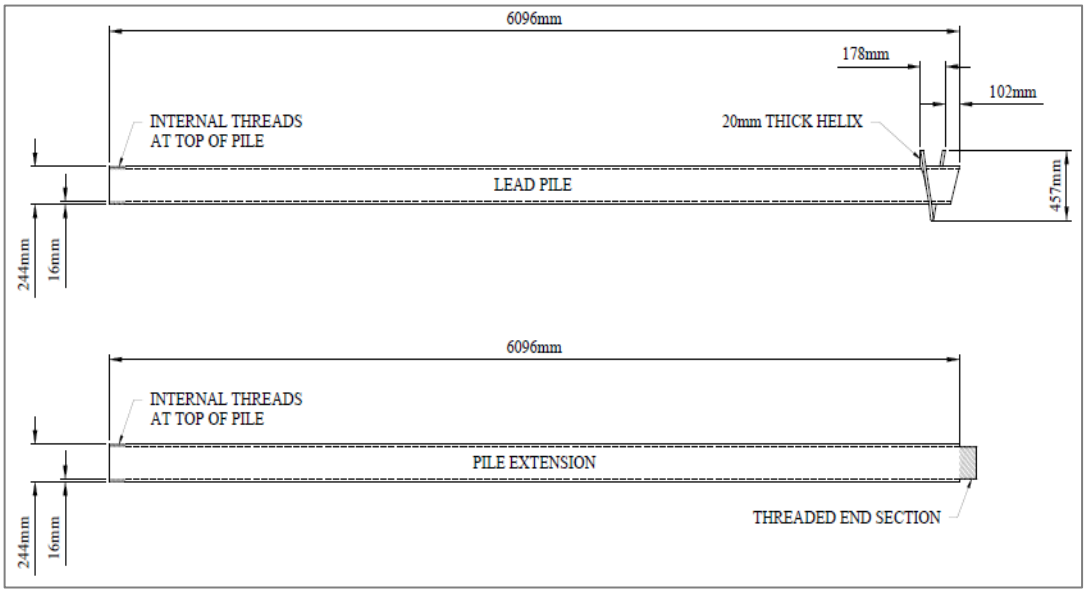


**Figure 3.2 - Production Pile Geometry**

### *3.3.2 Pile Installation*

The piles were installed from November 2015 to October of 2016 by Fourpoint Industrial Services Inc. (Fourpoint) and all pile installations were monitored by TREK Geotechnical Inc. (TREK). TREK provided field personnel and technical support to the Geotechnical Engineer of Record, DRI. The helical piles were provided

by Fourpoint and manufactured in Texas, USA. Static load tests were performed by Mortenson Canada Corporation (Mortenson) with the support of TREK. Survey support during construction was provided by Allnorth Consultants Ltd. (Allnorth).

Prior to installation, the helical pile location was marked with a ground pin and two offset pins 0.5 m from the pile were also installed to assist the ground crew in maintaining pile location. The pile location was then pre-bored using American Piling Equipment Ltd's (APE) Polar Penetrator™ to the target pre-bore depth of either 75 m asl or 72.5 m asl (i.e., below the TSS). The Polar Penetrator is a pneumatic tool with 305 mm diameter drive head, designed to pass through cobbles, boulders and frozen soils. The pre-boring was completed to reduce the risk of piles not advancing to the target depth. Piles were then installed through the pre-bored hole using APE's HD-200 hydraulic drive head affixed to a CAT374D excavator until installation criteria were met (see Section 3.3.3). The HD-200 has a maximum rated torque of 200,000 ft-lbs (271 kN-m) and was calibrated prior to pile installation.

During installation, TREK recorded torque measurements at 1 m intervals and observed pile advancement relative to helix pitch and rotation. Generally, an abrupt increase in torque was observed when the helix advanced past the pre-bored hole. Following refusal, plumbness was recorded in two directions and piles that were greater than 2.0% from vertical were identified for further review by the structural engineer. Other measurements were also recorded such as embedment depth, embedment below pre-bore, stick up, depth of soil plug and if water was present within the pile. In general, pile embedment ranged from 16.5 m to 20.9 m with an

average of 18.5 m. Torque at refusal was generally between 170 kN-m and 246 kN-m, however was as low as 46 kN-m on one occasion and as high as 286 kN-m.

### *3.3.3 Installation Criteria*

To ensure project specifications were met and reduce the risk of piles not meeting performance requirements, a detailed pile installation criterion was established for the pre-bore and pile installation. The installation criteria are discussed below.

Pre-bore:

The pre-bore was advanced to not less than the design depth of the TSS using a 305 mm diameter Polar Penetrator™ drilling tool.

Helical Pile Installation:

Following completion of the pre-bore, a helical pile was installed within the clay till until the helix met the following embedment criteria:

- Top of the helix is completely embedded below the bottom of the pre-bore, without augering or churning. The primary criteria is to achieve embedment without augering or churning. If the pile achieves this condition the underside of the helix will be in full contact with undisturbed soil.

- Torque refusal: The piles should be installed to meet the primary criteria (i.e. embedment without augering or churning) while ensuring that the torque begins to increase from the bottom of the pre-bore hole to the point where installation is halted once the pile embedment is achieved. The pile could be installed deeper provided the

pile is still advancing downward with rotation at a rate equivalent to the helix pitch. An increase in torque (minimum 15 kN-m) should be observed below the pre-bore depth as a confirmation that the pile has been installed into intact soils below the bottom of the pre-bore hole.

- Re-torque criteria: all piles were re-torqued approximately 48 hours after initial installation. Piles that advance more than 50 mm during re-torqueing were re-torqued again after an additional 48-hour period had passed. The re-torqueing continued until the re-torqueing criteria is achieved.

The annulus between the helical pile shaft and the pre-bore wall (at the surface) was backfilled loosely with clay cuttings from the prebore process, without compaction. After the helical pile installation was reviewed by the project team and approved, the pile top was cut to its design elevation and a pile cap installed.

### *3.3.4 Load Testing Program*

Sixty-eight axial compressive load tests were completed as part of the overall program. This included 6 instrumented load tests (4 during pre-production and 2 on non-production piles during production) and 62 non-instrumented load tests on production piles. Of the 62 production pile tests, 3 had issues with the load cell and the results are not considered reliable. An additional 2 had issues with the deflection dial gauges. In this regard, 57 of the 62 tests were included in the analysis. For the pre-production tests (instrumented), the raw load test data including the load per time

increment was not available and in this respect they are only included in the consideration of shaft adhesion.

Eight re-tests were also performed to evaluate atypical performance during the initial test or to adjust the load frame due to safety concerns. In the cases of atypical performance, the piles were generally re-driven to ensure no augering or churning at the pile bottom (i.e. the pile underwent the retorquing program and the pile was then retested). Piles were selected for load tests randomly or to confirm satisfactory performance when select aspects did not meet the installation criteria (e.g. minimum embedment or target increase in torque were not achieved). The results of initial tests and re-tests are shown for clarity, and retests always showed a stiffer pile response.

Following installation and selection as a candidate for load testing, the pile top was cut and a 50 mm thick steel plate was welded to the surface to support the jack. Loads were applied by a single 500-ton EnerPac double-acting ram in conjunction with an oil-filled gauge and hydraulic pump and loads were controlled via a hand operated switch. Loads were measured with a Geokon 3000-series load cell and the hydraulic gauge provided a backup reading to the load cell. The load cell and ram were calibrated prior to being shipped to site. A reaction frame, consisting of 16 helical piles and four steel H-beams were installed to support the test pile and jacking forces. Pile head deflection was measured by four dial gauges positioned on opposing quadrants of the steel plate which were mounted on magnetic bases affixed to two reference beams. The reference beams were each supported by rebar driven into the subgrade. The reference beams were located 1.5 m to 1.8 m from the nearest reaction

frame pile and 1.2 m to 1.5 m from the test pile. As this distance may be within the potential zone of influence of ground movement cause by pile deflection, tell-tale markers and independent survey of reference beams relative to local benchmarks was also completed. Photographs of the test pile set-up are shown in Figure 3.3 and Figure 3.4.

**Figure 3.3 - Typical Load Test Set Up**

**Figure 3.4 - Load Cell and Dial Gauge Set Up**

The pile load test was performed according to ASTM D1143 - Quick Test Method with the following exceptions:

- Distance between the reaction frame piles and the test pile was less than the minimum specified distance of 2.5 m for 6 of the 16 support piles. It is not anticipated this had a significant impact on the load test as reaction piles were installed to a relatively shallow depth when compared to the embedment of the test pile and loose backfill surrounding the test pile.

- The distance between the test pile and the reference beams was less than the minimum specified distance of 2.5 m. To mitigate the risk of ground movement affecting displacement readings, the reference beams were surveyed relative to an

independent benchmark at various load increments to confirm negligible movement occurred.

The termination criteria for a majority of the pile load tests were either a maximum load of 2680 kN (double the ULS load of 1340 kN) or about 25 mm of head displacement (whichever occurred first). For piles corresponding to more lightly loaded foundation elements, the ULS and SLS capacities were 1021 kN and 817 kN, respectively and these piles were either loaded to approximately 25 mm head displacement or 2000 kN (roughly double the ULS load). The pile was then unloaded and deflections measured as the pile rebounded. A summary of general production pile load test data is provided in Table 3.2.

**Table 3.2 - Pile Load Test Summary [(1)]**

| Load Test No.[(2)] | Pile No. | Max Load (kN) | Defl at Max Load (mm) | Pile Length (m) | Embedment (m) | | Torque (kN-m) | |
|---|---|---|---|---|---|---|---|---|
| | | | | | Below Grade | Below Prebore | End of Install | Re-Torque |
| 1 | 1073 | 2651 | 26.20 | 19.26 | 18.60 | 0.30 | 101 | 101 |
| 2 | 1062 | 2002 | 26.08 | 19.50 | 18.90 | 0.40 | 43 | 43 |
| 3 | 7076 | 2135 | 25.56 | 19.80 | 19.30 | 0.70 | 142 | 142 |
| 4 | 7010 | 1739 | 26.65 | 20.00 | 19.40 | 0.70 | 72 | 72 |
| 5 | 1063.2 | 2002 | 25.42 | 19.49 | 18.80 | 0.12 | 130 | 130 |
| 8 | 5008 | 2002 | 25.60 | 18.35 | 17.60 | 1.24 | 72 | 246 |
| 10 | 2023 | 2097 | 27.37 | 18.45 | 17.65 | 0.30 | 119 | 119 |
| 11 | 2094A | 1717 | 11.79 | 18.73 | 18.56 | 1.21 | 43 | 246 |
| 13 | 4128 | 2002 | 24.22 | 17.70 | 16.92 | 0.64 | 142 | 142 |
| 14 | 6058 | 2002 | 26.06 | 21.41 | 20.61 | 0.61 | 188 | 188 |
| 15 | 2119 | 1737 | 24.86 | 18.69 | 17.89 | 1.12 | 119 | 159 |
| 16 | 1038 | 1735 | 25.79 | 21.21 | 20.07 | 0.17 | 72 | 72 |
| 17 | 2046 | 2224 | 22.42 | 18.92 | 18.12 | 1.62 | 101 | 188 |
| 21 | 2123 | 1868 | 29.00 | 17.99 | 17.19 | 0.94 | 142 | 246 |

| | | | | | | | | |
|---|---|---|---|---|---|---|---|---|
| 22 | 4121 | 2002 | 18.64 | 19.58 | 18.78 | 1.38 | 182 | 246 |
| 23 | 2016 | 1334 | 25.04 | 17.70 | 16.91 | 0.64 | 113 | 72 |
| 24 | 3050 | 1600 | 33.35 | 18.44 | 17.64 | 1.06 | 55 | 124 |
| 25 | X128 | 2002 | 16.80 | 18.80 | 18.18 | 0.76 | 261 | 232 |
| 26 | X172 | 2002 | 19.00 | 18.70 | 18.15 | 0.65 | 289 | 203 |
| 27 | 4028 | 2002 | 17.30 | 18.30 | 17.73 | 0.30 | 159 | 260 |
| 28 | 4011 | 1868 | 24.60 | 17.40 | 16.84 | 0.30 | 179 | 78 |
| 30 | 6013 | 1468 | 33.20 | 18.30 | 17.15 | 0.90 | 93 | 188 |
| 31 | 5052 | 1468 | 29.60 | 18.35 | 16.77 | 0.66 | 162 | 246 |
| 32 | 6078 | 1735 | 30.50 | 18.90 | 18.23 | 0.83 | 220 | 130 |
| 33 | 5016 | 1735 | 27.40 | 18.35 | 17.20 | 0.95 | 174 | 153 |
| 34 | 6112 | 1868 | 24.00 | 19.44 | 18.84 | 1.16 | 185 | 159 |
| 35 | 6040 | 1735 | 18.60 | 19.53 | 18.93 | 1.75 | 232 | 246 |
| 36 | 5033 | 2002 | 24.10 | 19.77 | 18.91 | 1.41 | 232 | 130 |
| 37 | 5017.2 | 1882 | 17.40 | 18.06 | 17.50 | 1.40 | 246 | 220 |
| 38 | 5014 | 1468 | 34.80 | 19.56 | 17.05 | 0.80 | 174 | 133 |
| 39 | X166 | 1735 | 12.00 | 18.73 | 18.67 | 1.05 | 174 | 130 |
| 40 | X730 | 2002 | 28.00 | 19.81 | 18.71 | 1.19 | 246 | 220 |
| 41 | X315 | 1868 | 19.68 | 19.26 | 17.77 | 0.47 | 174 | 261 |
| 42 | X360 | 1735 | 34.90 | 22.87 | 20.69 | 3.19 | 203 | 159 |
| 43 | X375 | 1340 | 42.00 | 21.62 | 18.05 | 0.74 | 203 | 133 |
| 47 | X778 | 1468 | 47.00 | 18.36 | 17.99 | 0.69 | 188 | 148 |
| 48 | X370 | 2002 | 12.50 | 18.75 | 18.29 | 0.59 | 289 | 246 |
| 49 | X318 | 1468 | 48.50 | 20.14 | 19.64 | 2.29 | 174 | 174 |
| 50 | X323 | 2002 | 26.00 | 18.72 | 17.85 | 0.40 | 261 | 217 |
| 51 | X537 | 2002 | 18.10 | 21.43 | 19.98 | 2.43 | 289 | 289 |
| 52 | X578 | 1588 | 39.10 | 19.16 | 18.16 | 0.74 | 174 | 133 |
| 53 | X780 | 1601 | 47.49 | 18.67 | 18.12 | 0.81 | 188 | 159 |
| 54 | X777 | 1468 | 25.60 | 19.60 | 18.65 | 0.90 | 169 | 130 |
| 55 | X745 | 2002 | 18.19 | 17.72 | 17.94 | 0.36 | 318 | 203 |
| 56 | X739 | 2002 | 19.52 | 19.16 | 18.50 | 1.04 | 203 | 159 |
| 57 | X781 | 2002 | 22.52 | 18.77 | 18.17 | 0.89 | 261 | 217 |
| 58 | X469 | 2002 | 12.75 | 19.04 | 18.54 | 1.05 | 261 | 234 |
| 59 | X406 | 2002 | 25.50 | 19.05 | 18.51 | 1.10 | 203 | 159 |

| | | | | | | | | |
|---|---|---|---|---|---|---|---|---|
| 60 | X447 | 2002 | 16.80 | 18.51 | 17.89 | 0.48 | 174 | 130 |
| 61 | X581 | 2002 | 14.30 | 18.69 | 18.19 | 0.58 | 246 | 200 |
| 62 | X402 | 2002 | 20.00 | 19.71 | 19.03 | 1.72 | 261 | 223 |
| 63 | X545 | 2002 | 19.97 | 19.69 | 18.69 | 1.17 | 203 | 130 |
| 64 | X515 | 2002 | 24.60 | 19.91 | 18.91 | 0.43 | 174 | 174 |
| 65 | X550 | 1601 | 30.58 | 19.96 | 19.46 | 1.02 | 142 | 188 |
| 66 | X434 | 2002 | 19.80 | 20.21 | 19.42 | 2.01 | 232 | 188 |
| 67 | X737 | 2002 | 18.90 | 19.66 | 19.26 | 1.18 | 261 | 217 |
| 68 | X734 | 1868 | 27.40 | 19.79 | 19.14 | 0.50 | 174 | 145 |

*Notes:*
*1 – Tests 6 and 7 are non-production, instrumented tests. Test #29 was never completed. Tests 44, 45 and 46 were uplift tests. Tests 18, 19 and 20 are not reliable due to a malfunctioning load cell. Test 9 and 12 are not reliable due to malfunctioning dial gauges.*
*2 – Pile load test #29 was never completed due to a numbering error in the load test tracking*

A summary of the pile load tests which were not used in the analysis, along with the corresponding rationale, is provided in Table 3.3.

**Table 3.3 - Excluded Load Tests**

| Load Test No | Pile ID | Rationale for Excluding Results |
|---|---|---|
| 9 | 5036 | Dial gauge malfunction – deflection measurements not reliable |
| 12 | 3004 | |
| 18 | X114 | Load cell malfunction – load readings not reliable |
| 19 | X180 | |
| 20 | 2066 | |

3.3.4.1 Instrumented Load Tests

Instrumented axial loads tests were completed on four preproduction piles and two sacrificial piles during production. The length of the test piles varied however all were the same dimensions as the production piles as noted above. The pile location was pre-bored to a predetermined depth and then the pile installed beyond the pre-bore to the installation criteria described above, with the exception of the two tests

during production. For these tests, the pre-boring was completed to over 5 m below the helix depth. The intent of these tests was to maintain an open bottom below the helix, allowing for a more accurate assessment of shaft adhesion (as the end bearing would be minimized). The instrumented pile test IDs, pile lengths, pre-bore depths, embedment depths and strain gauge locations are shown in Table 3.4.

**Table 3.4 - Installation Summary for Instrumented Tests**

| Test ID | Pile Length (m) | Prebore Depth (m) | Embedment Depth (m) | Strain Gauge Locations, Pairs (m) |
|---|---|---|---|---|
| HP2-3 | 21.4 | 20.7 | 20.9 | 2.6, 6.1, 9.6, 13.1, 16.5, 20.0, 20.9 |
| HP2-6 | 20.9 | 20.1 | 20.4 | 0.5, 2.6, 6.1, 9.6, 13.1, 16.5, 20.0, 20.9 |
| HP8-2 | 18.6 | 14.9 | 18.3 | 0.1, 2.9, 5.5, 9.0, 12.4, 15.0, 18.6 |
| HP8-5 | 19.4 | 17.2 | 18.8 | 0.2, 3.4, 6.8, 10.3, 13.7, 15.5 |
| Test #6 | 20.40 | 18.98 | 24.07 | 5.20<br>11.30<br>17.80 |
| Test #7 | 20.50 | 19.20 | 23.94 | 4.37<br>10.46<br>16.56 |

For the preproduction tests, eight Geokon 4200 Series Concrete Embedded Vibrating Wire Strain Gauges (VWSGs) were installed within the piles at regular intervals to measure load transfer along the pile. The VWSGs were affixed to PVC piping (shown below in Figure 3.5) and lowered into the pile and the pile was then grouted to surface.

**Figure 3.5 - Typical Strain Gauge Installation**

For the sacrificial pile tests, three pairs of RST VWSGs were affixed to the inside of the piles via welded brackets. These piles were not grouted in an attempt to obtain a more accurate reading of the shaft adhesion as the steel-grout-interaction would not have to be accounted for. Additionally, a measurement was taken to ensure an open end was present at the pile bottom, confirming that minimal resistance was being provided by the pile toe. For Test #6, the VWSGs were over-tensioned during placement which may have influenced their readings. The extent of this influence could not be determined, however based on discussion with RST, the readings would not be off by more than 1 to 10% of their usual values. During Test #7 one of the strain gauges at 10.64 m began giving erroneous readings and therefor the data from this depth was not included in the analysis.

The load testing procedure for the instrumented tests was the same as the production tests described above. Strain gauge readings were taken with either data loggers or a

VW readout box at regular intervals throughout the test and at the end of each load increment.

## 3.4 Chapter 3 Discussion

Over 1,100 helical piles with shaft diameters of 244mm, lengths of 17.3 m to22.9 m and helix diameters of 457 mm were installed into hard clay tills. Test hole information shows that the site stratigraphy consists of a 3 to 5 m granular pad followed by glaciomarine sediments overlying clay tills. The undrained shear strength of the clay varied significantly across the site. Piles were installed with conventionally available construction equipment powered by hydraulic drive heads.

The pile installation was facilitated by preboring the pile location to below the anticipated depth of thaw sensitive soils. This approach was designed to minimize shaft adhesion as a result of the degradation of suspected permafrost. Throughout installation, 68 axial compressive load tests were completed, however only 57 of these tests provide results usable for the analysis. Additionally, 6 instrumented tests were completed to assess the contribution from shaft adhesion.

# Chapter 4: Theoretical Capacity of Piles

## 4.0 Theoretical Capacity of Piles

The theoretical capacity of piles is separated into the Individual Bearing Method (IBM) and Cylindrical Shear Method (CSM). Either of the methods may or may not include contribution from skin friction. The theoretical capacity for the piles installed are calculated based on the methods discussed in Section 2.0 and the selection of input parameters is discussed based on the information review and field data. Capacity to Torque Correlations (CTCs) are also provided using a range of $K_T$ factors and torque measurements from the field data.

## 4.1 Individual Bearing Method

The theoretical capacity of the piles was estimated using Equations 2.4 and 2.5 presented by Tappenden and Sego (2007) and Equation 2.7 presented by Layni-Bennet and Deng (2018). These equations are shown again below:

$$Q_{ult} = A_b(N_c s_u + \gamma' H) + \pi d H_{eff}\, s_u \alpha \qquad \text{(Equation 2.4 and 2.5)}$$

$$Q_{ult} = N_t s_u A_b n + \alpha s_u (\pi d H_{eff}) \qquad \text{(Equation 2.7)}$$

Side by side, the only difference between these equations is the consideration of embedment depth by Tappenden and Sego and the selection of the value for $N_c$ or $N_t$.

Inclusion of the shaft resistance component requires additional consideration for this project beyond simply applying an adhesion factor (α). Regardless of the loose compaction of backfill within the pre-bore to pile annulus, there is still some soil-pile

contact and thus some amount of shaft resistance would have been developed. This shaft resistance will be significantly less than typical adhesion factors would suggest and the selection of an appropriate $s_u$ value would be erroneous given the disturbed nature of the backfill. To more accurately represent the conditions in which the piles were installed, the calculation of shaft resistance was not included in the summation of the calculated ultimate capacity ($Q_{uc}$) but rather is discussed separately based on the results of the instrumented pile load tests. Through these testing results it will be demonstrated that shaft adhesion is relatively small compared to the ultimate capacity of the pile.

### *4.1.1 **Input Parameters***

The selection of the bearing capacity factor and undrained shear strength will play the largest role in determining the theoretical capacity. The value of $N_c$ for an undrained analysis is typically assigned a default value of 5.14, however $N_c$ was originally developed to evaluate the capacity of a long strip footing acting on the surface of soil represented as a homogeneous half-space. Several factors (denoted as $\zeta$) accounting for the rigidity of the soil, foundation shape, inclination, foundation tilt, surface inclination and foundation depth have been developed to adjust $N_c$ based on project specific conditions. These factors are presented in detail in Poulos (2001) and have been calculated based on project conditions as provided in Table 4.1.

**Table 4.1 - Calculation of Modified $N_c$ Factor**

| Nc Factor | Parameter | Value | Comments |
|---|---|---|---|
| $\zeta_{cr}$ = | Rigidity | 1.10 | B/L = 1 |
| $\zeta_{cs}$ = | Shape | 1.19 | |
| $\zeta_{ci}$ = | Inclination | 1 | no inclination (1) |
| $\zeta_{ct}$ = | Foundation Tilt | 1 | no foundation tilt |
| $\zeta_{cg}$ = | Surface Inclination | 1 | no surface inclination |
| $\zeta_{cd}$ = | Depth | 1.20 | |
| **$N_c\zeta$ =** | | **8.11** | |

*1 – See discussion below regarding effect of tilt*

When accounting for the soil rigidity, foundation shape and depth, an increase in $N_c$ is calculated from the default of 5.14 to 8.11. Although there is some inclination of the helix, the foundation tilt term, $\zeta$ ct, is equal to 0.99 and therefore was not considered in the analysis. $N_t$ is assigned a value of 9 based on the CFEM (2006) having a helix diameter of less than 0.5 m (457 mm). In this regard, Equations 2.4 and 2.7 will give very similar results, with the exception of the $\gamma$'H term included in Equation 2.4. Equation 2.7 will give the same results for all piles as $N_t$, $s_u$ and $A_h$ do not vary. The range of values from 5.14, which should be considered a low bound, up to 8.11 is within the range of values presented in the literature, with the exception of Elsherbiny Z.H. and El Naggar (2013) who recommended $N_c$ be increased to 12.

A saturated unit weight of 13.5 kN/m$^3$ along with the pile embedment was used in the calculation of the $\gamma$'H term. The consideration for using the effective unit weight of the clay till was deemed reasonable as the depth of the groundwater table, where observed, was generally above the embedment depth and in some instances was a

shallow as 3 m. In the instances where the groundwater table is below 3 m, for sake of argument even 10 m lower, this would only account for a difference in capacity of only 5% to 10% of the ultimate value. In this regard, accounting for the variability in groundwater elevation, even with the large differences from 3 to 20 m was considered marginal. Similarly, the variation in embedment depths between piles results in very little difference in ultimate capacity between the piles in Equation 2.4.

The CFEM (2006) states that for Limit States Design (LSD), which is the design framework most jurisdictions operate under, that selection of a nominal or characteristic value is generally the mean undrained shear strength of soil, $s_u$ or a cautious estimate of the mean.

As noted by Hoyt and Clemence (1989), the interpretation of these properties involves engineering judgement and the accuracy and precision of the 'algorithm' used to predict capacities must take that into account. In this regard, obtaining reliable strength data is key in producing accurate predictions of pile capacity. A challenge from the practical side is balancing the costs of obtaining a sufficient amount of reliable strength data (more reliable data can be considerably more expensive) with the level of risk associated with the project. Obtaining sufficient data is important as the designer needs to be confident the design values used are representative of the in-situ soil conditions.

In this regard, a relatively simple statistical analysis was undertaken showing the cumulative distribution function of the undrained shear strength testing results to

evaluate an appropriate value. The data was assumed to be normally distributed and the mean $s_u$ as measured by undrained, unconfined compression tests, is shown (i.e. the $s_u$ has a 1 in 2 chance of being at least that high). Additionally, the value required to meet the unfactored ultimate capacity, based on average embedment depth and $N_c$ of 8.11 is also presented. Providing a probability for these values gives a framework to justify the selection of a mean value, or a cautious estimate thereof. This analysis is shown graphically in Figure 4.1.

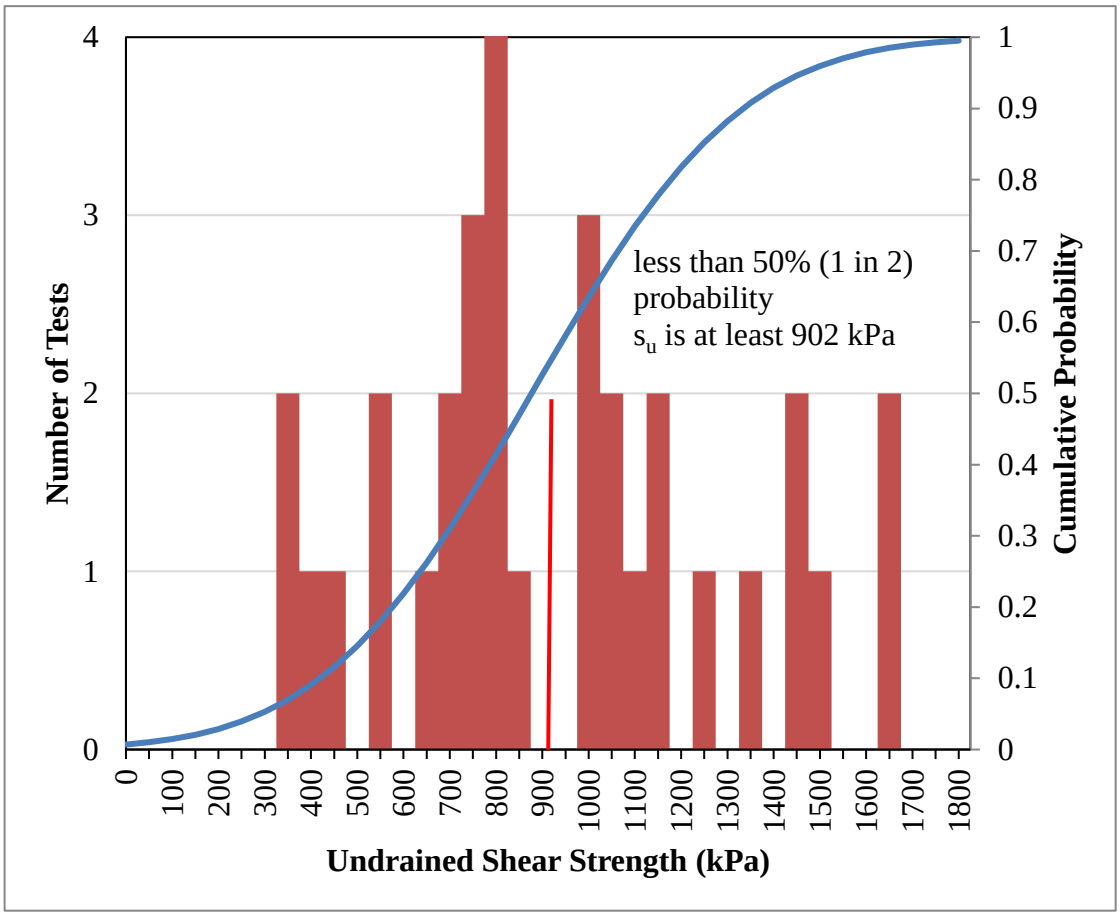


**Figure 4.1 - Cumulative Distribution of $s_u$**

The mean value for $s_u$ of the 33 tests is 902 kPa (Std Deviation = 347 kPa) which was used in the analysis. The $s_u$ required to meet the ultimate (unfactored) pile capacity of 2680 kN, using an $N_c$ of 8.11, is 915 kPa (essentially the same as the mean). In this regard, using the mean would result in a capacity slightly less than the required unfactored, ultimate capacity, adding credence to the idea a cautious estimate should be selected. Little guidance is provided on what criteria define a cautious estimate, for example 10% less than the mean or within one standard deviation. In this regard, the mean was selected for calculation purposes and recommendations for a cautious estimate are provided in Section 5.0.

## 4.2 Theoretical Ultimate Capacity

During preliminary design it is not common to have knowledge of load test data. Therefore, adjusting input parameters based on the load test results at this stage was not considered appropriate. The results of the theoretical capacities calculated from Equation 2.4 (denoted as $Q_{uc}$) using the mean $s_u$ at project specific $N_c$ are presented in Figure 4.2.

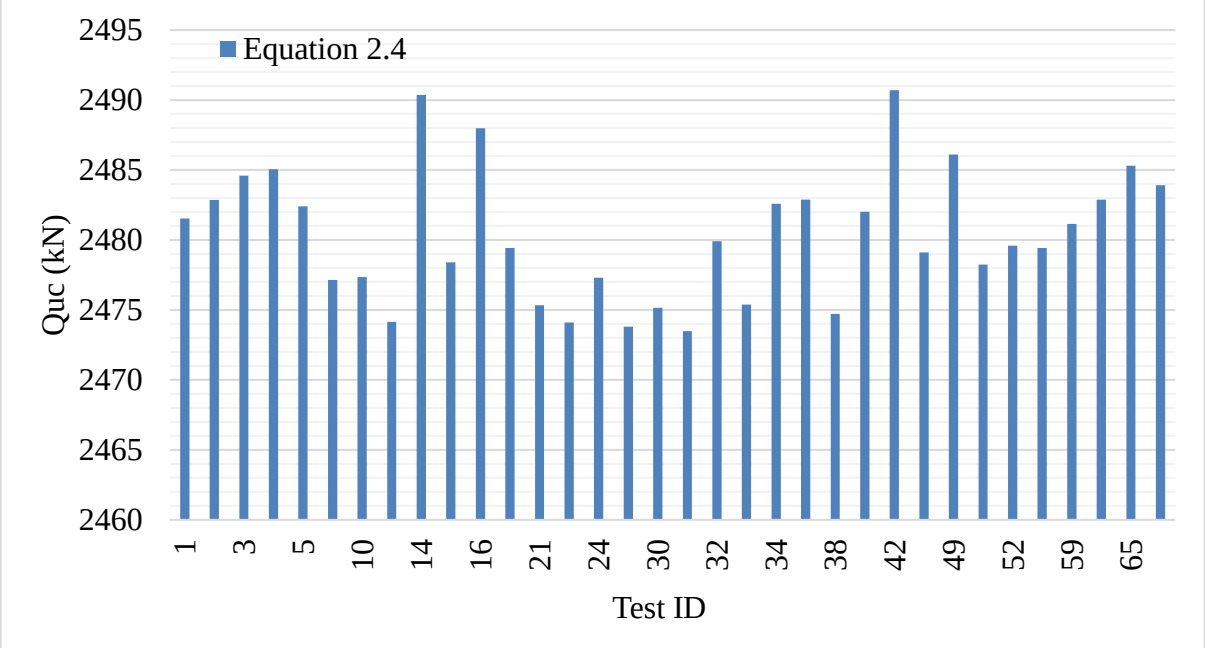


**Figure 4.2 - Theoretical Ultimate Capacity**

As shown above, the range in capacities from Equation 2.4 are small, from 2470 kN to 2490 kN with an average of 2480 kN. The small difference can be attributed to the embedment depths being similar for all piles. Equation 2.7 resulted in an ultimate capacity of 2663 kN, the higher capacity is due to the higher bearing capacity factor ($N_c$ of 8.11 vs $N_t$ of 9). To further assess the potential range of calculated ultimate capacities that could be reasonably defended in design, the following additional values were used:

- $N_t$ 6.2 to 7.7 - Layni-Bennet and Deng (2018)
- $s_u$ =545 kPa, which is 1 standard deviation from the mean.

The use of low bound $N_c$ values and an $s_u$ of 545 kPa results in a calculated pile capacity with an average of 1190 kN. Using an $N_c$ of 7.7 increases the average to

1460 kN. Designers should be hesitant to use these low bound values as it will likely result in increased cost to their clients. This shows how the selection of input values for theoretical calculations can have a significant impact on the design capacity, which alone is a good reason to use load testing data to refine theoretical predictions, or at least account for a large margin of error (e.g. lower reduction factors). Comparison of these calculations with load test results is presented in Chapter 5.

### *4.2.1 Shaft Adhesion*

The values presented above do not include a contribution from shaft adhesion. Using Equation 2.5, an $H_{eff}$ of 17.9 m (average embedment minus 1 helix diameter), an adhesion factor of 0.3 estimated from Figure 18.1 in CFEM (2006) and the mean $s_u$ of 902 kPa, the contribution from shaft adhesion would be on the order of 3700 kN (much greater than calculated from end bearing). As the pile shaft was not in contact with the surrounding soil, the use of an intact shear strength is not reasonable. The backfill material was essentially loose, small pieces of sand and gravel backfill from the pad or clay till (on average 25 mm or less) that were blown out of the hole during preboring. In this regard, it makes more sense to evaluate shaft adhesion using methods employed for cohesionless soils. The CFEM provides the following equation:

$$q_s = \beta \sigma'_v \qquad \text{Equation 4.1}$$

Where β is a combined shaft resistance factor and $\sigma'_v$ is the average effective stress at the pile depth. The CFEM (2206) recommends a β value 0.2 for silts and loose sands

around cast in place piles, which given the backfill method is appropriate. From Equation 4.1 and using half the average pile embedment to determine the effective stress, a groundwater level of 3 m and $H_{eff}$ from above, a shaft adhesion on the order of 400 kN is calculated. Instrumented load testing results will show that even this low-bound estimate is an overprediction of the actual shaft adhesion.

## 4.3 Torque to Capacity

The pile capacity was estimated using the values proposed by Harnish (2015), CFEM (2006) and Tappenden (2007) from Equation 2.9. This value is denoted as $Q_{ut}$. The $K_T$ value of 23 was used from the CFEM, which is similar to that proposed by Lanyi (2017). The relationship proposed by Perko (2009) was developed for pile diameters up to 271 mm and produces a small $K_T$ value of 5.1 therefore was not considered in the analysis. Additionally, the maximum interpreted capacity from the load tests (described in the follow chapter) were used to back calculate a project specific $K_T$. The Capacity Torque Correlations (CTC) capacities are shown in Figure 4.3 and ranged from 396 to 7501 kN. This figure is presented to illustrate the immense scatter in the data.

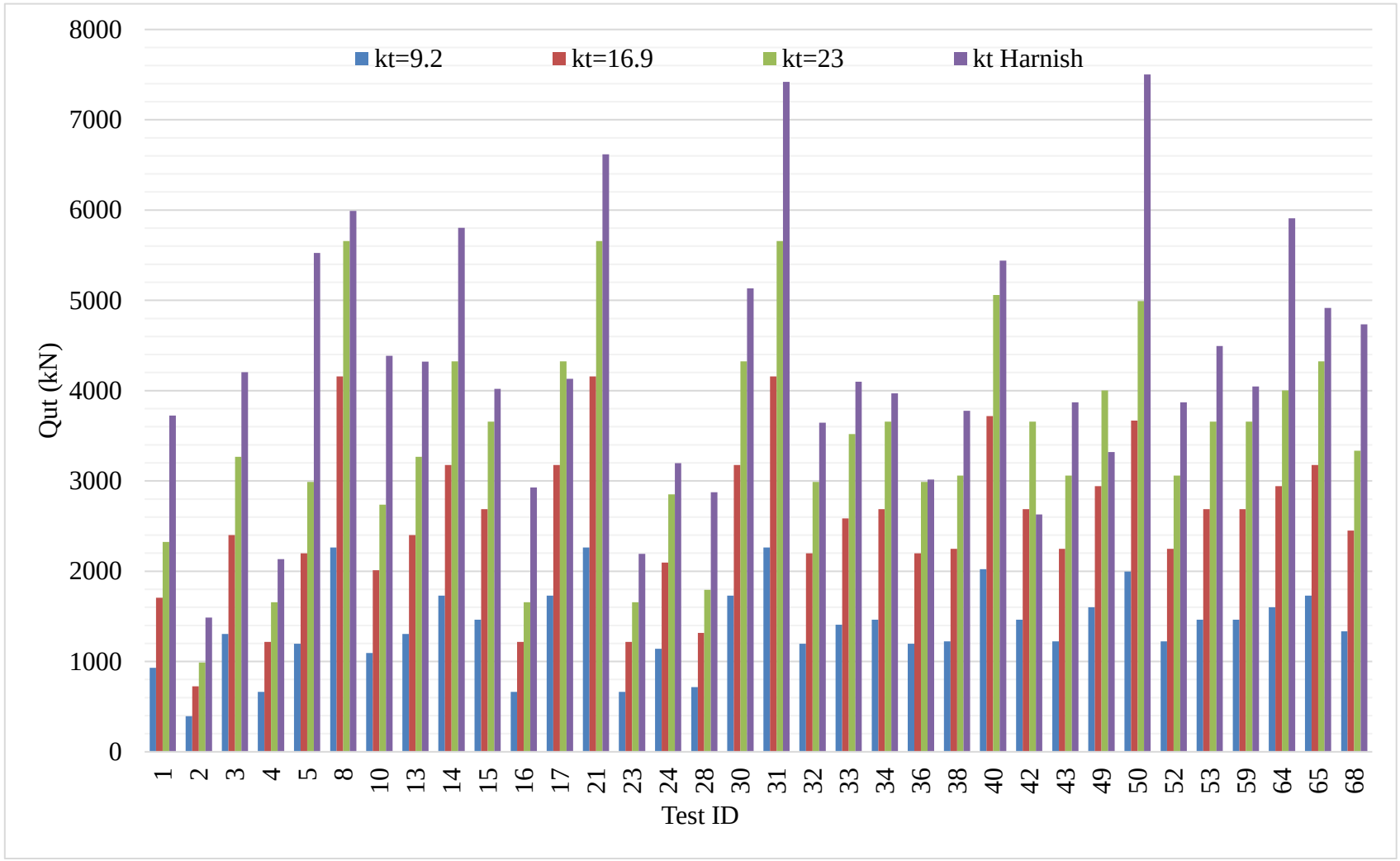


**Figure 4.3 - CTC Capacities**

The relationship between the calculated capacity and $K_T$ factor is obvious, with the higher capacities associated with the higher $K_T$ factors. The above plot is shown to display the range of capacities and how variable CTC methods can be without applying some judgement.

To determine if there was a relationship between torque and ultimate capacity, the maximum torque and ultimate capacity were also plotted on the abscissa and ordinate, respectively, as shown in Figure 4.4.

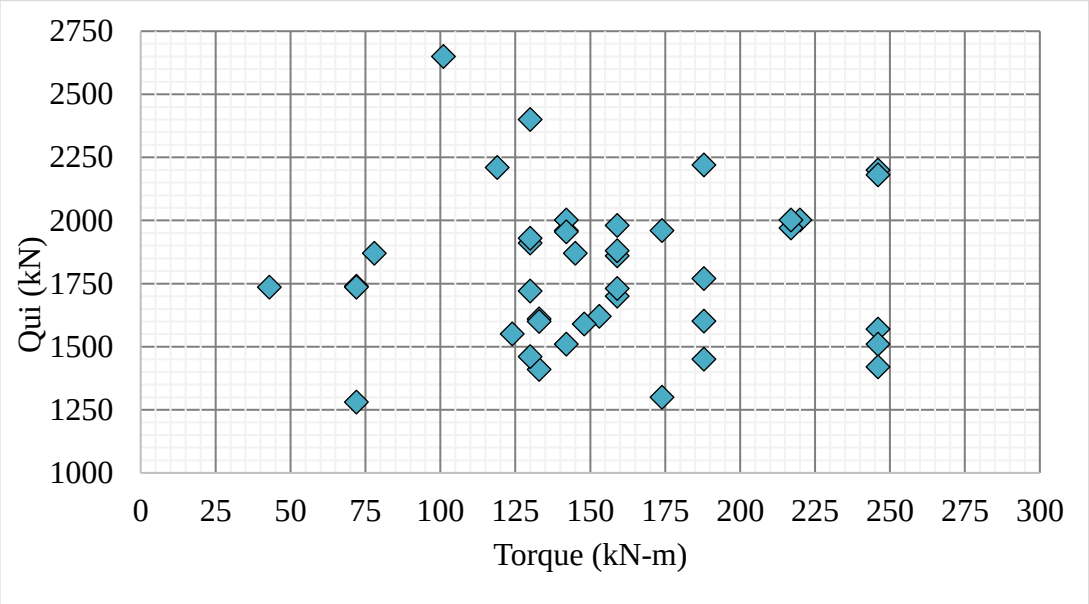


**Figure 4.4 - Torque vs Ultimate Capacity**

Visually it is apparent there is no clear trend between capacity and torque. In the absence of a project specific, parametric analysis of $K_T$ factor (e.g. this could consider embedment depth, embedment beyond prebore, pile diameter, etc.) a project specific $K_T$ value could be calculated by dividing ultimate capacity by torque at refusal. This exercise is discussed in the succeeding Chapter. Further, based on the above results,

using default values for $K_T$ is not recommended and only site-specific values, calibrated from load data appear appropriate.

## 4.4 Chapter 4 Discussion

The theoretical capacity of the test piles were calculated based on two similar methods proposed in literature. The input parameters from these methods were adjusted based on reasonable estimates of the mean $s_u$ and $N_c$ values presented in literature. Calculated ultimate capacities ranged from 1190 kN to 2660 kN. The results of this analysis shows that the basic approach followed for a preliminary design would more than likely over predict the capacity. CTC relationships were also used to predict capacity using ranges of values found in literature. Capacities ranged from as low as 400 kN to upwards of 7,000 kN, owing to the large range of $K_T$ factors available. From site specific data, an average $K_T$ value of 11.9 was back-calculated. The significant range in calculated values adds credence not only to the need for reduction factors in design but also the value of load testing to confirm design values.

# Chapter 5: Results of Axial Load Tests

## 5.0 Results of Axial Load Tests

Sixty-eight axial compressive load tests were completed during the piling program and 57 tests were considered as part of this study. From the tests considered, maximum loading ranged from 1334 kN to 2402 kN with deflection at those maximum loads from 12 mm to 49 mm. The load versus deflection, load test interpretation, shaft adhesion and the load test results as compared to the theoretical values are discussed below.

## 5.1 Load versus Deflection

The maximum load and the deflection at that load (following an 8-minute load step) are presented in Figure 5.1. The maximum deflection at the maximum load is also plotted in Figure 5.2 as an additional method of comparison, which has been shown with and without elastic compression of the pile.

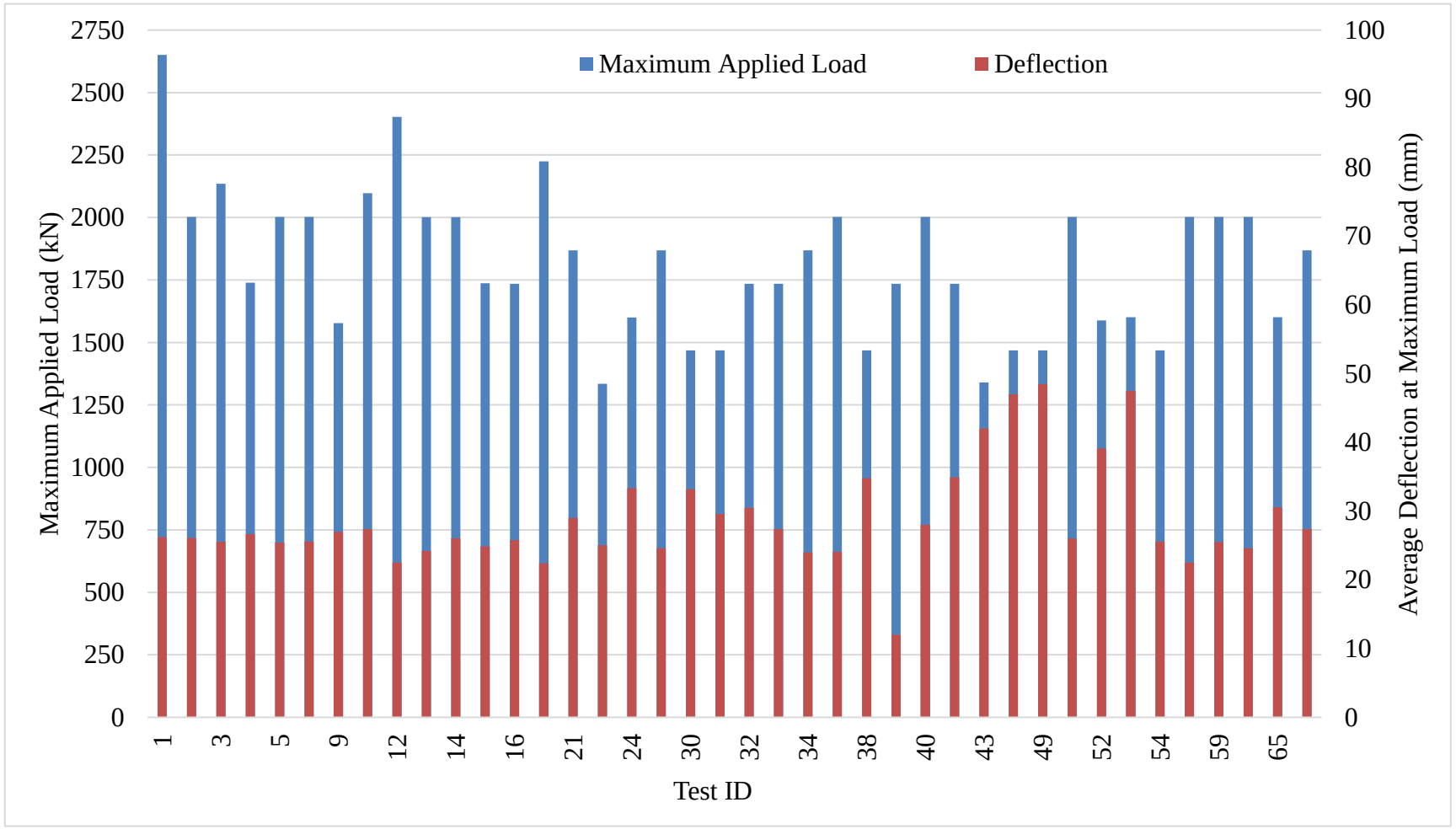


**Figure 5.1 - Summary of Maximum Applied Loads**

A clear trend between deflection and load is not apparent from Figure 5.1 or 5.2, and some of the highest deflections are for the lowest maximum loads and vise versa. For piles which are installed in a similar manner into the same soil types, the deflection at the maximum load is a representation of the overall pile-soil interaction and it is reasonable to expect similar performance. The elastic compression is not a function of the pile-soil interaction and therefore removing this from the deflection provides a more discrete estimate of movement at the pile toe (assuming small contributions from shaft), as shown in Figure 5.2.


**Figure 5.2 - Maximum Applied Load vs Deflection**

Figure 5.2 does show a slight trend towards decreasing deflection with increasing load. Similar to the discussion above, this is the opposite of what would be intuitively

expected (i.e. higher loads should result in higher deflections). This may be explained when considering the test protocols and soil stiffness - areas with softer soils required more deflection to reach a point where the load test would be terminated (i.e. the ULS or SLS values). The wide range in results also supports the wide range in measured undrained shear strengths, i.e. if there is a known variability in a factor that is expected to influence capacity, it is reasonable to expect this would be reflected in load tests. It is also important to note the cluster of values near the 25 mm range – often the value where the tests were halted, which ranged from approximately 1300 kN to 2600 kN. The variability in performance is further shown by the tests which were all terminated at a load of 2002 kN that resulted in deflections from 12 mm to 28 mm, indicating the same load could still result in a wide array of deflections (i.e. soil stiffness varied widely across the site). This trend may be explained due to the load tests simply not being carried to higher/failure loads. If the tests towards the right side of Figure 5.2 would have been carried to failure, their deflections would increase and the expected trend may have been observed. Either way, there is a clear variability in the pile performance at the site.

The trend for data with and without elastic compression (shortening) show comparable results, with perhaps a slightly clearer trend towards decreasing settlement with increasing load, once the elastic compression is removed. The similar trend is not surprising given the similar pile lengths and loading (i.e. the elastic compression is similar for all piles).

To determine if IBM was a suitable method to evaluate capacity, confirming load was fully transferred to the pile toe would be valuable. This can be interpreted in two ways: by subtracting the calculated elastic compression from the measured pile head deflection at max load (a theoretical method), and: by measuring the actual, permanent deflection of the pile head after unload, the remaining movement can be attributed to compression of the soil at pile toe. Both assume the yield point of the steel has not been exceeded. The movement for either method is expected to be positive (i.e. downwards) and in theory should be equal between methods for a free standing column.

A comparison of the difference between the deflection at maximum load minus the elastic compression of the pile (i.e. theoretical movement at pile toe) to the deflection upon unload (i.e. actual movement at the pile toe) is plotted on Figure 5.3.

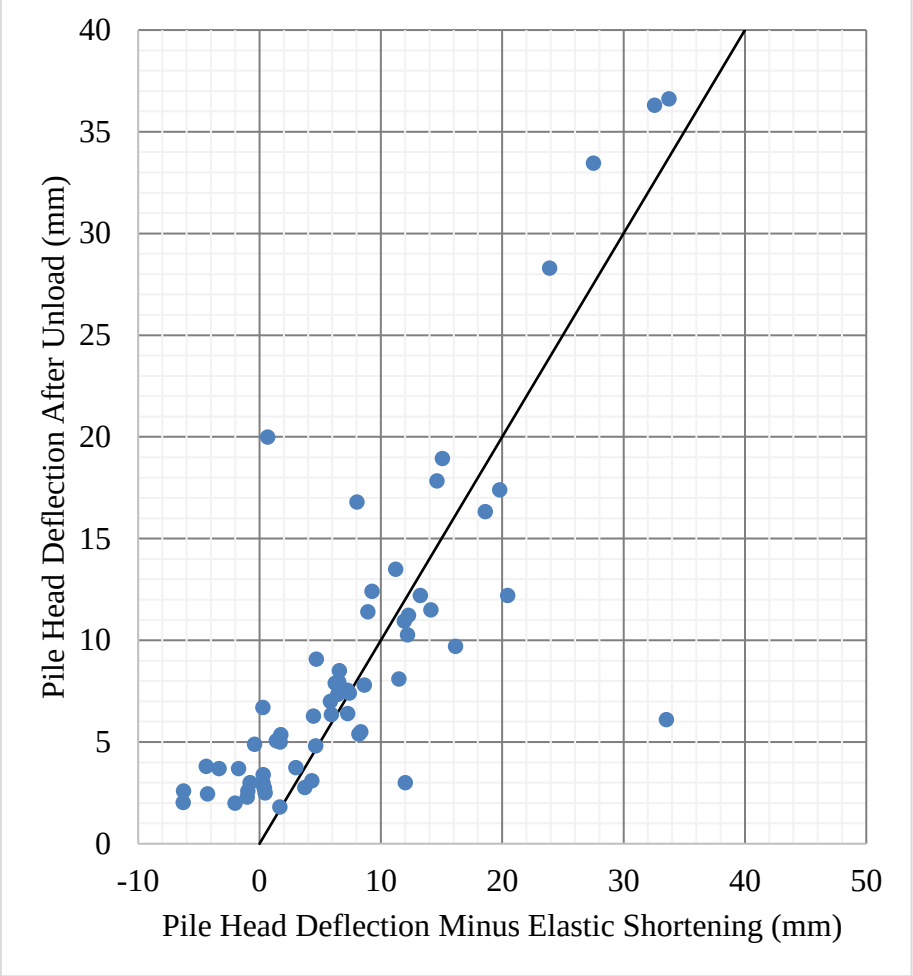


**Figure 5.3 - Deflection at Max Load and Unload**

Figure 5.3 shows the values plotting near a 1:1 line, indicating they are approximately equal and the contribution from shaft adhesion was minimal. When the theoretical deflection is less than the unload value (i.e. values are above the 1:1 line and the theoretical elastic compression is more than what actually occurred), this can be an indication that the pile gained shaft adhesion. Conversely, when the theoretical deflection is more than the unload value (i.e. values are below the 1:1 line), this can be an indication that the pile did not gain much shaft adhesion, the toe continued to move during unload, or a combination thereof. These observations support the idea

that IBM is an appropriate method to evaluate the theoretical capacity and the majority of pile capacity was developed at the helix.

Several tests also show negative values for the theoretical method, that is, the calculated elastic compression is greater than the total pile deflection (which is impossible). This again can be explained by the contribution from shaft adhesion. Where shaft adhesion is present, the entire length of the pile was not being compressed under the maximum load, i.e. the $Q$ and $L$ in Equation 2.11 are both less than used in calculation, and the assumption of a free-standing column is not valid.

The above figures do not consider more detailed pile performance such as whether or not the pile failed and the overall load-deflection response. To further assess pile performance simply beyond comparing maximum deflections and loads, the various failure criteria discussion in Chapter 2 were applied to the load tests. From this application, the pile load tests were separated into three distinct types based on the observed load-deflection curves and their intersection on the plots with the various failure criteria, as described below:

- Type 1: The load-displacement curve did not intersect any of the criteria and therefor an ultimate capacity could not be interpolated from the graph. Type 1 accounted for 23 of the 57 tests. An example is shown below in Figure 5.4.

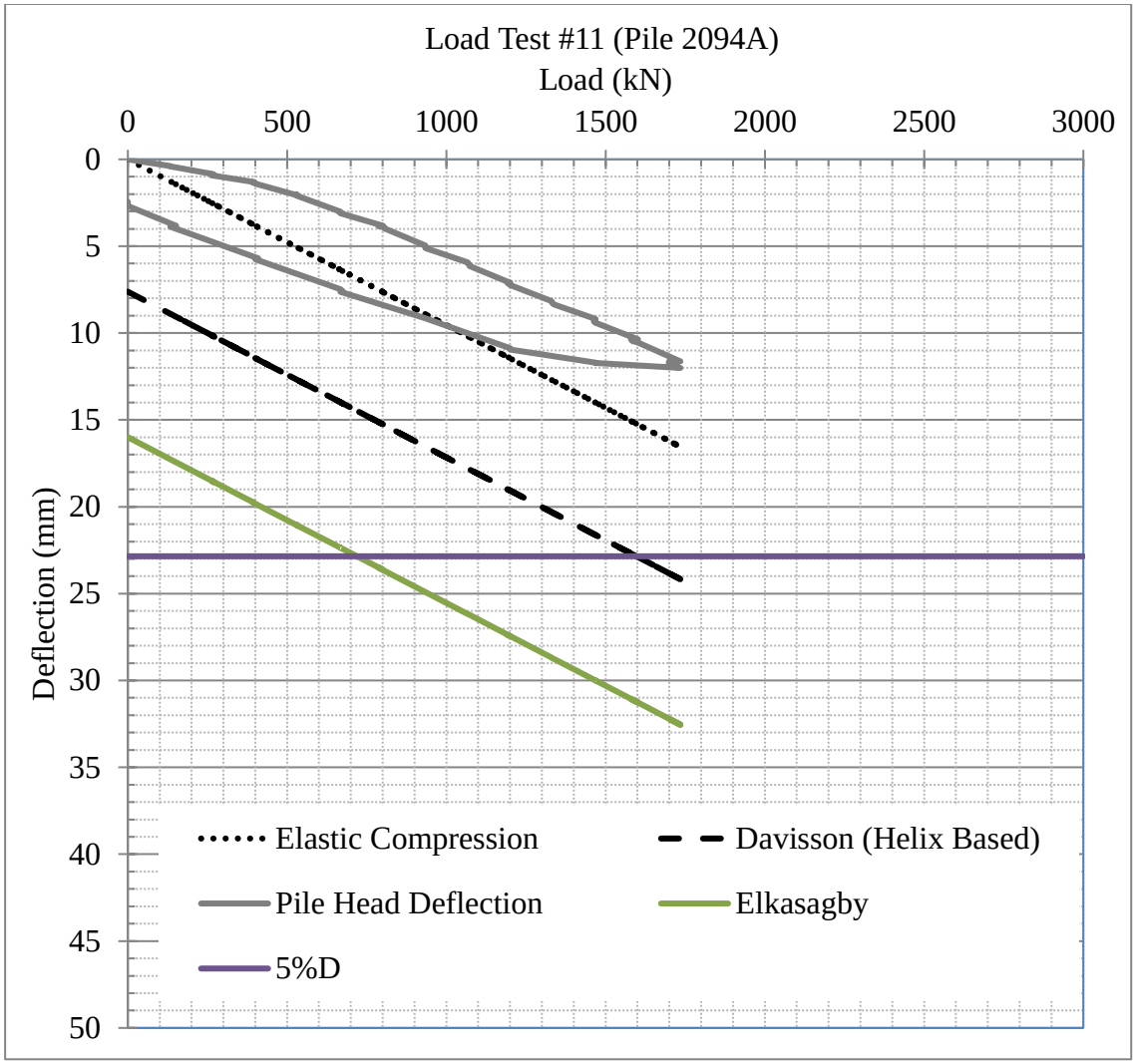


**Figure 5.4 - Type 1 Behavior**

- Type 2: The load displacement curve intersected at least one of the failure criteria, however a distinct plunging failure was not observed. Type 2 accounted for 24 of the 57 tests. An example is shown below in Figure 5.5.

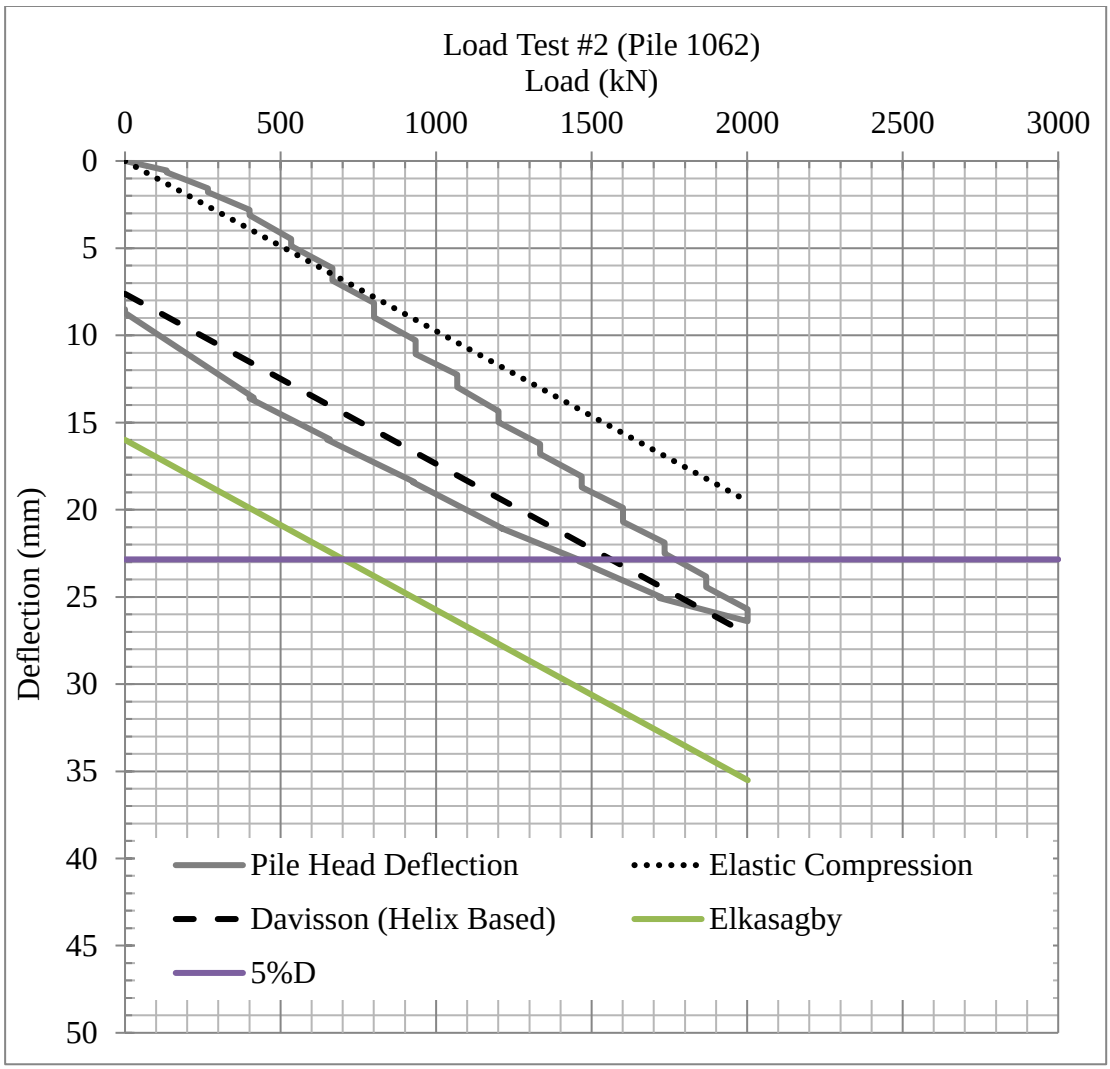


**Figure 5.5 - Type 2 Behavior**

- Type 3: The load-displacement curve intersected more than one failure criteria and a distinct plunging failure was observed. Type 3 accounted for 10 of the 57 tests. An example is shown below in Figure 5.6.

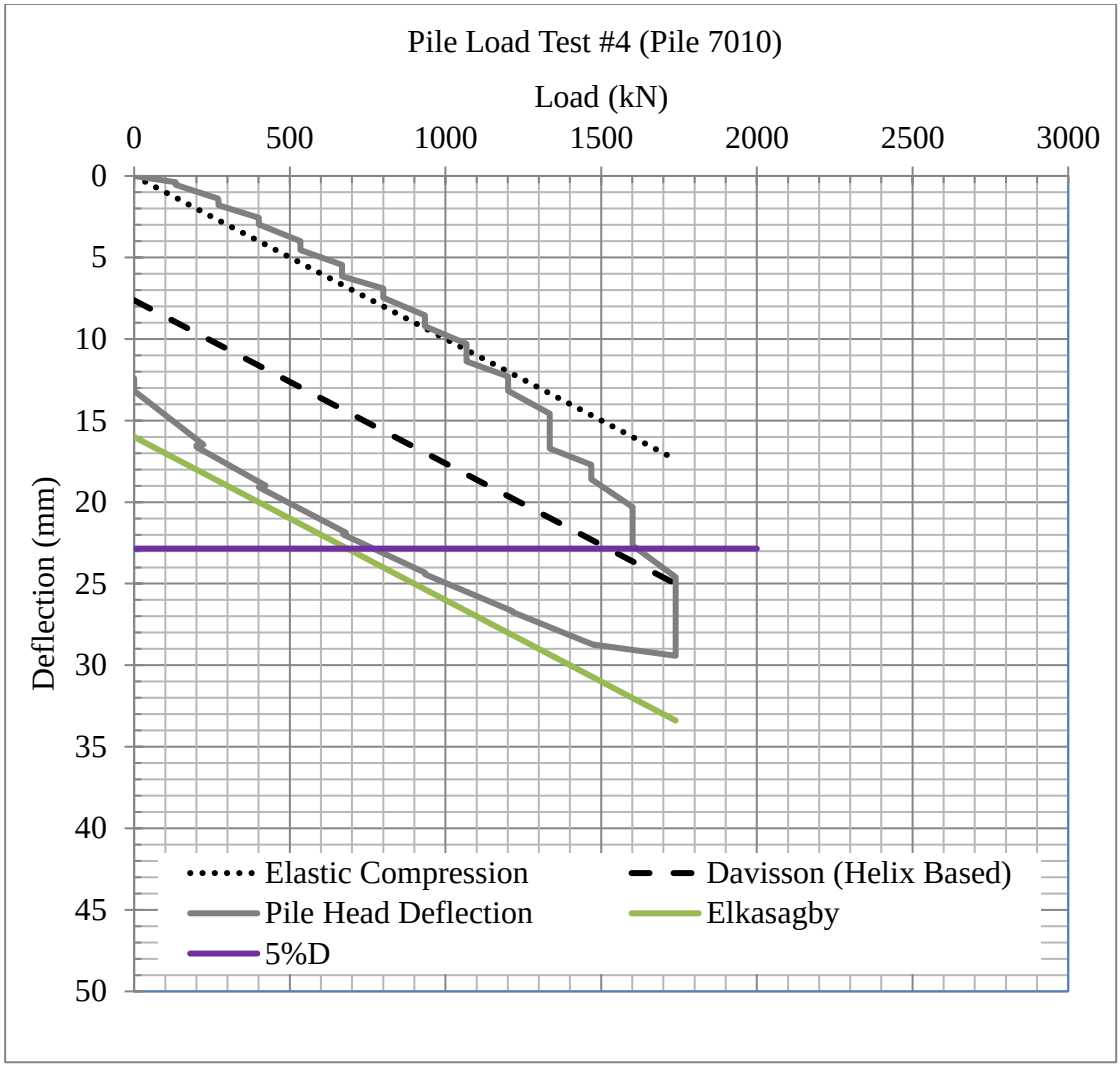


**Figure 5.6 - Type 3 Behavior**

The results of Type 1 tests were not considered further in the analysis as no ultimate capacity could be obtained. Type 2 and Type 3 tests were used to compare the theoretical ultimate capacity to the interpreted value(s). Where multiple failure criteria were applicable, the calculated ultimate capacity was compared to the highest interpreted capacity.

## 5.2 Load Test Interpretation

The 5%D and Davisson criteria were found to underestimate the pile capacity where the Elkasabgy criteria was always the highest. The 5%D and Davisson criteria were also found to be applicable in the most cases (i.e. they most commonly provided an intersect with the load-deflection curves). The Elkasabgy criteria provided a more accurate estimate of an actual failure load however wasn't applicable in as many cases. From this point, an exercise was undertaken to expand on these graphical and numerical methods to investigate a means which may be applicable in more cases than Elkasagby and also produce higher loads than the 5%D or Davisson criteria.

### *5.2.1 The Creep Limit*

Figure 2.5 and Figure 2.6 illustrate how the De Beer failure criteria did not develop in the Type 3 tests, which is consistent with all 10 of the Type 3 tests. Recall for the De Beer criteria to be applicable, plotting the logarithm of load and displacement needs to result in two straight lines, the intersection at which the ordinate corresponds to the interpreted load. This is due to the deflection not being of high enough magnitude for the study load tests. A modified method of the De Beer criterion is proposed where the deflection is not plotted on a log scale. This results in two linear portions as indicated in the original De Beer criterion. When the load at the intersection of these lines is plotted on the load deflection curve, it tends to represent the onset of the second, non-linear region of the data. It is at this value where the deflections begin to creep – that is deflections are no longer proportional to the load. The value obtained at the intersection of the two lines alone underestimates capacity (e.g. loading can still

occur with little relative deflection) and in this regard, interpreting a higher load is appropriate. Adding the elastic compression to the deflection at this load, results in the summation being within the third, low stiffness region of the curve. The process for obtaining this load, denoted as the Creep limit going forward, along with the other failure criteria, is shown in Figure 5.7 and Figure 5.8.

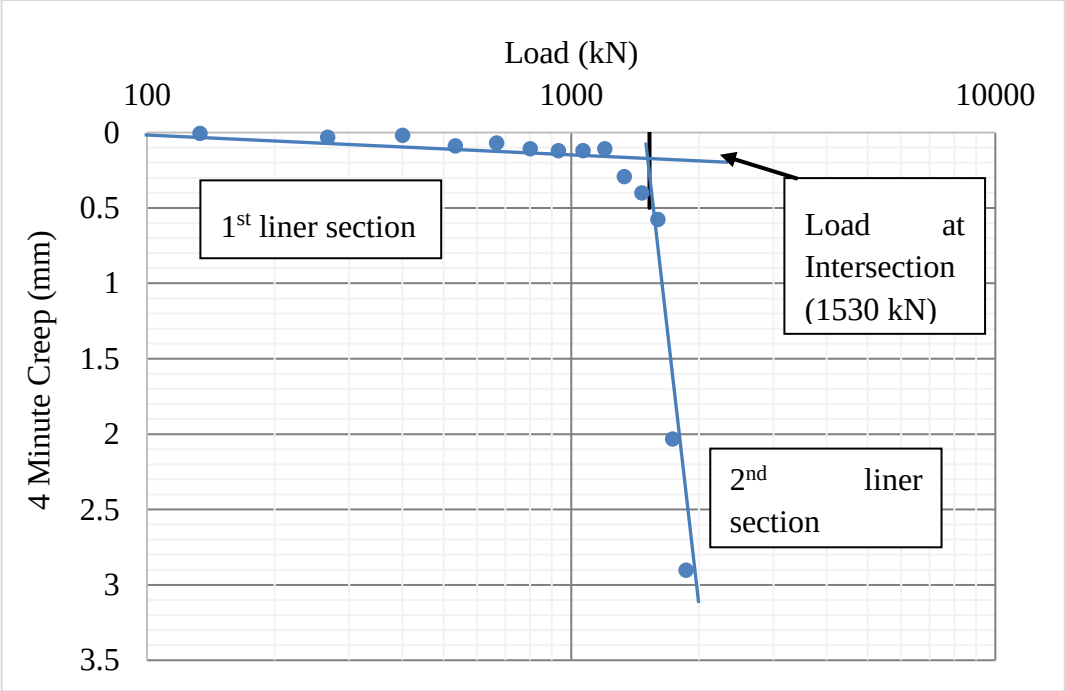


**Figure 5.7 - Determining Modified De Beer Limit (Creep Limit)**

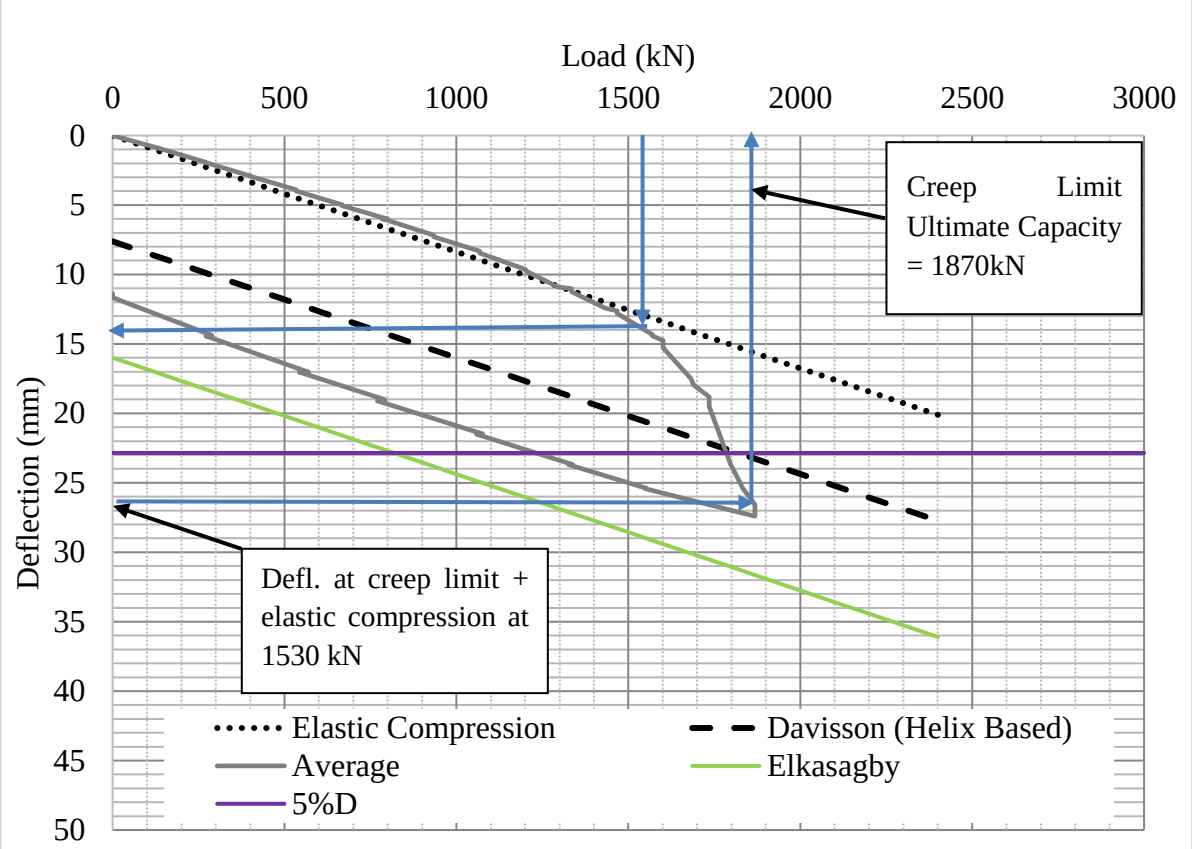


**Figure 5.8 - Ultimate Capacity from Creep Limit**

The Creep limit was applicable in 14 cases and was always higher than the 5%D and Davisson Criteria. The Creep and Elkasabgy criterion produced very similar results, with the Elkasabgy criterion producing higher values in 5 out of 7 tests, however the values were within 0.6 to 6.4% of each other

### *5.2.2 **Comparison of Interpretation Methods***

Multiple criteria regularly pass the load-deflection curve for Type 2 tests and the maximum predicted capacity was either Elkasabgy or the Creep limit in all cases. In these cases, the ultimate capacity was always obtained from the third, linear region of low stiffness indicating these methods are good approximations to represent a failure

load. Current practice applies reduction factors to ultimate capacity obtained from load tests (in the case of the National Building Code of Canada the factor is 0.6) and the resulting factored load would be well below the region of low stiffness and thus an appropriate design value, in the case above, 1,122 kN which corresponds to approximately 7mm of deflection. The ultimate capacity interpreted from the failure criteria are shown in Table 5.1 and a graphical comparison of the ultimate capacity is also provided in Figure 5.9.

**Table 5.1 - Interpreted Ultimate Capacity**

| Load Test ID | Failure Type | Pile No. | Max Load (kN) | Avg Defl at Max Load (mm) | $Q_{ui}$ (kN) | | | |
|---|---|---|---|---|---|---|---|---|
| | | | | | Creep Limit | Davisson | 5% D | Elkasabgy |
| 1 | 3 | 1073 | 2651 | 26.2 | 2540 | 2250 | 1910 | 2650 |
| 2 | 2 | 1062 | 2002 | 26.1 | -- | -- | 1735 | -- |
| 3 | 2 | 7076 | 2135 | 25.6 | -- | -- | 1960 | -- |
| 4 | 3 | 7010 | 1739 | 26.7 | 1740 | 1739 | 1600 | -- |
| 5 | 2 | 1063.2 | 2002 | 25.4 | -- | -- | 1910 | -- |
| 8 | 2 | 5008 | 2002 | 25.6 | *1750* [(1)] | -- | 1880 | -- |
| 10 | 2 | 2023 | 2097 | 27.4 | 2210 | 2200 | 2110 | -- |
| 13 | 2 | 4128 | 2002 | 24.2 | -- | -- | 2002 | -- |
| 14 | 2 | 6058 | 2002 | 26.1 | -- | -- | 1770 | -- |
| 15 | 2 | 2119 | 1737 | 24.9 | -- | 1700 | 1660 | -- |
| 16 | 2 | 1038 | 1735 | 25.8 | -- | 1735 | 1550 | -- |
| 17 | 2 | 2046 | 2224 | 22.4 | -- | -- | 2220 | -- |
| 21 | 2 | 2123 | 1868 | 29.0 | -- | 1780 | 1750 | -- |
| 23 | 2 | 2016 | 1480 | 23.9 | -- | 1210 | 1300 | -- |
| 24 | 2 | 3050 | 1600 | 33.3 | -- | 1330 | 1400 | 1550 |
| 28 | 2 | 4011 | 1868 | 24.6 | -- | 1870 | 1850 | -- |
| 30 | 3 | 6013 | 1468 | 33.2 | 1390 | 1210 | 1300 | 1410 |
| 31 | 2 | 5052 | 1468 | 29.6 | 1420 | 1240 | 1360 | -- |
| 32 | 2 | 6078 | 1735 | 30.5 | -- | 1540 | 1540 | -- |

| | | | | | | | | |
|---|---|---|---|---|---|---|---|---|
| 33 | 2 | 5016 | 1735 | 27.4 | -- | 1600 | 1620 | -- |
| 34 | 2 | 6112 | 1868 | 24.0 | -- | -- | 1860 | -- |
| 36 | 2 | 5033 | 2002 | 24.1 | -- | -- | 1950 | -- |
| 38 | 3 | 5014 | 1468 | 34.8 | 1320 | 1080 | 1240 | 1410 |
| 40 | 2 | X730 | 2002 | 28.0 | 2002 | 1850 | 1850 | -- |
| 42 | 3 | X360 | 1735 | 34.9 | 1730 | 1575 | 1575 | 1730 |
| 43 | 3 | X375 | 1680 | 35.2 | 1670 | 1480 | 1570 | 1610 |
| 49 | 3 | X318 | 1468 | 48.5 | 1320 | 1210 | 1260 | -- |
| 50 | 2 | X323 | 2002 | 26.0 | -- | 1970 | 1950 | -- |
| 52 | 3 | X578 | 1588 | 39.1 | 1600 | 1470 | 1570 | 1600 |
| 53 | 3 | X780 | 1601 | 47.5 | 1880 | 1800 | 1820 | 1860 |
| 59 | 2 | X406 | 2002 | 25.5 | -- | 1980 | 1930 | -- |
| 64 | 2 | X515 | 2002 | 24.6 | -- | 1960 | 1840 | -- |
| 65 | 2 | X550 | 1601 | 30.6 | -- | 1320 | 1440 | 1601 |
| 68 | 3 | X734 | 1868 | 27.4 | 1870 | 1780 | 1780 | -- |
| | | | | **Count =** | **14** | **25** | **34** | **9** |

*Notes:*

*-- Indicates criterion never crossed load-deflection curve*

*(1) -Creep limit did not fully develop. This value is shown for further discussion.*

.

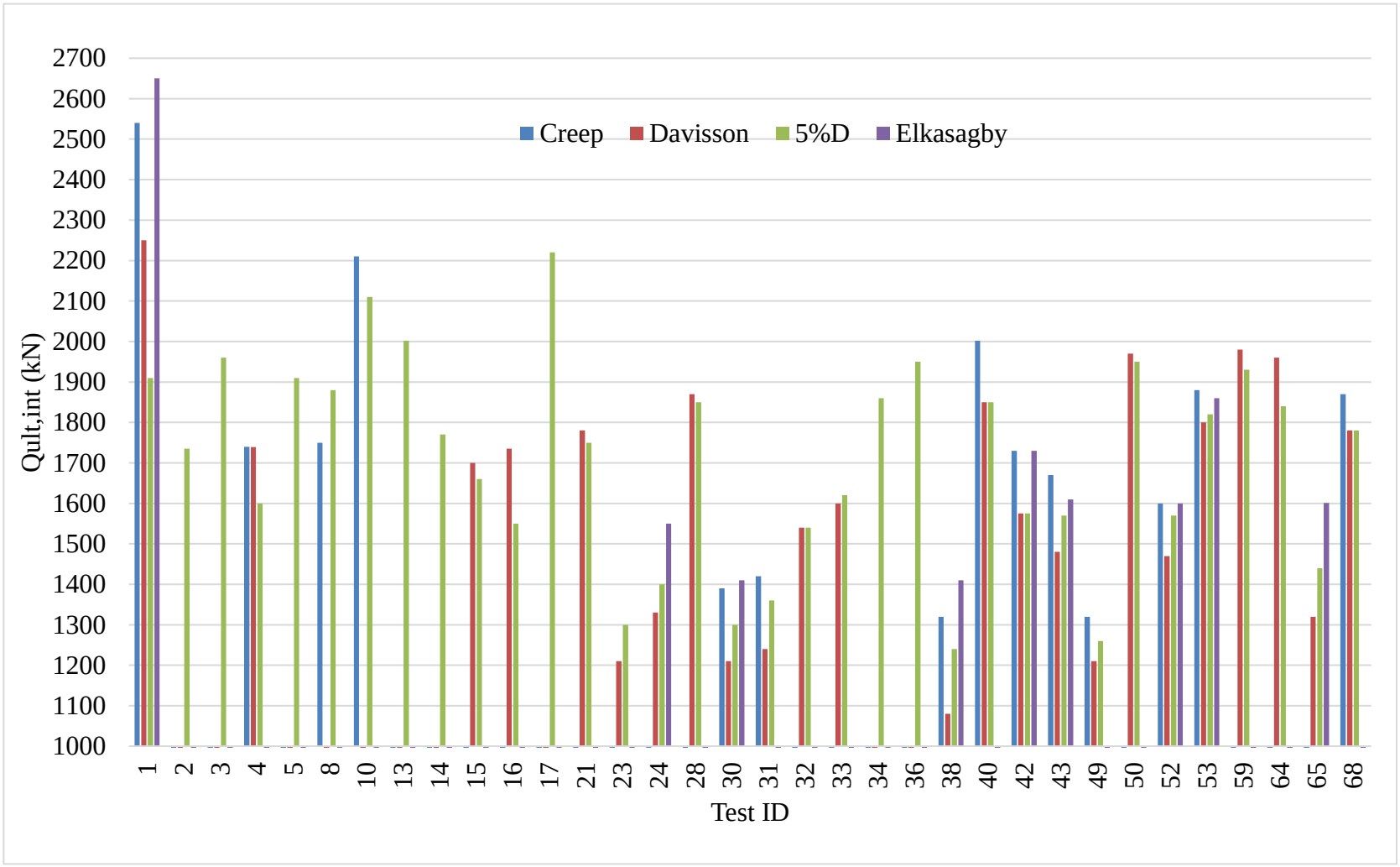


**Figure 5.9 – $Q_{ui}$ from Failure Criterion**

The 5%D criterion was applicable in every case, due to the fact that every test was taken to at least 25 mm deflection (i.e. beyond 22.9 mm or 5% of the helix diameter). The 5%D criterion underestimated pile capacity by an average of 7% but by as much as 28% when compared to the interpretation method which produced the highest load. The 5%D criterion and the Davisson criterion were generally very close, within 100 kN or so of each other. Where a low stiffness response was present in the load-deflection behavior, the Davisson criteria was intersected first and a lower capacity was interpreted. The Davisson criteria was applicable in 25 of 34 tests and will always produce a lower capacity than the Elkasabgy criterion given the initial offset is less. The Davisson criteria underestimated capacity by an average of 10% and by as much as 18% when compared to the interpretation method which produced the highest load. The Elkasabgy criterion was applicable in 9 tests and generally produced the highest capacity, always within the third region of low stiffness of the curve. The Creep limit was applicable in 14 cases and was always higher than the 5%D and Davisson criteria. Seven of the tests were appliable in all criteria, which were all Type 3. Two tests which were applicable to Elkasabgy but not the Creep limit (tests #24 and #65) due to not having a well-defined plunging failure and poor dial gauge readings also affected the results of test #65. The Creep failure load is shown in Appendix A for load test #65 to illustrate how a poorly defined plunging failure results in an inappropriate interpretation of the ultimate capacity (see Figure A33b).

## 5.3 Shaft Adhesion

Contribution from shaft adhesion is expected to be relatively low for the production pile tests given the loose backfill surrounding the piles. For pile HP8-2 there were issues with the grout set up and the strain gauge readings ended up being erroneous and therefore the results are not discussed. Table 5.2 presents the interpreted shaft adhesion from the 5 loads tests.

**Table 5.2 - Unit Shaft Resistance**

| Test ID | Unit Shaft Resistance (kPa) |
|---|---|
| HP2-3 | 7 to 12 |
| HP2-6 | 0 to 10 |
| HP8-5 | 0 to 10 |
| #6 | 0 to 10 |
| #7 | 0.5 to 1 |

The relatively high unit shaft resistance in HP2-3 is attributed to the prebore hole sloughing in at 1.8 m prior to pile install. Advancing the pile likely resulted in densification of the soils which in turn may have increased the unit shaft resistance. In the remaining tests, the pre-bore remained open close to the target pre-bore depth and was then loosely backfilled following pile installation. Based on these unit shaft resistances and an average pile embedment of 18.4 m, the shaft adhesion is anticipated to account for as little as 14 kN (=1 kPa) to as high as 170 kN (=12 kPa). Compared to the theoretical, low range value of 400 kN, it is clear that the backfilling method significantly reduced shaft adhesion. Given this represents such a small portion of either the interpreted or calculated capacity and the uncertainty in the

actual value for each test, the shaft adhesion portion is not included when comparing calculated to interpreted values with the exception of noting that variations in expected capacities may be minorly affected by shaft adhesion. The low shaft adhesion lends further support to IBM being an appropriate method for evaluating theoretical capacity.

## 5.4 Comparison with Theoretical Calculations

The theoretical capacities calculated for each pile using the mean $s_u$ and $N_c$ of 8.11 were compared to each of the failure criterion. These results are shown in Figure 5.10 as $Q_{uc}$ divided by $Q_{ui}$. A statistical breakdown of $Q_{uc}$ divided by $Q_{ui}$ is also provided in Table 5.3.

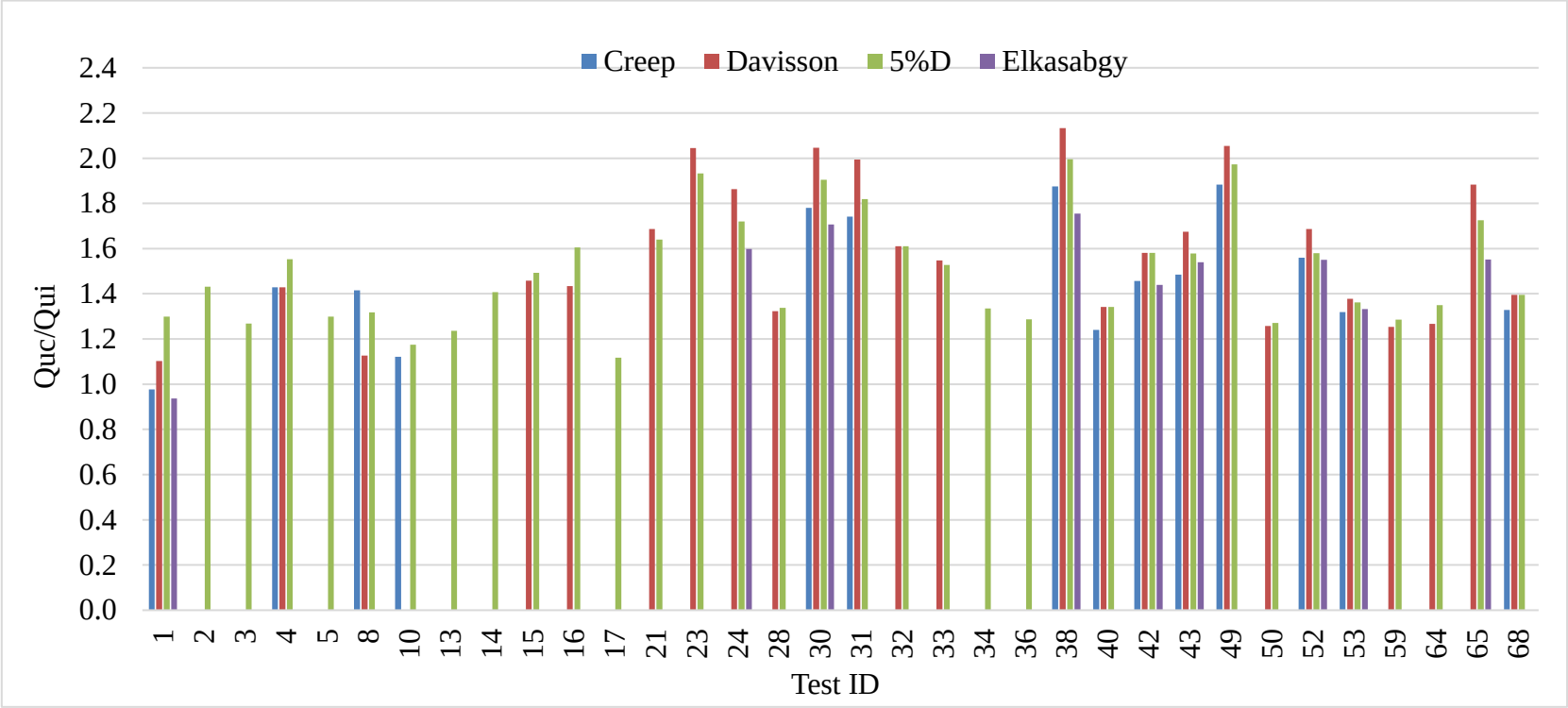


**Figure 5.10 - Calculated vs Interpreted Capacity**

**Table 5.3 - Calculated vs Interpreted Capacity Data**

| Method | Quc/Qui | | | | | |
|---|---|---|---|---|---|---|
| | Count | Minimum | Average | Maximum | Std Dev | CV |
| Creep Limit | 14 | 0.98 | 1.47 | 1.88 | 0.26 | 0.18 |
| Davisson | 25 | 1.10 | 1.58 | 2.13 | 0.31 | 0.19 |
| 5%D | 34 | 1.12 | 1.49 | 2.00 | 0.23 | 0.16 |
| Elkasabgy | 9 | 0.94 | 1.49 | 1.76 | 0.23 | 0.15 |

The calculated capacity was always higher than that obtained from the failure criterion, on average 47% to 58% higher than interpreted across the 4 methods. The Creep and Elkasabgy criteria were closest to the calculated values, as they predicted the highest capacities when comparing tests. The coefficient of variation, which is a measurement of how far a set of values within a data set vary from the mean, shows a range from 0.15 (Elkasabgy) to 0.19 (Davisson), which given the data set is statistically nearly equivalent, i.e. each of the criterion developed similar results compared across all piles for which they were applicable.

The overestimated, calculated capacity can be attributed to selection of an undrained shear strength that is unrepresentatively high, the $N_c$ factor being too high, or a combination thereof. Since bearing capacity factors are determinate (e.g. it is a widely accepted formula based on the pile geometry and loading and not a function of the soil properties), it is more appropriate to re-evaluate selection of the shear strength than recalculate the bearing capacity factor.

A subsequent method of evaluating $s_u$ was undertaken where the $s_u$ required to produce the maximum interpreted ultimate capacity (presented in Chapter 5) was back-calculated using Equation 2.4 and the project specific $N_c$ of 8.11. For comparison with measured $s_u$ values, this exercise assumes that the shear strength has been fully mobilized (i.e. the UUC tests report fully mobilized strengths). The result of this calculation is shown in Figure 5.11.

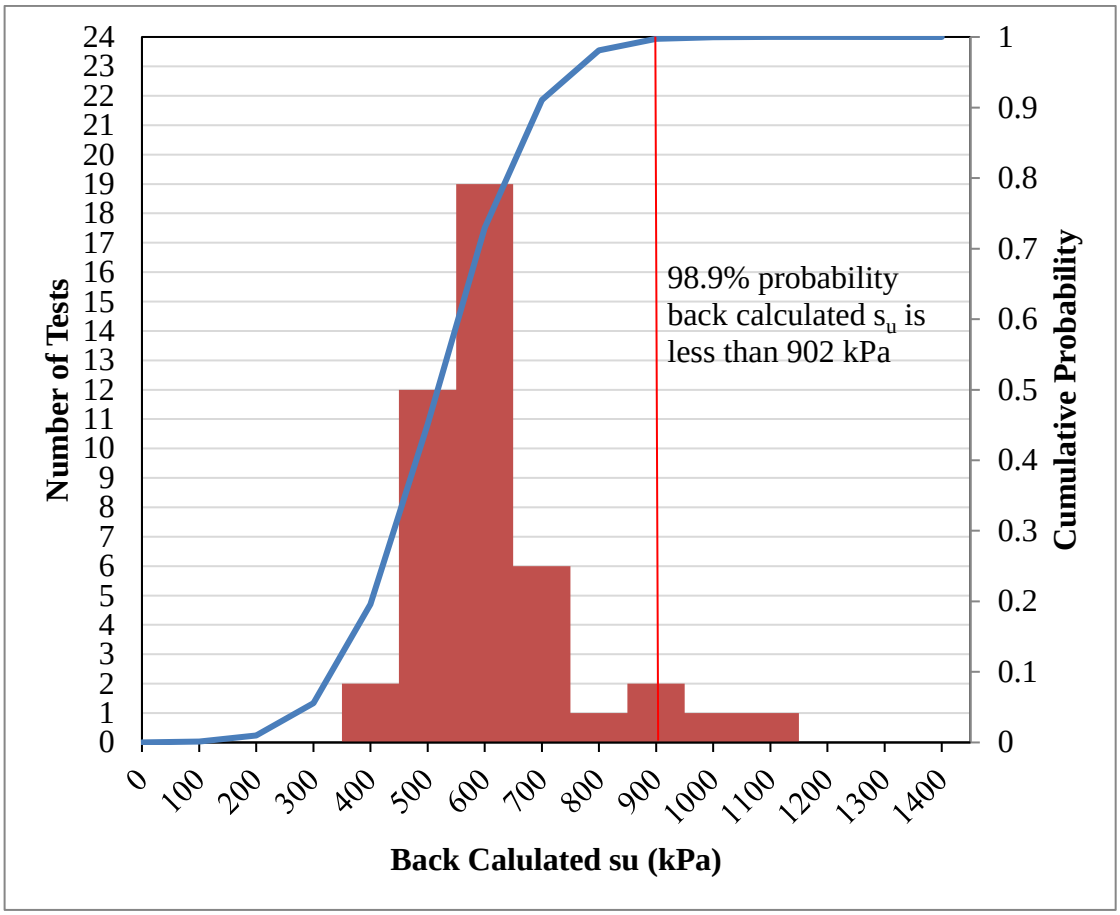


**Figure 5.11 - Back Calculated $s_u$**

The figure above shows how using the average $s_u$ is almost certainly going to over-predict the measured pile capacity. A mean $s_u$ of just over 500 kPa is shown in Figure 5.11. For a normally distributed $s_u$, using a range of values within 1 standard deviation less than the mean this would result in 68% of the values being at least this high (68% of values are within 1 standard deviation above or below the mean). An $s_u$ of 545 kPa is obtained with this process using the measured strength data which is about 60% of the mean presented in Figure 4.1. The use of this undrained shear strength would obviously underestimate the required, ultimate pile capacity, however

is near the mean of the back calculated mean in Figure 5.11 (around the 55% cumulative probability).

This degree of over-conservatism is not standard in practice however perhaps should be considered when there is significant scatter in the data (the coefficient of variation for the $s_u$ data was 0.4). When selecting a single nominal value, the coefficient of variation is ideally small, say closer to 0.1, indicating that most values are near the mean. This gives good confidence that the selection of a nominal value closer to the mean will not result in erroneous capacities. In cases such as this study where the variation is rather large (e.g. the standard deviation is 40% of the mean), a more cautious estimates are warranted.

A similar exercise was undertaken to evaluate the $N_c$ factor using mean $s_u$ values, particularly since the suggested values of $N_c$ can range from approximately 5 to 10. To accomplish this, a range of $N_c$ values was back calculated from Equation 2.4 using the average undrained shear strength (902 kPa) and maximum interpreted capacity, as shown in Table 5.4.

**Table 5.4 - Back Calculated $N_c$**

| Min | Average | Max | Std Dev. | CV |
|---|---|---|---|---|
| 4.07 | 5.78 | 8.70 | 0.96 | 0.17 |

Table 5.4 shows approximately the same range of values as suggested in the literature, however are slightly less, indicating the value of 8.11 used in this study may be around 25% high but appropriate, albeit the overprediction is arguably better attributed to the selection of undrained shear strength.

## 5.5 Comparison with CTC

Calculated values from the various CTCs were compared by diving each result by the ultimate capacity from failure criteria (the highest value). The results of this analysis are shown in

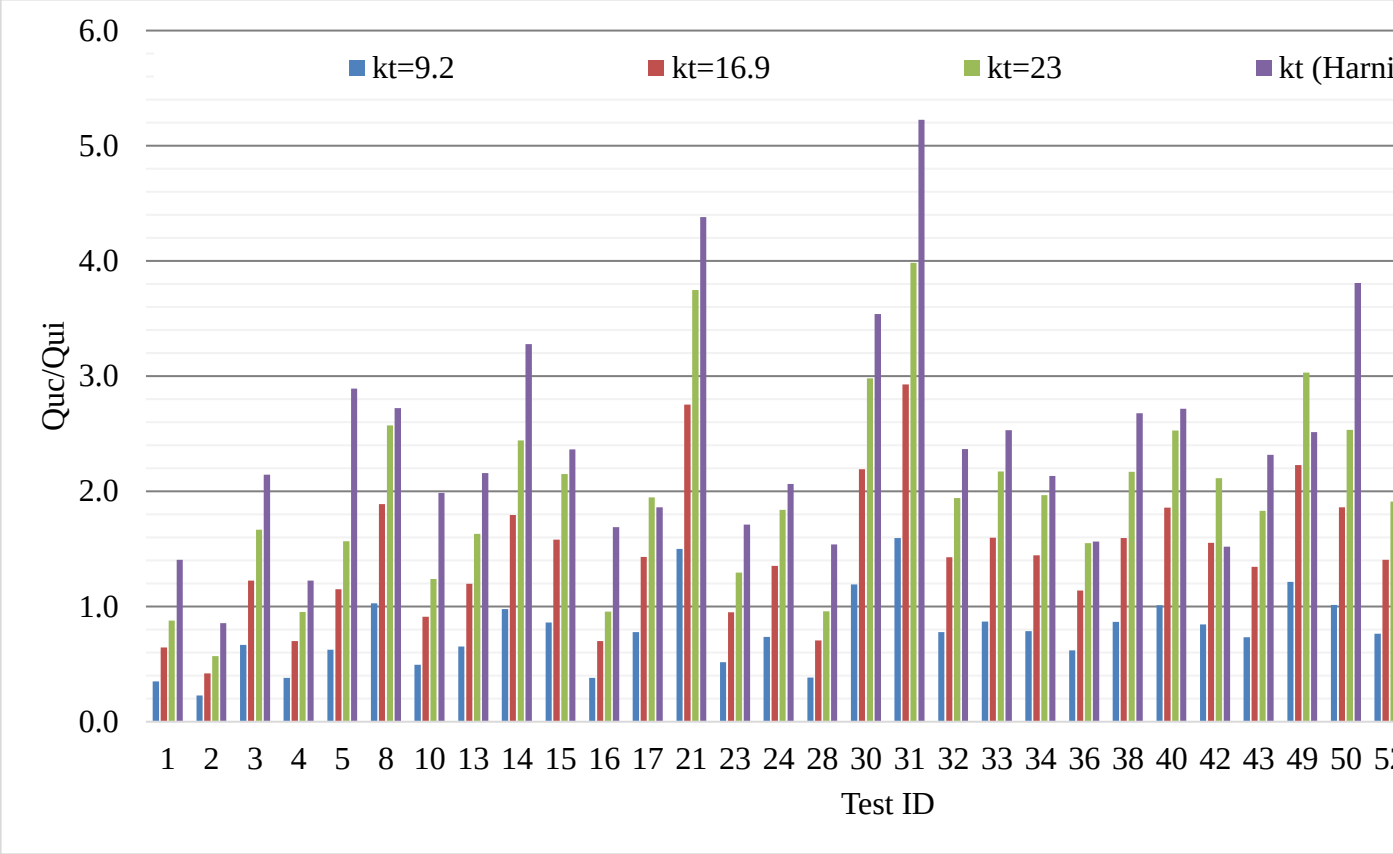


**Figure 5.12** and presented as $Q_{ut}$ divided by $Q_{ui}$.

The lower $K_T$ values generally underpredicted capacity by 11% to 21% while the higher values overpredicted capacity by 98% to 143%, showing there is significant range in predicted values using CTC methods. A site-specific value was then calculated by dividing the average ultimate capacity as interpreted from failure criterion by the maximum torque of each test (within 3 helix diameters). This results

in an average $K_T$ value of 11.9. When the calculated $K_T$ value is then used to determine ultimate capacities for each load test, reasonably close values to unity are achieved (

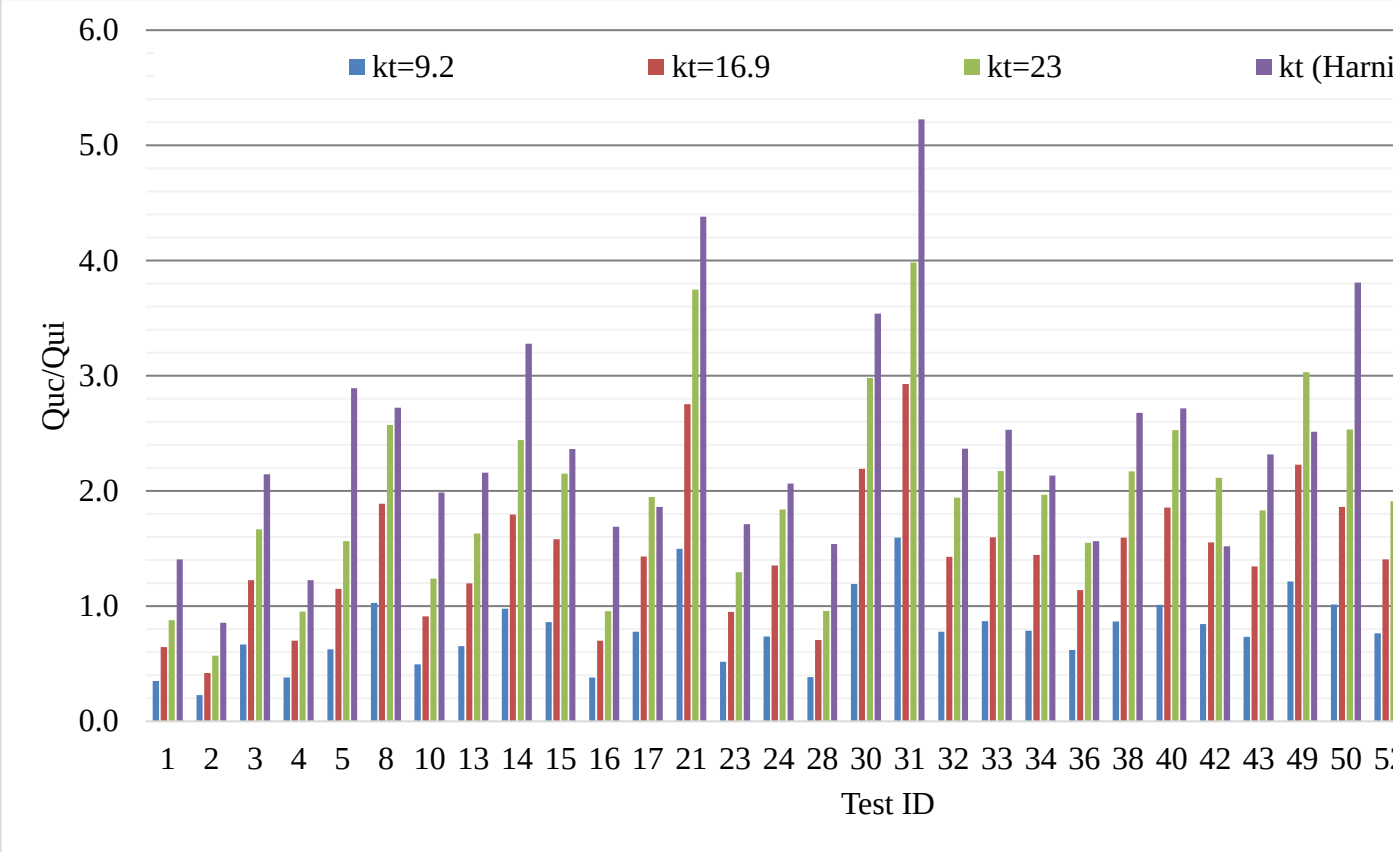


**Figure 5.12 - CTC vs Interpreted Capacities**

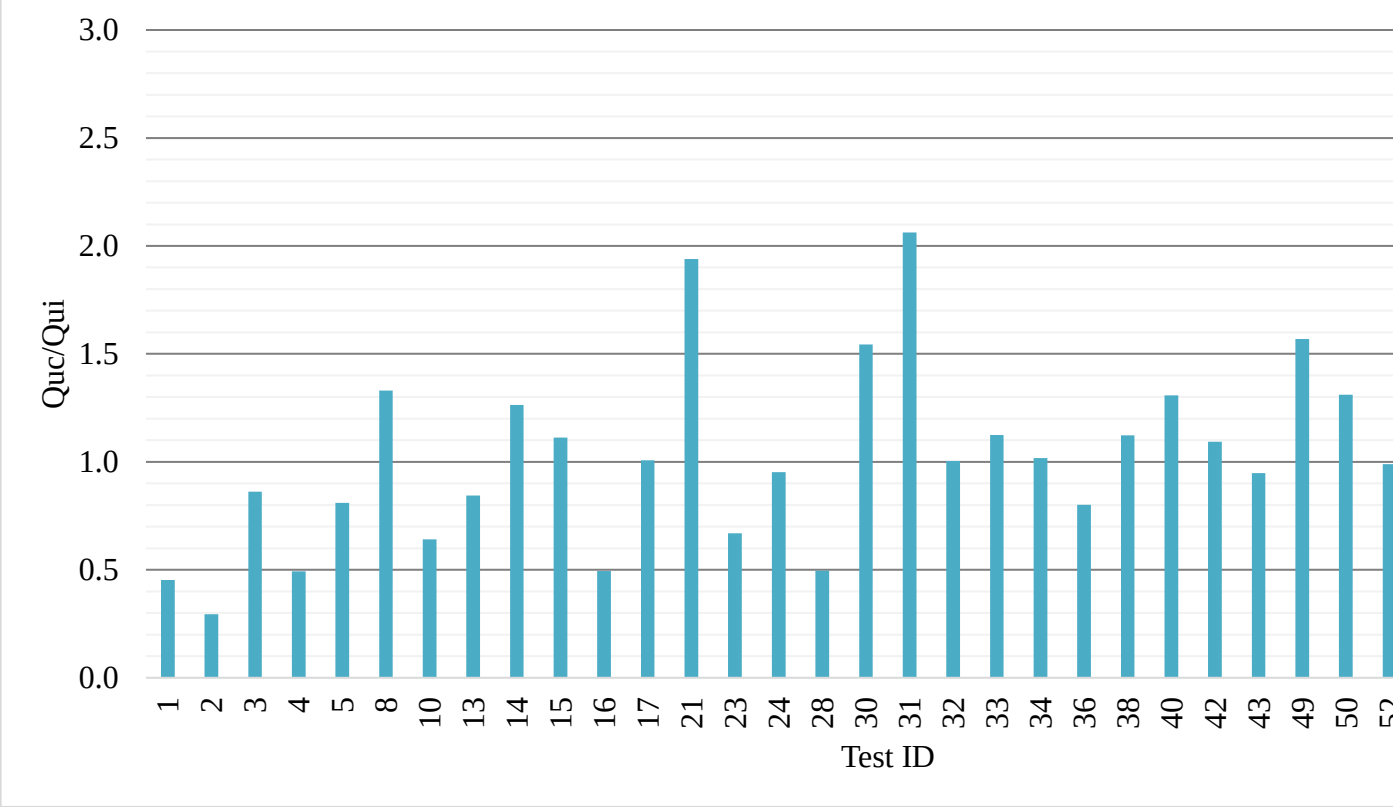


Figure 5.13, shown on the same scale). Although this is a simple mathematic exercise to generate a $K_T$ value that will predict more normalized values, it is at a minimum, a demonstration of the calculated $K_T$ being close to those presented in literature and an indication they should be used cautiously.

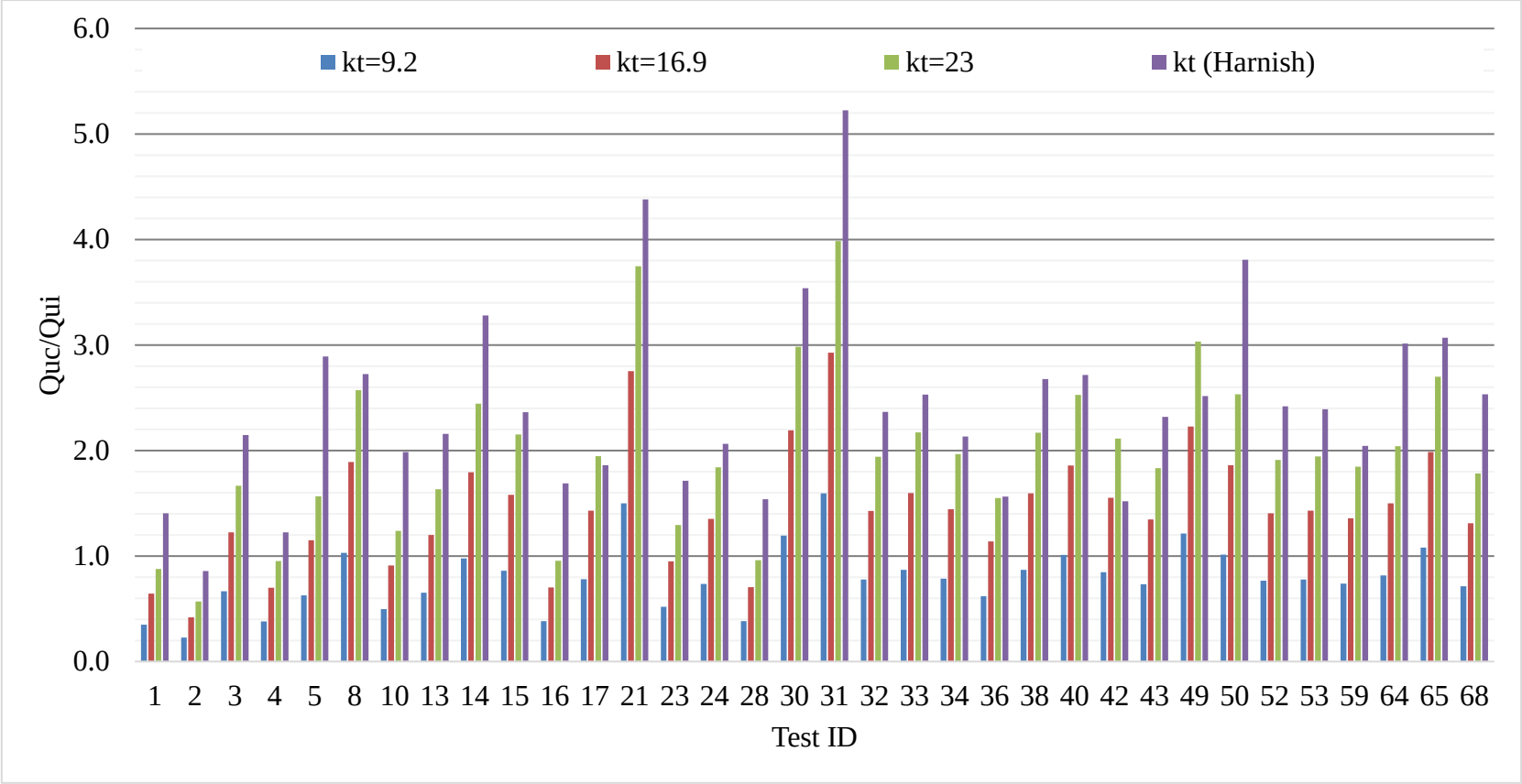


**Figure 5.12 - CTC vs Interpreted Capacities**

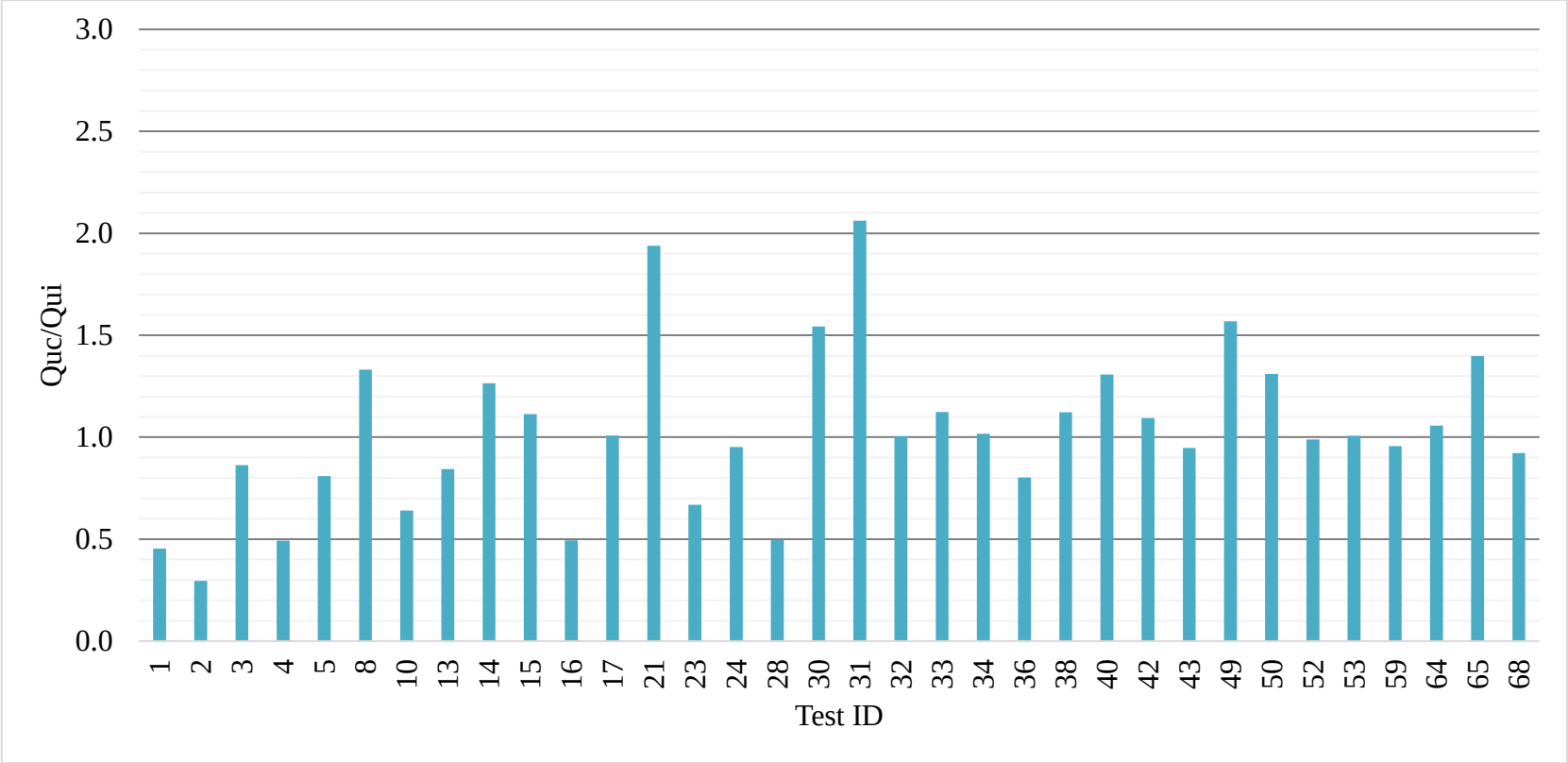


**Figure 5.13 - $Q_{ut}$ from Average $K_T$**

Notes:

Qcalc = $K_T$ x T, where T is torque at pile refusal and $K_T$ = 11.9 (Equation 2.9)

Interestingly, Pack (2000) notes the refusal condition is generally met with a reduction in torque. He indicates that this does not mean that the pile will not meet its ultimate capacity, but simply that capacity can't be predicted by measuring torque. The reduction in torque with refusal was not noted ubiquitously throughout this program, although where it was is likely due to the prebore or over churning at the pile toe. The statement by Pack still provides insight into the use (or non-use) of torque to predict capacity, particularly for piles driven to refusal – this should be done with caution and the appropriate engineering judgement is needed.

## 5.6 Chapter 5 Discussion

Sixty-eight static axial load tests were completed and 57 of these tests were reviewed as part of the current study. The load-deflection performance of the piles were compared and there is a clear variability in the results with respect to applied load and deflection at that load. The results showed a trend of lower deflections with increasing load, i.e. lower stiffness was observed as loads increased. This variability is attributed to the range in soil stiffness, as evidenced by the undrained shear strength test results along with procedures of the load testing itself.

The tests were separated into three types (Type 1, 2 and 3) based on their observed load-deflection curve and intersection with the failure criteria. From this exercise it was noticed that methods which were appliable in most cases (5%D and Davisson) underestimated the capacity by an average of 7% to 10% when compared to the highest interpreted value. The Elkasabgy method which produced the highest capacity

in most cases was found to only be applicable in 9 cases. Based on the De Beer failure criteria, a modified method, denoted the Creep limit, was developed which utilizes graphical and mathematical approaches to interpret a failure load. The Creep limit was found to be applicable in 15 instances and resulted in capacities near plunging failure and within 0.6% to 6.4% of Elkasabgy.

Based on the ultimate capacity obtained from failure criteria, the theoretical methods over predicted capacity in every case. This is attributed to the selection of unrepresentatively high shear strengths, $N_c$ factors or a combination thereof, although a preference to re-evaluating the selection of shear strength. When there is significant scatter in the data, as determined from statistical methods, the cautious estimate of the mean should be re-evaluated and in this case was approximately 60% of the mean (545 kPa vs 902 kPa). The ultimate capacity as interpreted from the failure criteria was then used to back calculate the $N_c$ factor assuming an average shear strength of 902 kPa. This resulted in $N_c$ factors ranging from 4.07 to 8.70 with a mean of 5.78, compared to the theoretical value used of 8.11.

The results of the instrumented pile load testing show that shaft adhesion was minimized as a result of the backfilling procedures. Conservative (i.e. low bound) theoretical predictions of shaft adhesion were significantly higher, in the range of 400 kN where measured shaft adhesion was in the range of 14 kN to 170 kN. The small contribution from shaft was further confirmed by comparing the deflection at maximum load (minus elastic compression) to the deflection following unload.

Torque to Capacity Correlations (CTC) were also analyzed by comparing the maximum interpreted load to the torque at refusal. This generally resulted in an overprediction compared to interpreted capacity from the load tests. A site specific $k_T$ values of 11.9 was also calculated using the average torque near refusal and the maximum interpreted load.

# Chapter 6: Summary, Conclusions and Recommendations

## 6.0 Summary, Conclusions and Recommendations

## 6.1 Project Summary

Helical piles are gaining popularity in use and further study is required to better understand their performance and develop more efficient designs. Over 1,100 helical piles were installed to support power generation infrastructure in northern Manitoba. The piles were installed into hard clay tills using hydraulicly powered drive heads affixed to conventionally available construction equipment. The capacity of 57 of these helical piles was evaluated based on results of axial compressive load tests. Multiple failure criteria were reviewed, and ultimate capacities were determined from load-deflection curves. The capacity of the 57 piles was also calculated using theoretical methods and empirical relationships. The ultimate capacities between the failure criterion and theoretical and empirical methods were compared.

## 6.2 Theoretical and Empirical Predictions of Capacity

The theoretical methods tended to over predict the capacity as determined from load test data. The over prediction may be attributed to the selection of high, mean shear strengths and to a lesser extent selection of high bearing capacity factors. As these two terms have the largest influence on calculating pile capacity, their selection as a group must be considered. It is not common to have load test data at a preliminary design stage (the point at which theoretical relationships are often first used in a design) and the recommended practice of selecting a shear strength value that is a

cautious estimate of the mean needs to consider the quality of the data. Bearing capacity factors are well defined in literature and in this regard, the selection of an mean shear strength was further scrutinized.

The theoretical methods were found to underestimate capacity (in one occasion) by 7% and overestimate capacity on average by 42% but up to 94% in the 33 remaining cases. This is attributed to the selection of a relatively high mean value for the undrained shear strength. By comparing the measured strength data to back-calculated strength data from the load tests it was determined that a selected value closer to 60% of the mean would be more appropriate (545 kPa vs 902 kPa). This was attributed to a large scatter in the strength data. The bearing capacity factor, Nc, also has a significant impact on the bearing capacity and a project specific value of 5.78 was back-calculated based on the results of the load tests, compared to 8.11 used in predictions.

CTC methods under predicted capacity by as much as 21% and over predicted capacity by up to 141%. When the back calculated $K_T$ value of 11.9 is used, CTC methods over estimated capacity on average by 50%, indicating large scatter in the data (as demonstrated in Figure 4.4). The reliability of torque readings obtained from dial gauges during pile installation also likely contributes to the variability of CTC relationships. These relationships could be improved by methods to record torque such as the fabricated torque pin presented by Harnish (2015). Again, this range in predicted capacities highlights the need for appropriate reduction factors such that the service or ultimate limit states are not reached during a foundation service life. When

a reduction factor of 0.4 is applied to the estimates (recommended in NBCC for design using lab testing data), an average capacity of 994 kN is obtained. At this load, the deflection for all tests were below 15 mm, well within the tolerance of the structures. However, the two distinct SLS and ULS capacities of the piles were 1021 kN/1340 kN and 871 kN/1075 kN, respectively, i.e. higher than 944 kN, indicating a need for a higher capacity. When load testing is completed, design codes often allow for the use of higher resistance factors, and in the case of NBCC, this can be increased to 0.6 and an average capacity of 1484 kN is calculated, well above the SLS and ULS required. This results in a significant cost savings to owners in the form of less piles (i.e. less materials, personnel and time), provided capacities in production are representative of theoretical values. Further, at this load, all of the piles were less than the SLS deflection limit of 25 mm, indicating an acceptable service limit would be obtained for a helical pile foundation, albeit some of the piles required re-torquing to achieve this performance.

## 6.3 Failure Criterion

Failure criteria should be selected on a project specific basis, as randomly applying methods will likely result in under estimation of pile capacity, deflections beyond what is reasonable for most structures, or the criteria simply won't be applicable to the pile response. Using offset methods that are a function of pile dimensions provide a quick means to evaluate ultimate capacity however are likely to result in under estimation. The under estimation of capacity can result in in-efficient designs and significant cost increases for owners. Other failure criteria which rely on large

deflection or plunging failures are not appropriate for load tests on production piles and an additional method to estimate ultimate capacity termed the Creep limit was developed. The Creep limit was applicable in 41% of the cases, compared to 26% for other methods which predicted failure loads within the appropriate portion of the load deflection curve. The Creep limit was within 6% of the maximum, ultimate capacities predicted by other the methods.

## 6.4 Recommendations for Further Research

The Creep limit should be expanded to additional helical pile geometries, loading and soil conditions to further evaluate its applicability. Ideally this could be completed on non-production piles such that a large plunging failure could be developed. Comparing this to the original De Beer criteria would be interesting to see which resulted in a higher predicted capacity and in which region of the load-deflection curve it crossed.

The variability in the shear strength data presented significant uncertainty when calculating ultimate capacity. Several Pile Driving Analyzer (PDA) tests were completed on-site with open ended steel pipe piles. These tests were completed to depths upwards of 24 m below grade and thus could provide an estimate of shear strengths below the helical pile embedment. This data could be used to refine the ultimate capacity predictions by serving as a check as to the selection of shear strength values. Similarly, other load test data could be valuable to complete a statistical analysis to develop criteria for selection of nominal values, that is, describe what a ‘cautious estimate of the mean’ entails.

The theoretical prediction of helical piles should continue with specific attention to the shear strength. A study with a larger data set of reliable strength data would be even more valuable such that this could be removed as an uncertainty in the prediction. Evaluating the effect of helix diameter, pitch and orientation and their effect on $N_c$ could also reduce design uncertainty.

## References


Aydin, M. Bradka, T.D. Kort, D.A. 2011. Osterberg Cell Load Testing on Helical Piles. American Society of Civil Engineers. Geo-Frontiers 2011.

Baracos, A. Shields, S.H. Kjartanson, B. 1983. Geological Engineering Report for the Urban Development of Winnipeg. Department of Geological Engineering, University of Manitoba.

Belbas, R. 2013. The Capacity of Driven Steel H-Piles in Lacustrine Clay, Till and Karst Bedrock: A Winnipeg Case Study. M.Sc. Thesis, University of Manitoba, Winnipeg, Manitoba.

Brinch Hansen, J. 1961. The ultimate resistance of rigid piles against transversal forces. Bulletin No. 12, Danish Geotechnical Institute, Copenhagen, Denmark: 5-9.

Canada. 1995. Canadian Permafrost. National Resources Canada. Department of Energy, Mines and Resources.

Canadian Foundation Engineering Manual, 4th Edition. 2006. Canadian Geotechnical Society.

EBS Geostructural website. Accessed April 29, 2021. Capacity Charts. https://www.ebsgeo.com/helical-piles/capacity-charts

Elkasabgy, M. El Naggar, M.H. 2015. Axial Compressive Response of Large Capacity Helical and Driven Steel Piles in Cohesive Soils. Canadian Geotechnical Journal. 52: 224-243.

Elsherbiny, Z.H. El Naggar, M.H. 2013. Axial Compressive Capacity of Helical Piles from Field Tests and Numerical Study. Canadian Geotechnical Journal. 50:1191-1203.

Fellenius, B.H., 2006. Basics of foundation design. Electronic Edition. www.Fellenius.net, 275 p.

Fuller, F.M. Hoy, H.E. 1970. Pile Load Tests Including Quick-Load Test Method, Conventional Methods and Interpretations. *In* Proceedings of the 49th Annual Meeting of the Highway Research Board. Pp 74-86.

Gavin, K. Doherty, P. Tolooiyan, A. 2014. Field Investigation of the Axial Resistance of Helical Piles in Dense Sand. Canadian Geotechnical Journal, 51:1343-1354.

Ghaly, A. Hanna, A. 1991. Experimental and Theoretical Studies on Installation Torque of Screw Piles. Department of Civil Engineering, Concordia University. Montreal, Quebec.

GoliathTech Inc. website. Accessed January 20, 2021. Stamped Certification Sheets Canada. https://www.goliathtechpiles.com/dev/wp-content/uploads/2017/08/GoliathTech-Technical-Data-Sheet-CAN-MB.pdf

Harnish, J. 2015. Helical Pile Installation Torque and Capacity Correlations. M.Sc. Thesis, University of Western Ontario, London, Ontario, Canada.

Hirany, A., and Kulhawy, F.H. 2002. On the Interpretation of Drilled Foundation Load Test Results. Deep Foundations 2002, An International Perspective on Theory, Design, Construction, and Performance, Geotechnical Special Publication No. 116, ASCE, pp. 1018‑1028.

Hoyt, R.M. Clemence, S.P. 1989. Uplift Capacity of Helical Anchors in Soil. 12th International Conference on Soil Mechanics and Foundation Engineering, Rio de Janeiro, Brazil. Pp. 1019-1022.

Khan, U. Siddiqua, S. 2018. Study of compressive loading capacities of helical piles using torque Method and Induced Settlements. Environmental Earth Sciences (2018) 77:22.

Kumar, D. Yonan, J. Ruban, A. 2014. Oterberg Cell Pile Load Test in Calgary, Alberta – a Case Study. Canadian Geotechnical Society. GeoRegina 2014.

Lanyi, S. 2017. Behaviour of Helical Pile Groups and Individual Piles under Compressive Loading in a Cohesive Soil. Department of Civil and Environmental Engineering. University of Alberta. Edmonton, Alberta.

Lanyi-Bennet, S.A. Deng, L. 2018. Axial Load Testing of Helical Pile Groups in Lacustrine Clay. Canadian Geotechnical Journal, 56:187-197 (2019). dx.doi.org/10.1139/cgj-2017-0425.

Li, W. Zhang, D.J.Y. Sego, D.C. Deng, L. 2018. Field Testing of Axial Performance of Large-Diameter Helical Piles at Two Soil Sites. Journal of Geotechnical and Geoenvironmental Engineering, ASCE. ISSN 1090-0241.

Livneh, B. Naggar, M.H.M. 2008.Axial Testing and Numerical Modelling of Square Shaft Helical Piles under Compressive and Tensile Loading. Can. Geotech.J.45(8),1142–1155.

Lutenegger, A. J., and Tsuha, C. H. C. 2015. "Evaluating installation disturbance from helical piles and anchors using compression and tension tests." 15th Pan-American Conference on Soil Mechanics and Geotechnical Engineering, Buenos Aires, Argentina.

Matile, G.L.D. and Keller, G.R. 2006: Surficial geology of east-central (NTS 54C), Manitoba; Manitoba Science, Technology, Energy and Mines, Manitoba Geological Survey, Surficial Geology Compilation Map SG-ECMB, scale 1:250 000.

Mitsch, M.P. Clemence, S.P.1985. The Uplift Capacity of Helix Anchors in Sand. American Society of Civil Engineers, New York, pp.26–47.

Mohajerani, A. Bosnjak, D. Bromwich, D. 2016. Analysis and Design Methods of Screw Piles: A Review. The Japanese Geotechnical Society. 0038-0806. http://dx.doi.org/10.1016/j.sandf.2016.01.009.

Mooney, J.S. Adamczak, S. Clemence, S.P. 1985. Uplift Capacity of Helix Anchors in Clay and Silt. American Society of Civil Engineers, 48–72.

Nabizadeh, F. Choobbasti, A.J. 2017. Field Study of Capacity Helical Piles in Sand and Silty Clay. Transp. Infrastruct. Geotech. 4, 3–17. https://doi.org/10.1007/s40515-016-0036-0

NeSmith, W.M. Timothy, C.S. 2009. Shortcomings of the Davisson Offset Limit Applied to Axial Compressive Load Tests on Cast-in-Place Piles. International Foundation Congress and Equipment Expo 2009. DOI:10.1061/41021(335)71

O'Neil, M. W. & Reese, L. C. 1999. Drilled Shafts: Construction Procedures & Design Methods. Rpt. FHWA-IF-99-025, Federal Highway Admin., Washington, DC.

Pack, J.S. 2000. Design of Helical Piles for Heavily Loaded Structures. New Technological and Design Developments in Deep Foundations. American Society of Civil Engineers, USA, pp. 353-367

Perko, H.A. 2009. Helical Piles - A Practical Guide to Design and Installation. John Wiley & Sons, Inc. Hoboken, New Jersey.

Postech Screw Piles website. Accessed January 20, 2021. Technical Data Sheets. https://postechpiles.com/technical-informations/p178/

Poulos, H.G. Carter, J.P. Small, J.C. 2001. Foundations and Retaining Structures – Research and Practice. Proceedings of the 15th International Conference on Soil Mechanics and Foundation Engineering, Istanbul, Vol.4 pp.2527-2606.

Rao, N. Prasad, Y.V.S.N. Shetty, D. June 1991. The Behavior of Model Screw Piles in Cohesive Soils. Soils and Foundations. The Japanese Society of Soil Mechanics and Foundations Engineering. Vol. 31, No2, 35-50.

Sakr, M. 2009. Performance of Helical Piles in Oil Sand. Canadian Geotechnical Journal. 46: 1046-1061.

Sakr, M. 2011. Installation and Performance Characteristics of High-Capacity Helical Piles in Cohesionless Soils. Deep Foundation Institute Journal Vol. 5. No.1 (39).

Skaftfeld, K. 2014. Experience as a Guide to Geotechnical Practice in Winnipeg. M.Sc. Thesis, University of Manitoba, Winnipeg, Manitoba.

Tappenden, K.M. 2007. Predicting the Axial Capacity of Screw Piles Installed in Western Canadian Soils. M.Sc. Thesis, University of Alberta, Edmonton, Alberta.

Tappenden, K.M. Sego, D.C. 2007. Predicting the Axial Capacity of Screw Piles Installed in Canadian Soils. In: Proceedings of the Canadian Geotechnical Society Conference, OttawaGeo 2007, pp. 1608-1615.

Tappenden, K.M. Abazari, E. Sego, D.C. 2018. Load Transfer Behavior of Full-Scale Instrumented Helical Piles. GeoEdmonton 2018.

TREK Geotechnical Inc. November 9, 2015. Results of APE Helical Pile Installation Trial and Load Test Program – Revised.

Weech, C. Howie, JA. 2012. Helical Piles in Soft Sensitive Soils – a Field Study of Disturbance Effects on Pile Capacity. VGS Symposium on Soft Ground Engineering. Vancouver, B.C.

Weidong, Li. Zhang, D.J.Y. Sego, D.C. Deng, Lijun. 2017. Field Testing of Axial Performance of Lage-Diameter Helical Piles at Two Soil Sites. Journal of Geotechnical and Environmental Engineering. ASCE, ISSN 1090-0241.

# Appendix A

## Pile Load Test Results - Load-Deflection Curves

**Figure A1. Pile Load Test 1 – Pile 1073**

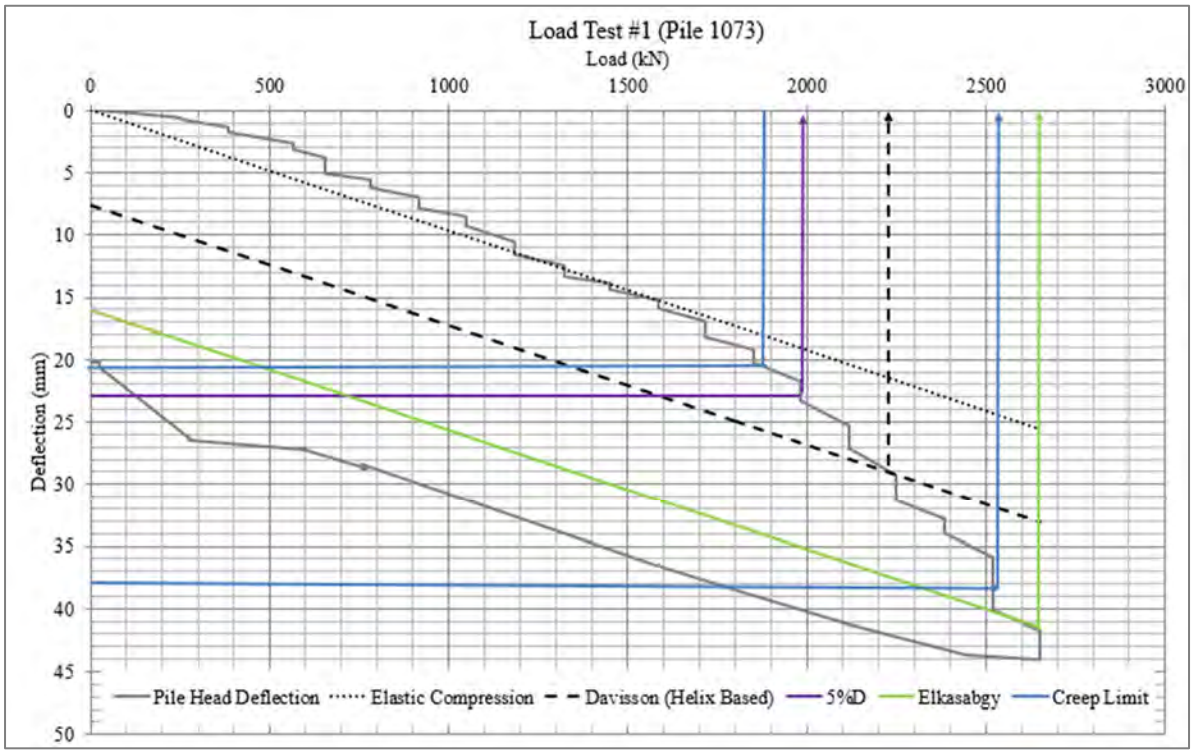


*Figure A1a. Load Test Interpretation*

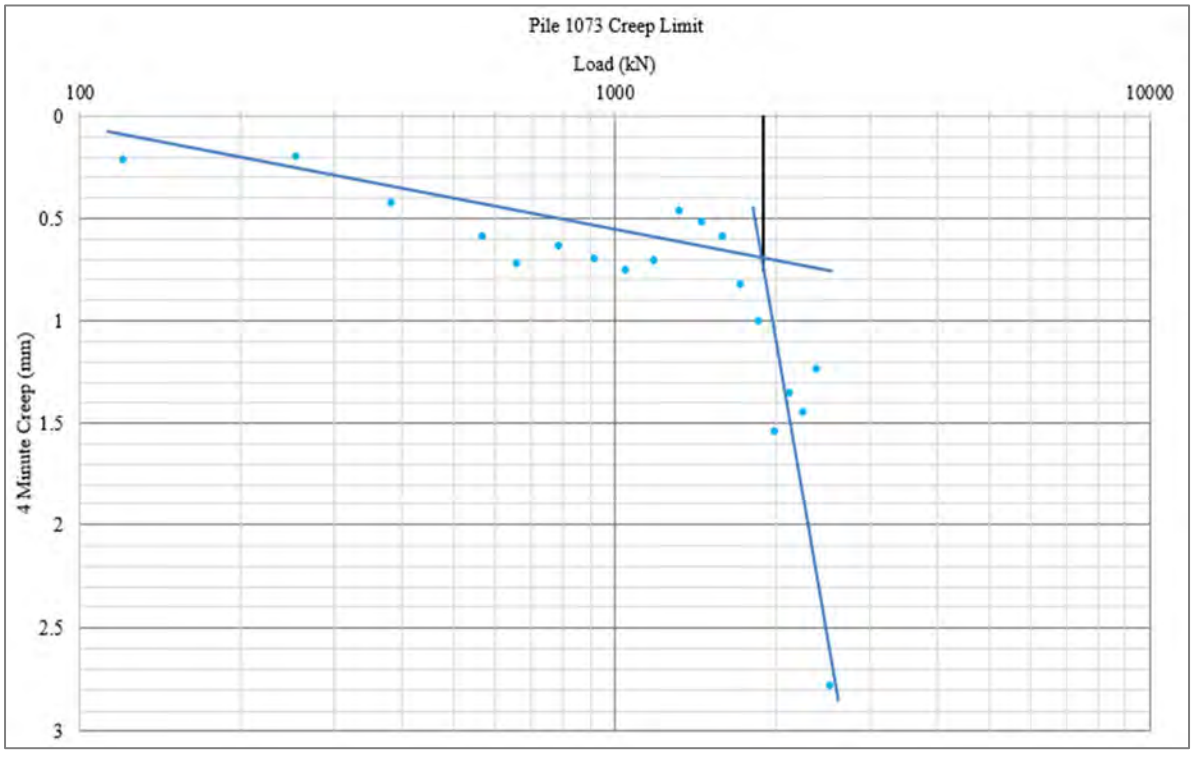


*Figure A1b. Creep Limit Interpretation, Creep limit=1890kN*

**Figure A2. Pile Load Test #2 – Pile 1062**


*Figure A2a. Load Test Interpretation*

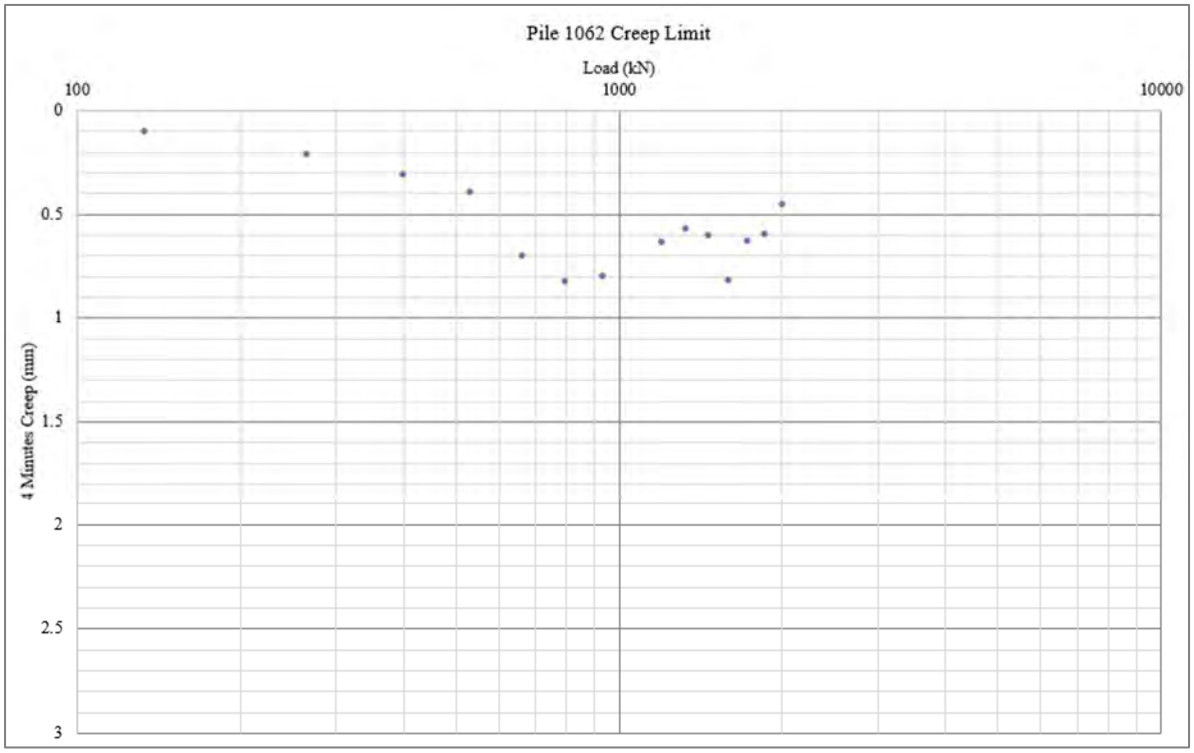


*Figure A1b. Creep Limit Interpretation, Creep limit=1890kN for Pile 1062 shown to illustrate how two distinct linear sections did not develop*

**Figure A3. Pile Load Test #3 – Pile 7076**

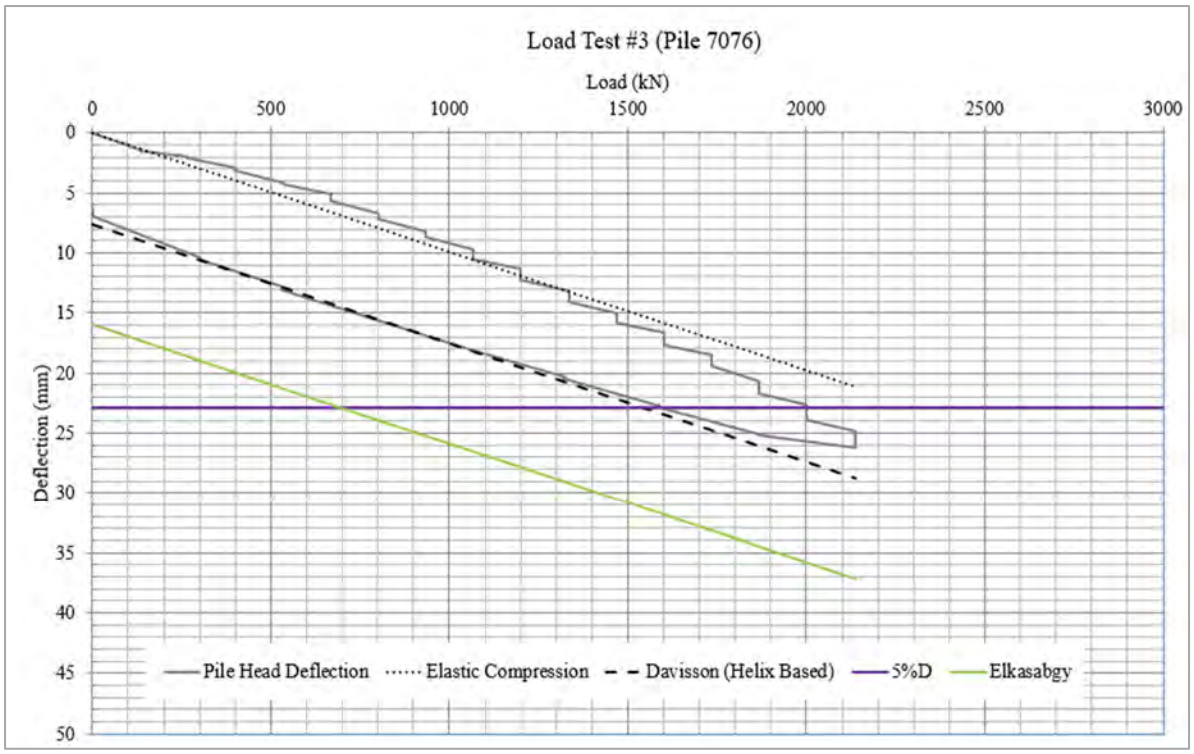


*Figure A3a. Load Test Interpretation*

Creep limit did not develop

**Figure A4. Pile Load Test #4 – Pile 7010**

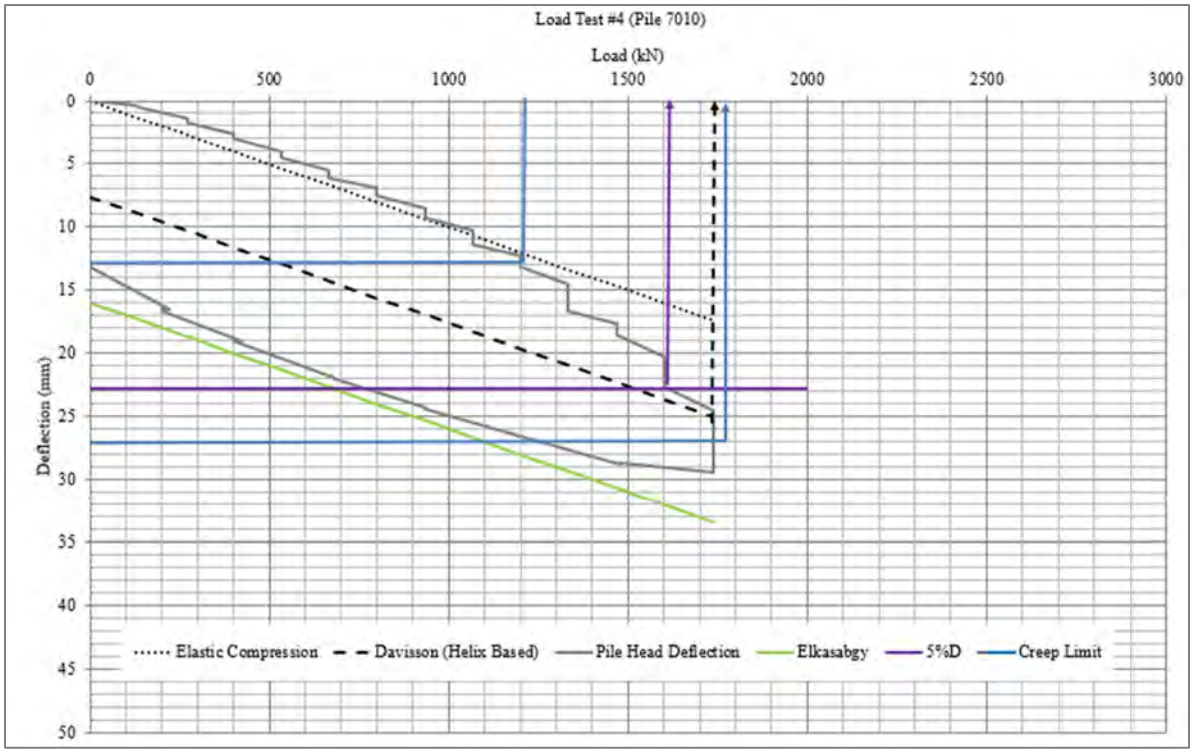


*Figure A4a. Load Test Interpretation*

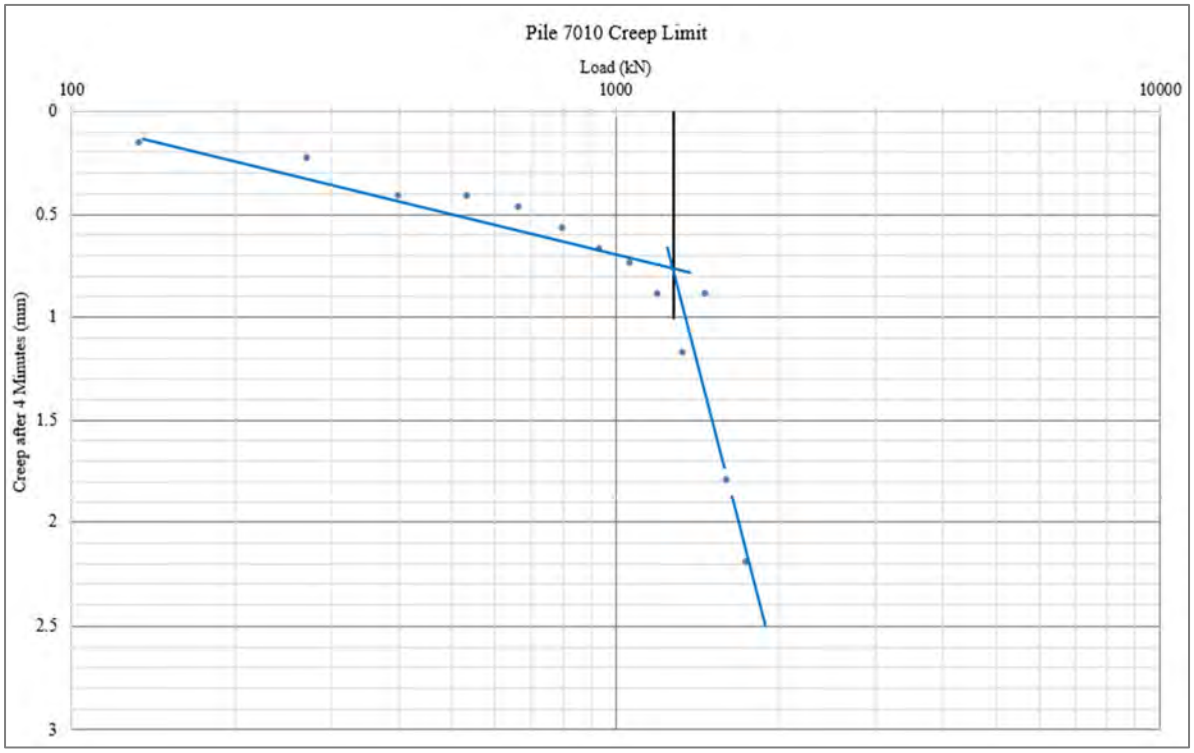


*Figure A4b. Creep Limit Interpretation, Creep limit=1280kN*

**Figure A5. Pile Load Test #5 – Pile 1063-2**

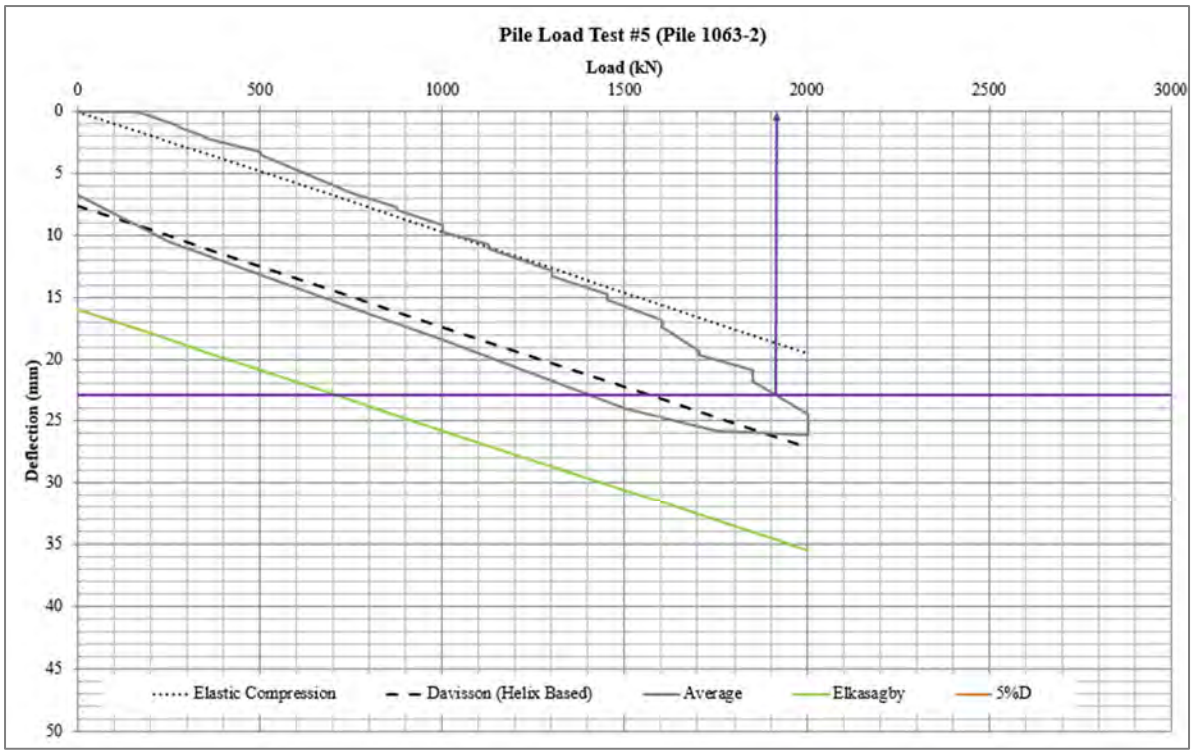


*Figure A5a. Load Test Interpretation*

Creep limit did not develop

**Figure A6. Pile Load Test #8 – Pile 5008**

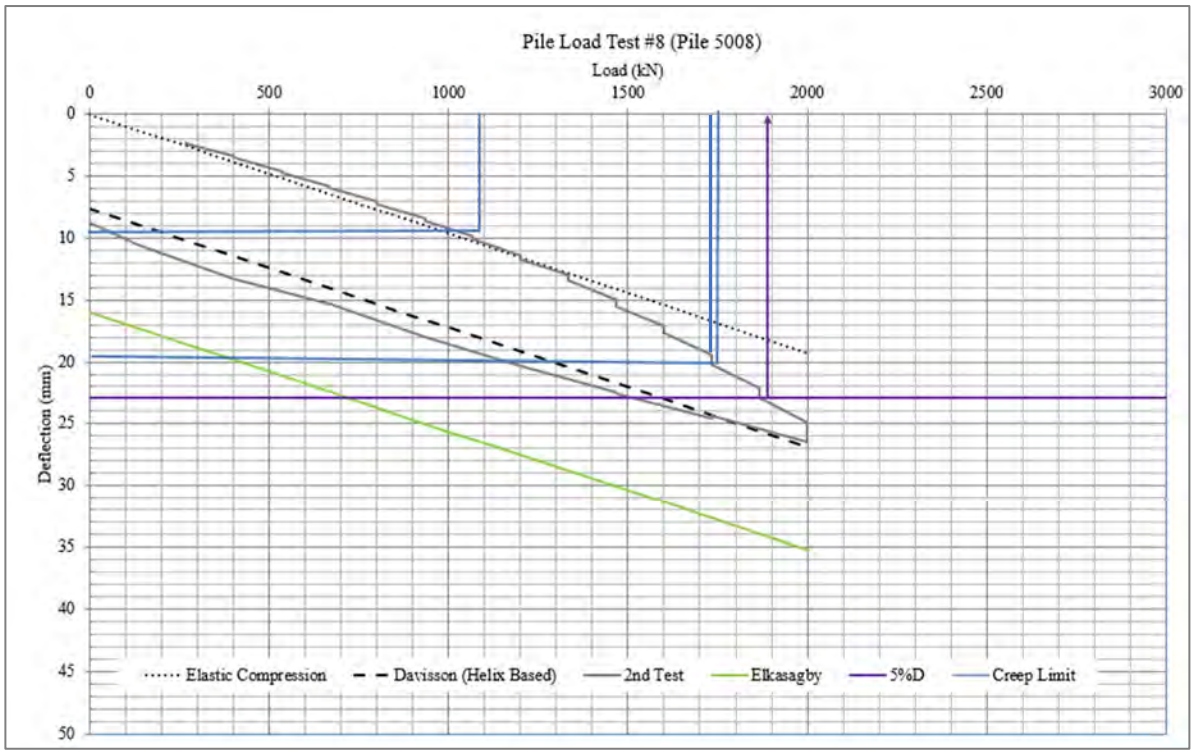


*Figure A6a. Load Test Interpretation*

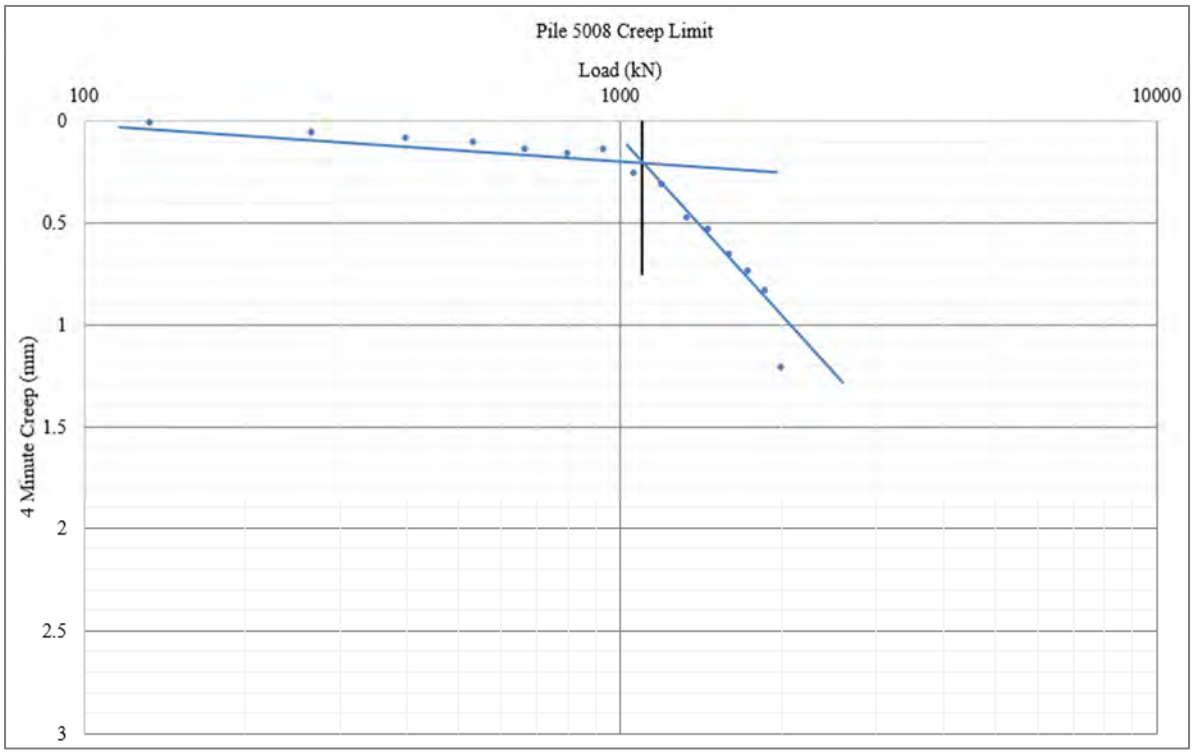


*Figure A6b. Creep Limit Interpretation Creep limit=1100kN*

**Figure A7. Pile Load Test #10 – Pile 2023**

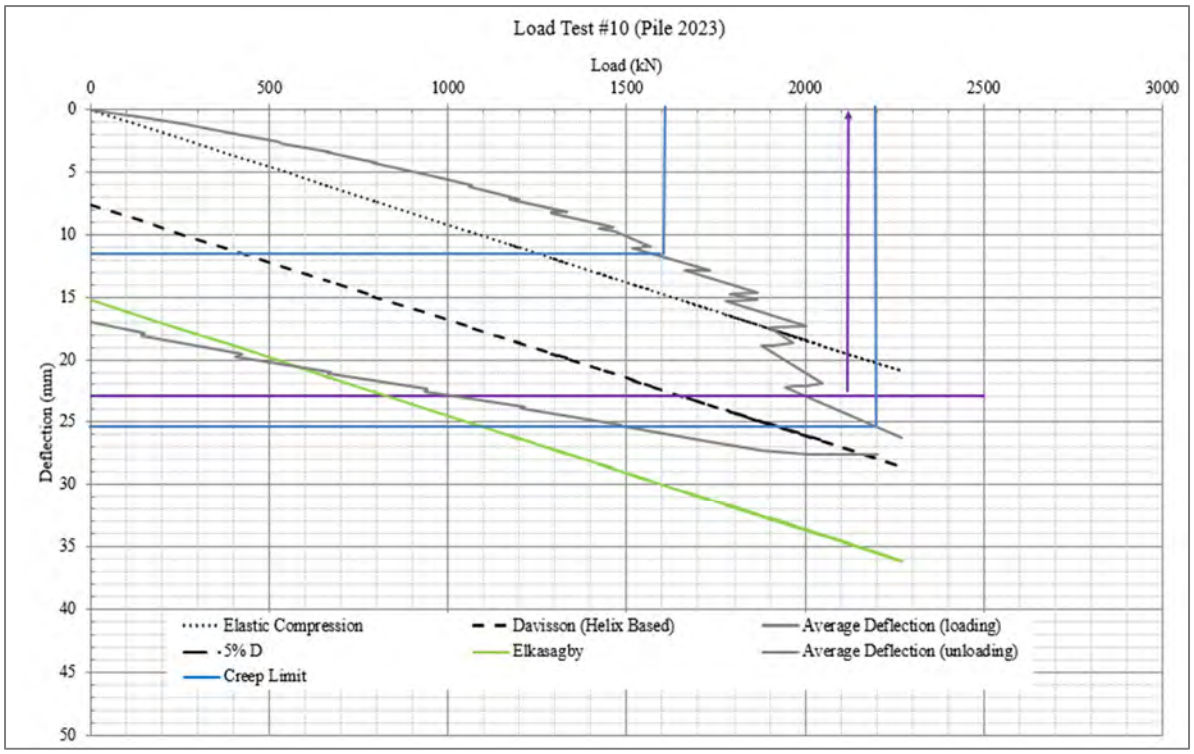


*Figure A7a. Load Test Interpretation*

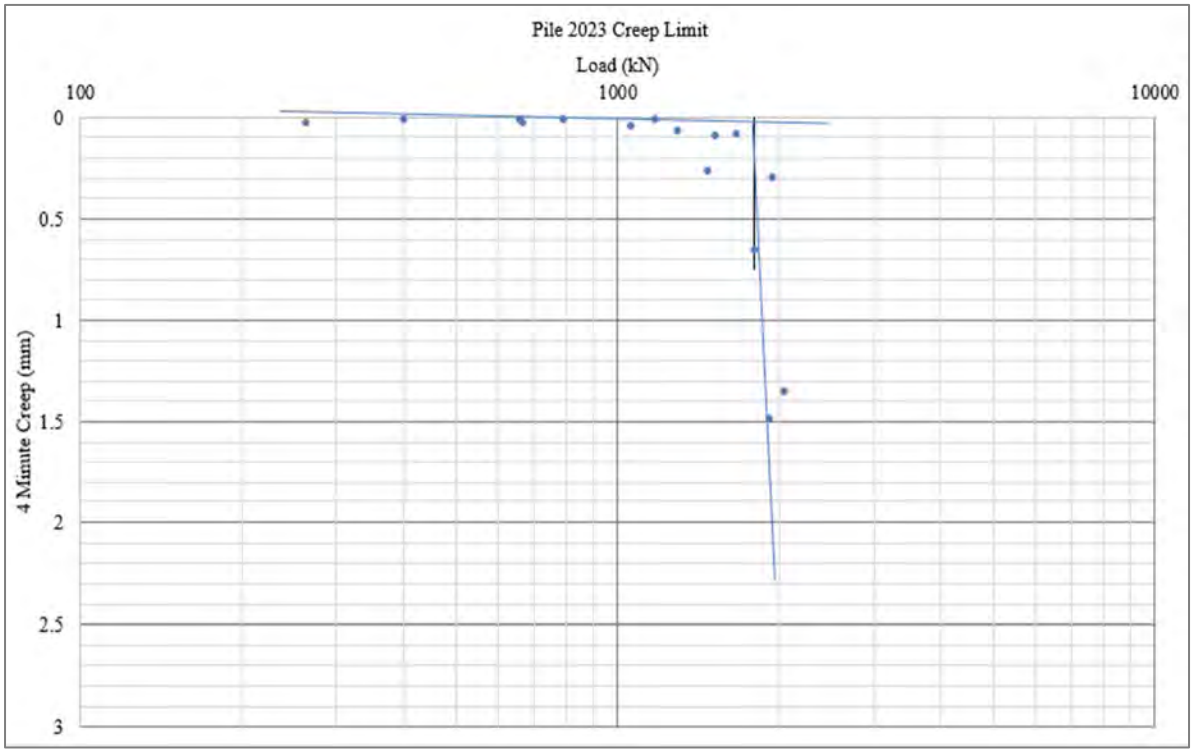


*Figure A7b. Creep Limit Interpretation. Creep limit=1560kN*

**Figure A8. Pile Load Test #13 – Pile 1428**

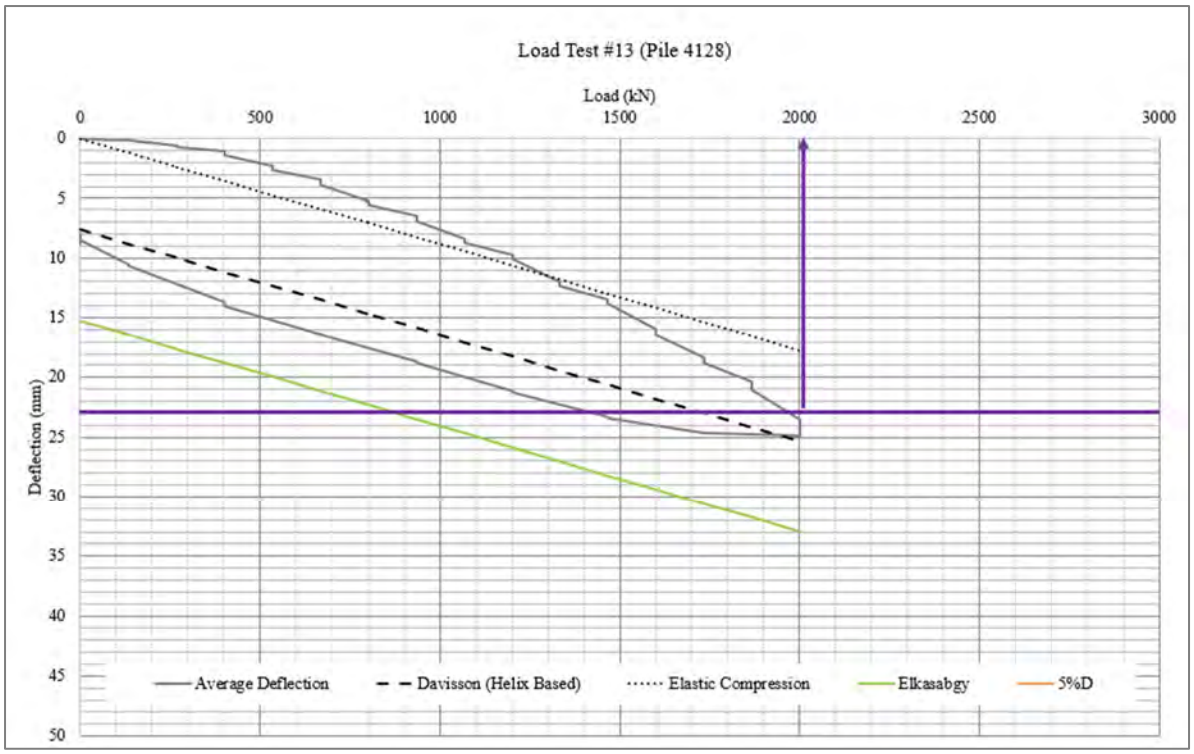


*Figure A8a. Load Test Interpretation*

Creep limit did not develop.

**Figure A9. Pile Load Test #14 – Pile 6058**

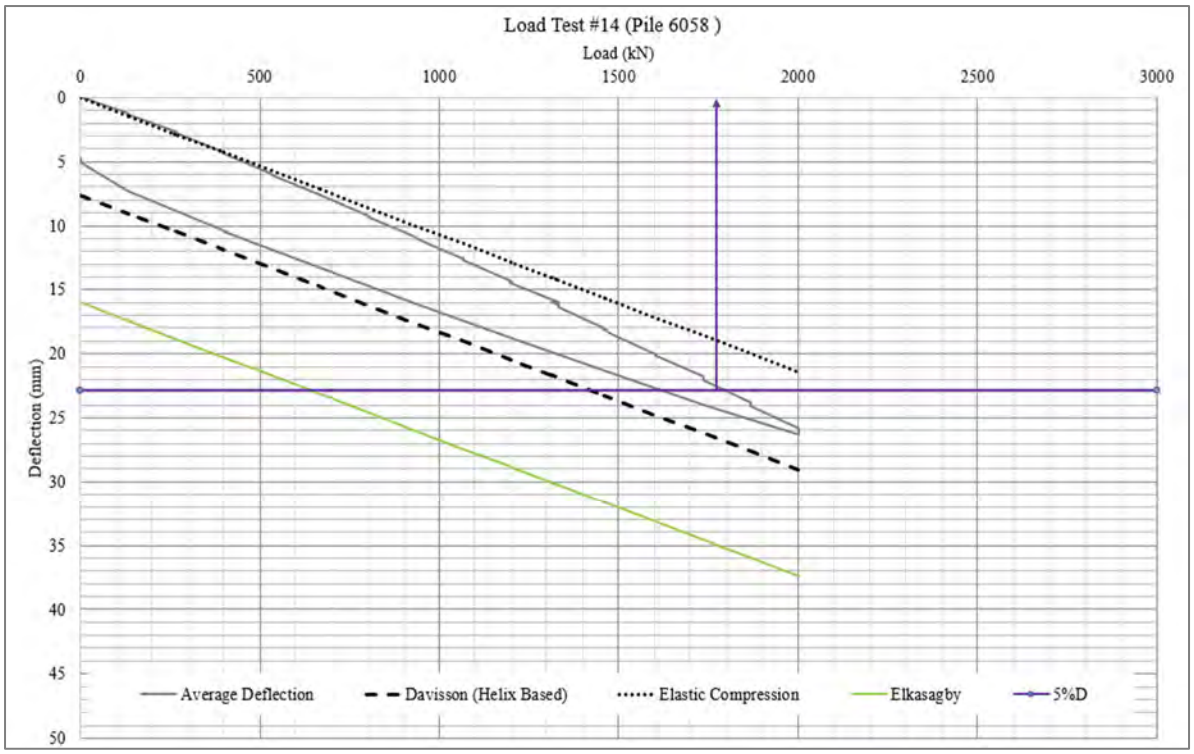


*Figure A9a. Load Test Interpretation*

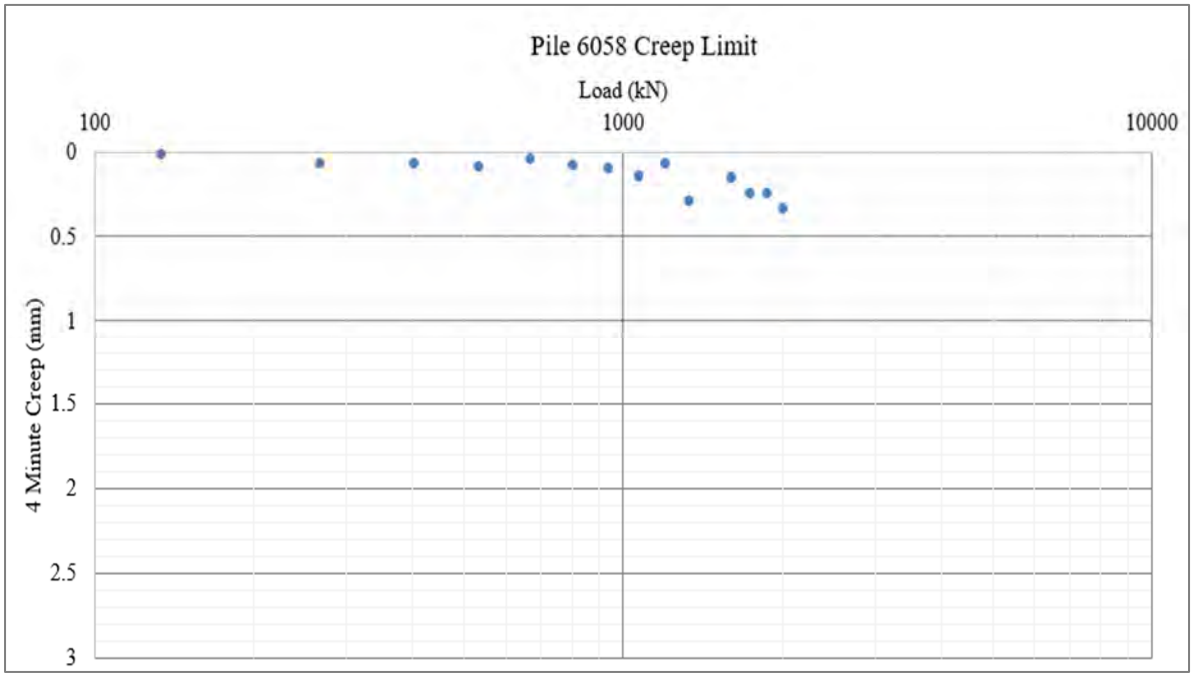


*Figure A9b. Creep limit did not develop. Creep results shown for illustration.*

**Figure A10. Pile Load Test #15 – Pile 2119**

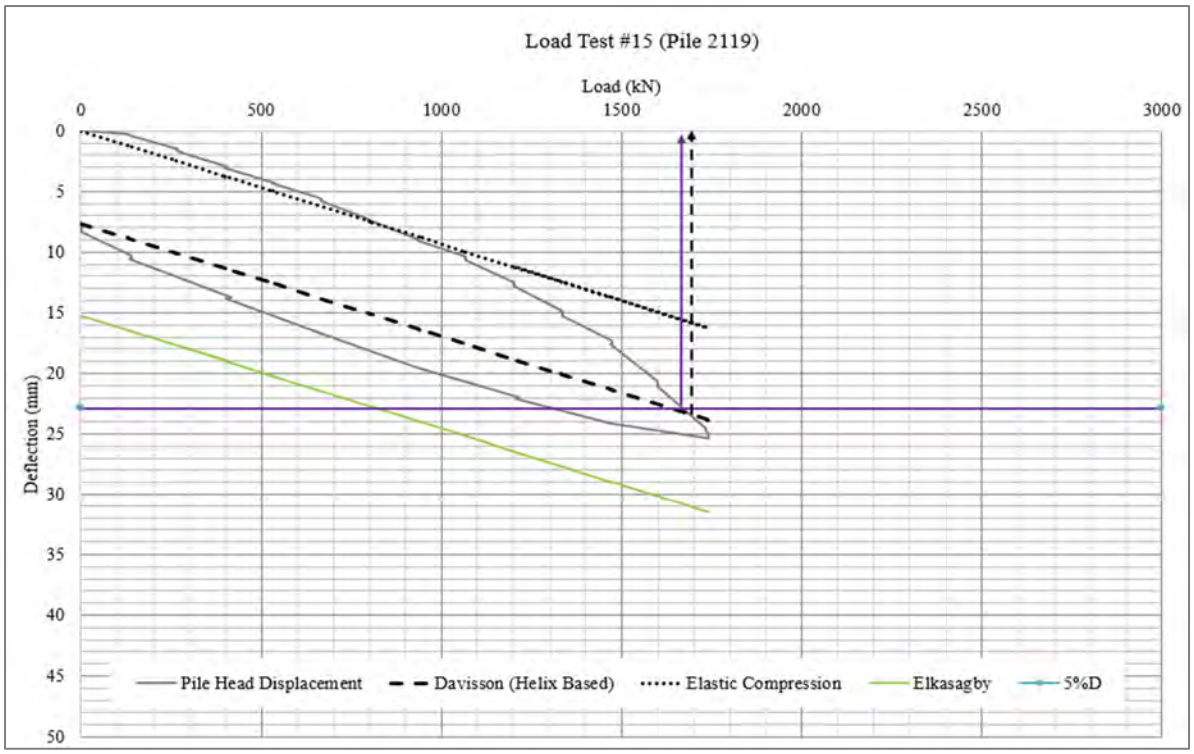


*Figure A10a. Load Test Interpretation*

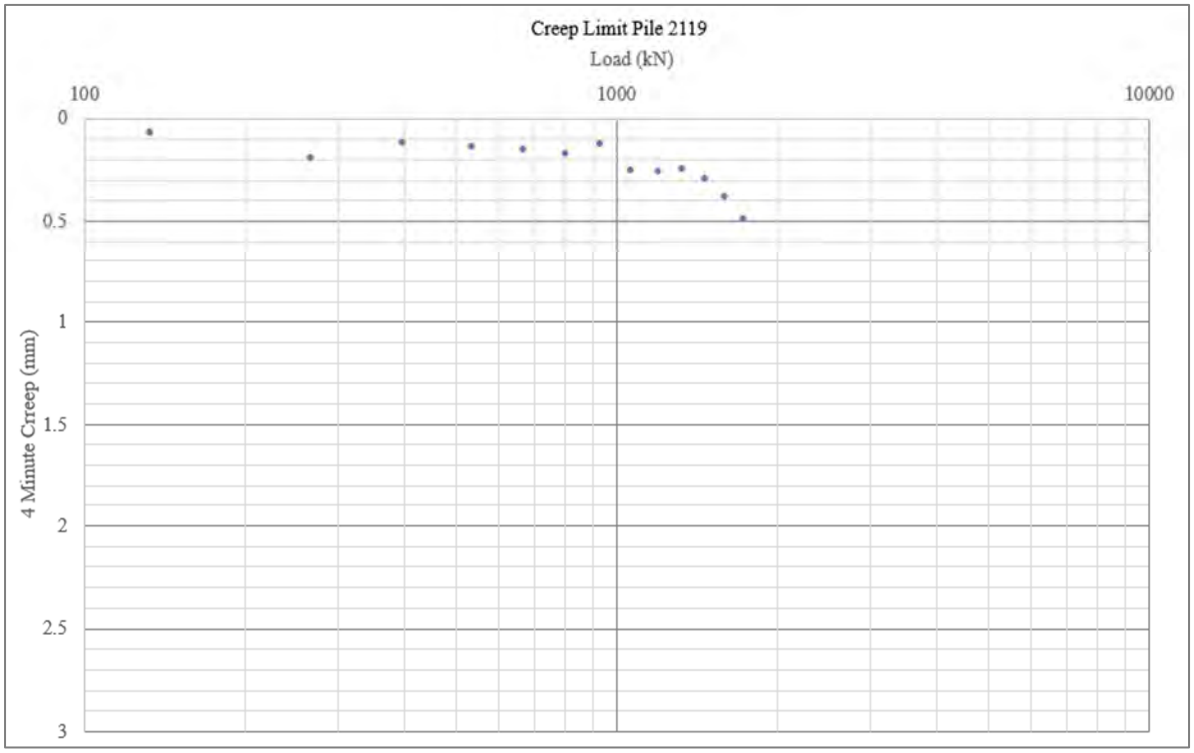


*Figure A10b. Creep limit did not develop. Test shown to illustrate how Type 2 tests progress into plunging failure but do not develop.*

**Figure A11. Pile Load Test #16 – Pile 1038**

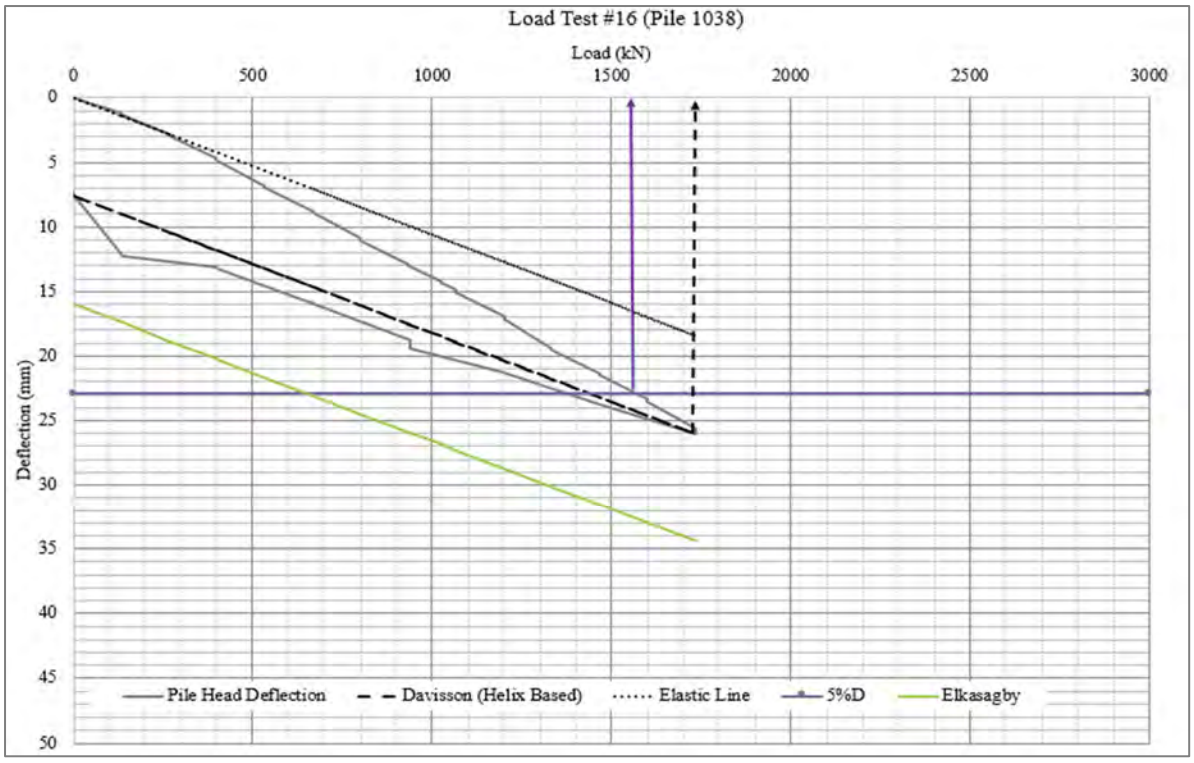


*Figure A11a. Load Test Interpretation*

Creep limit not developed.

**Figure A12. Pile Load Test #17 – Pile 2046**

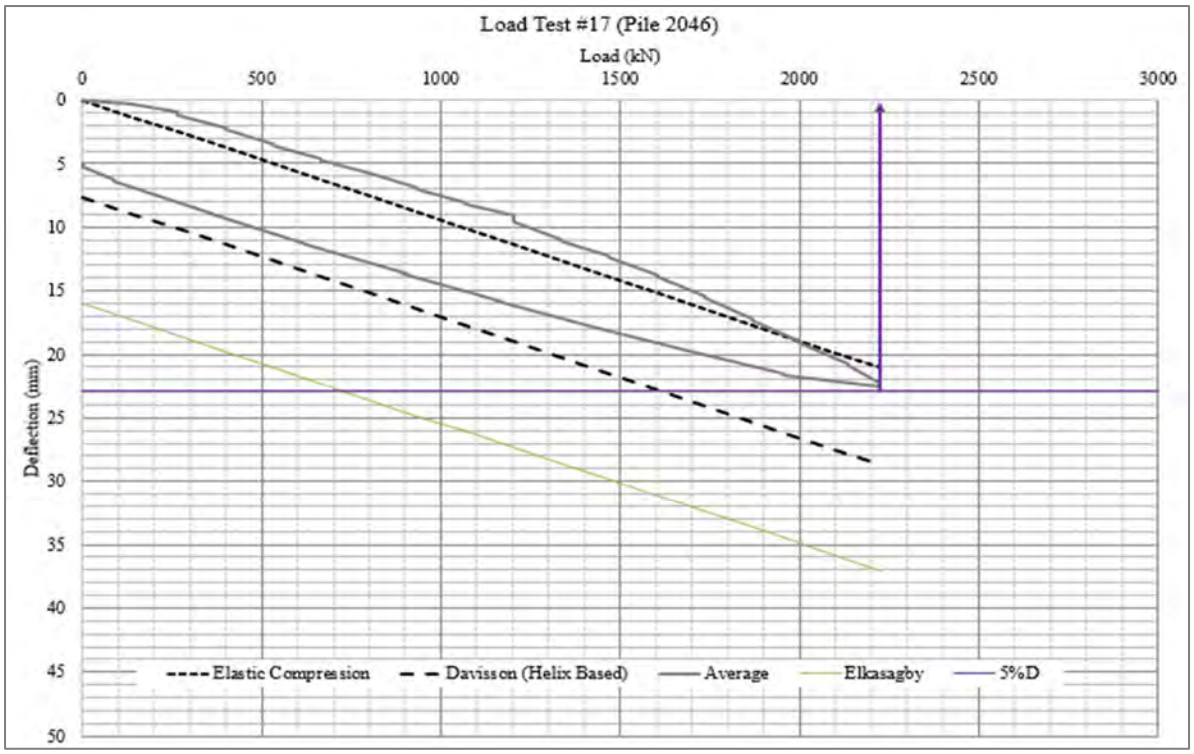


*Figure A12a. Load Test Interpretation*

Creep limit not developed.

**Figure A13. Pile Load Test #21 – Pile 2123**

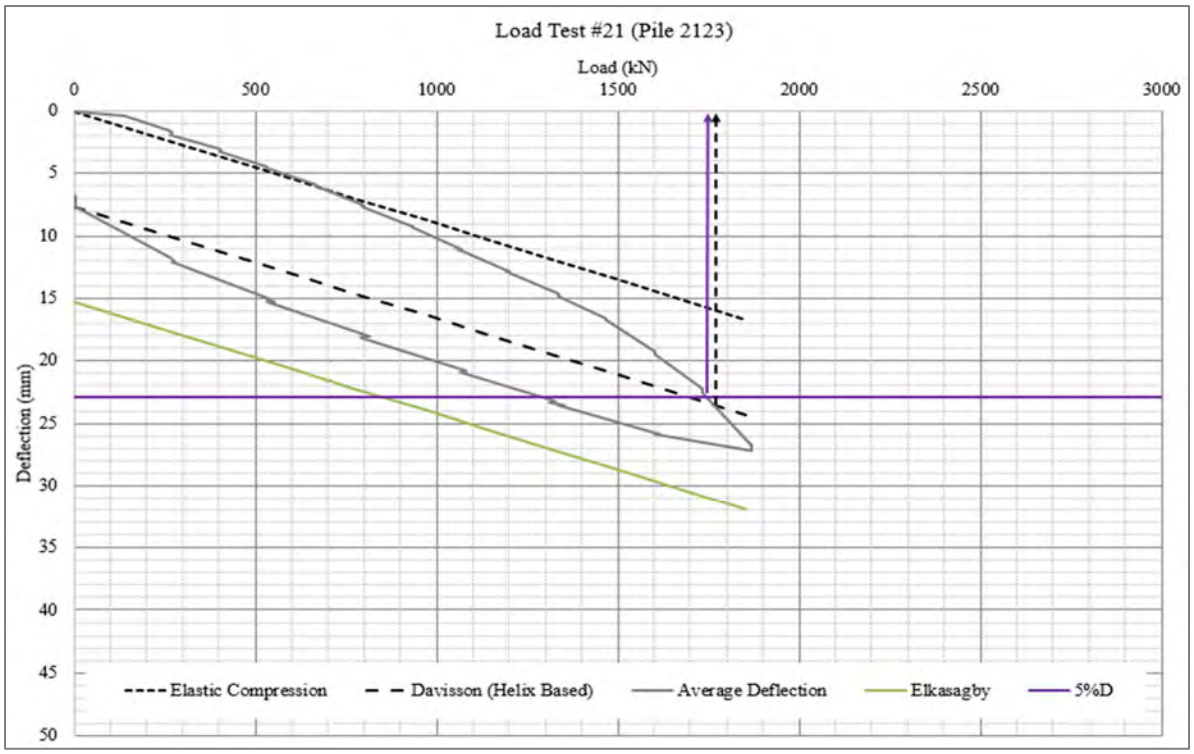


*Figure A13a. Load Test Interpretation*

Creep limit not developed.

**Figure A14. Pile Load Test #23 – Pile 2016**

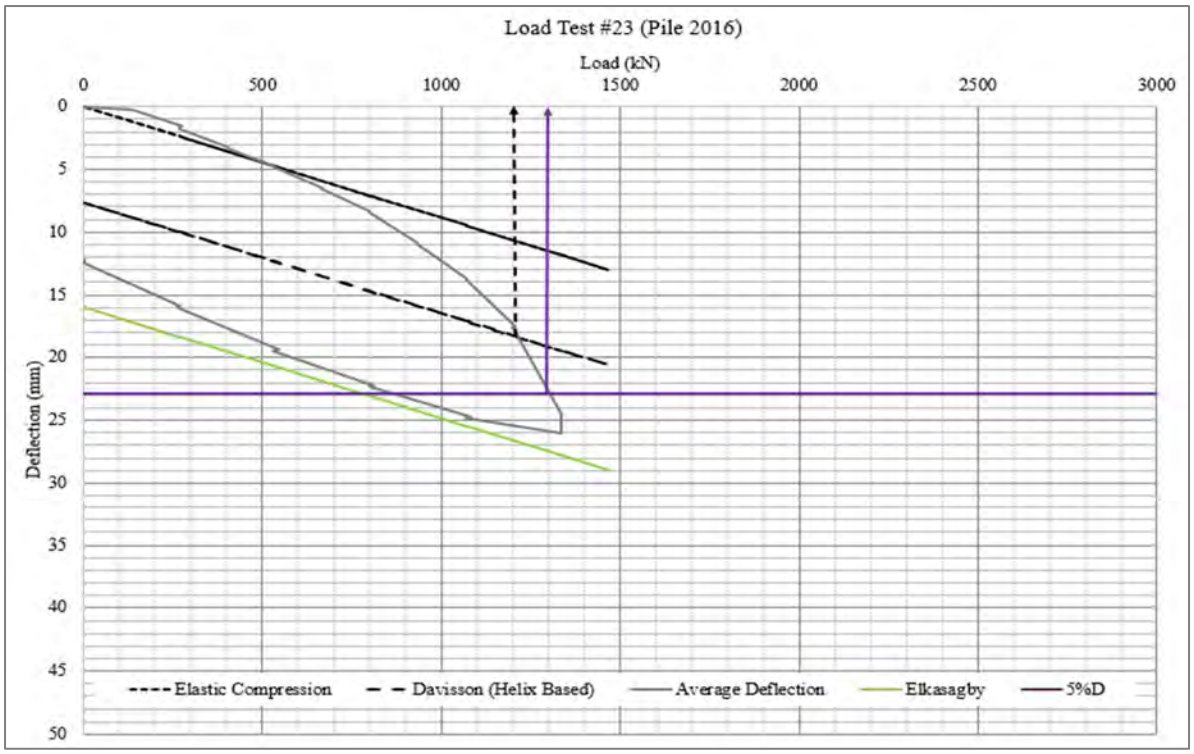


*Figure A14a. Load Test Interpretation*

Creep limit not developed.

**Figure A15. Pile Load Test #24 – Pile 3050**

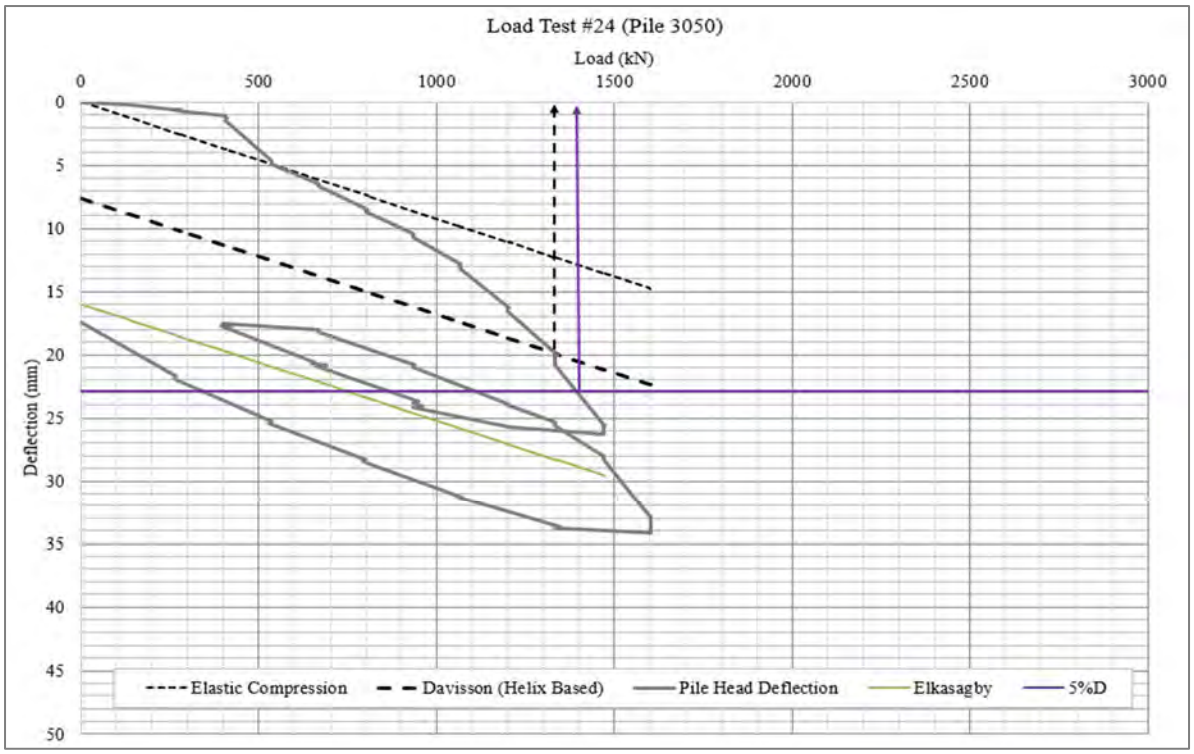


*Figure A15a. Load Test Interpretation*

Creep limit not developed.

**Figure A16. Pile Load Test #28 – Pile 4011**

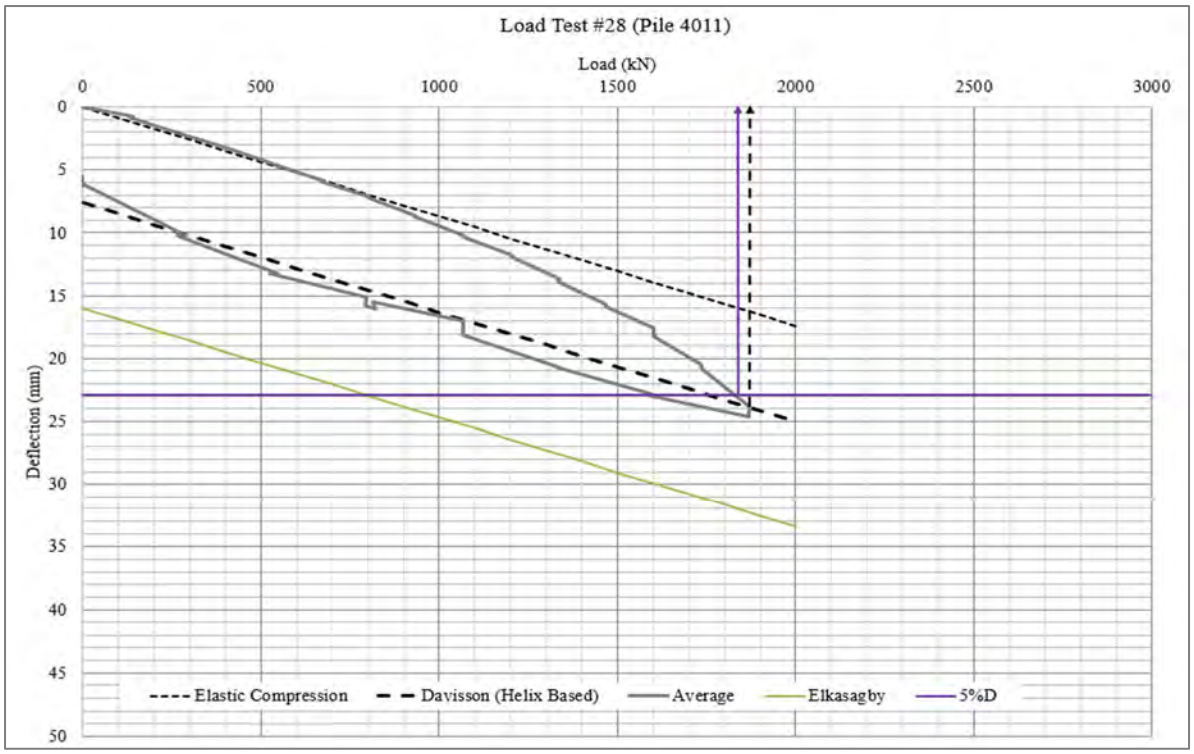


*Figure A16a. Load Test Interpretation*

Creep limit not developed.

**Figure A17. Pile Load Test #30 – Pile 6013**

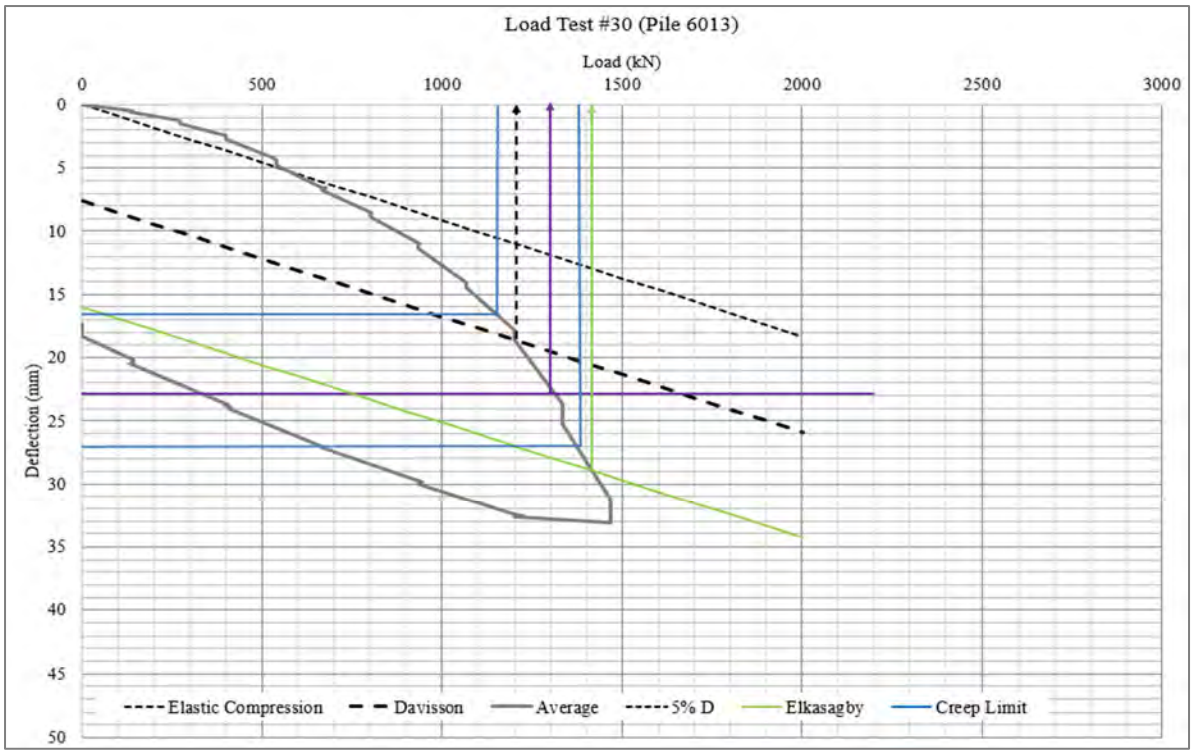


*Figure A17a. Load Test Interpretation*

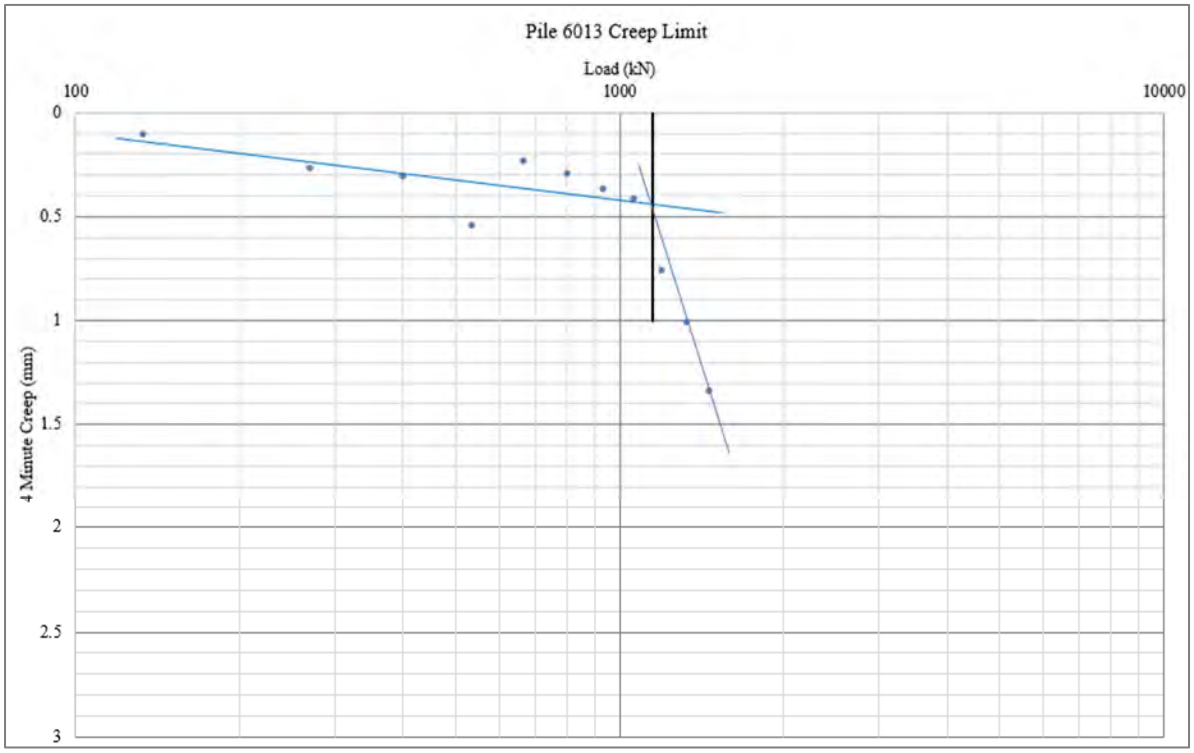


*Figure A17b. Creep Limit Interpretation. Creep limit=1150kN.*

**Figure A18. Pile Load Test #31 – Pile 5052**

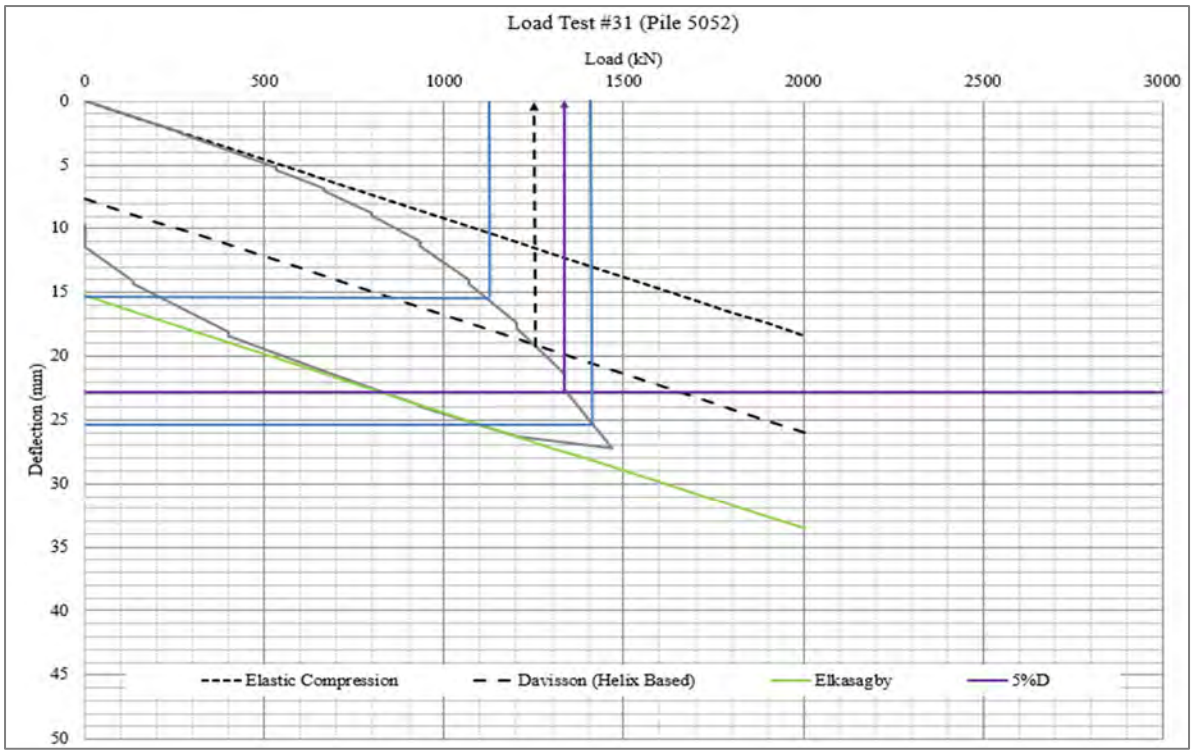


*Figure A18a. Load Test Interpretation*

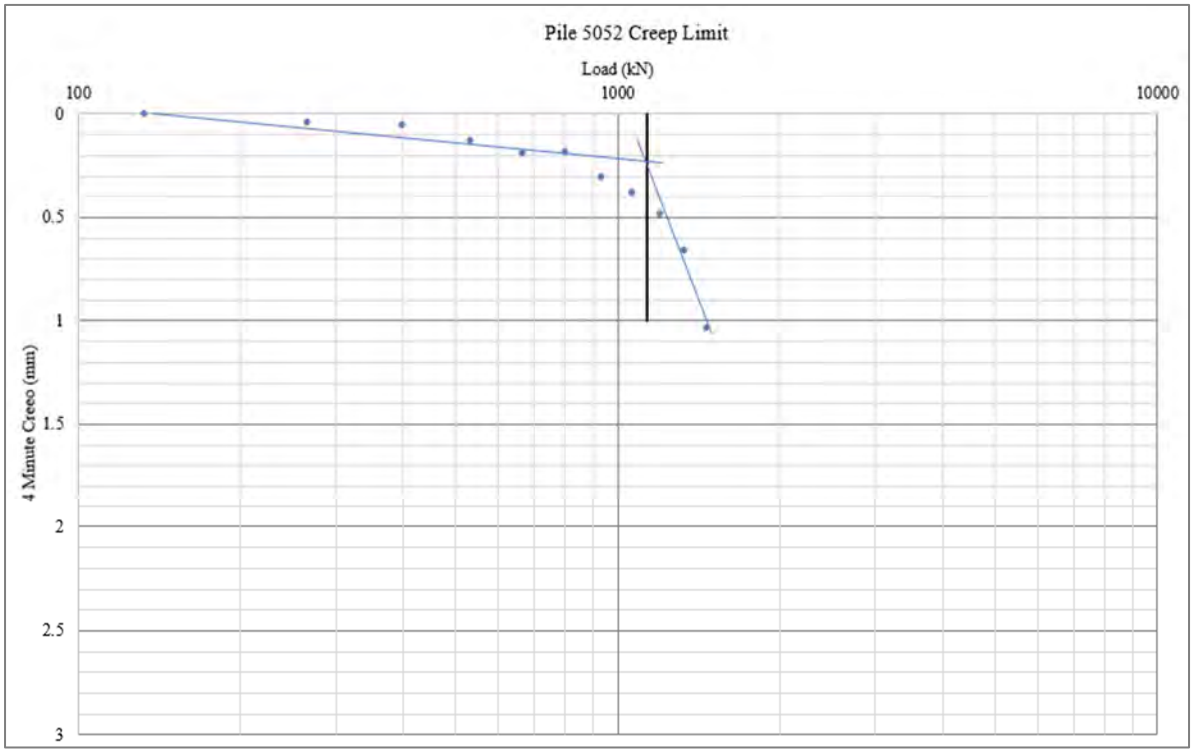


*Figure A18b. Creep Limit Interpretation. Creep limit=1130kN*

**Figure A19. Pile Load Test #32 – Pile 6078**

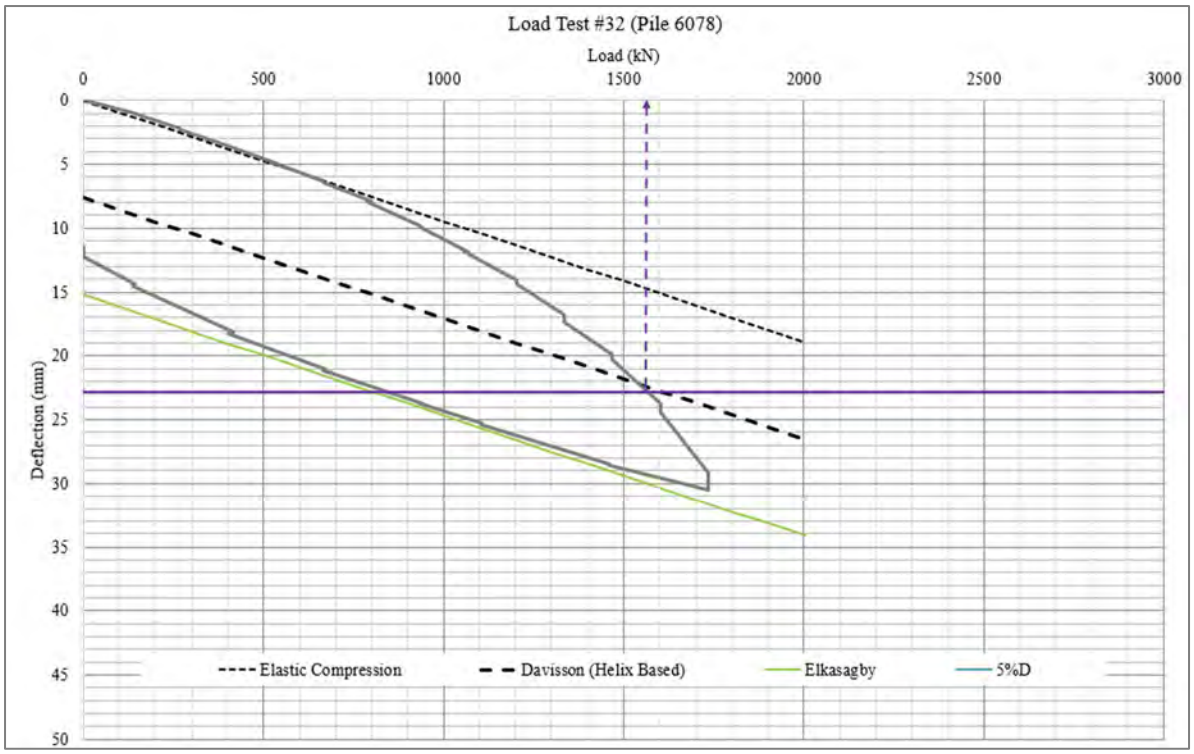


*Figure A19a. Load Test Interpretation*

Creep limit=1410kN. Creep method did not cross curve.

**Figure A20. Pile Load Test #33 – Pile 5016**

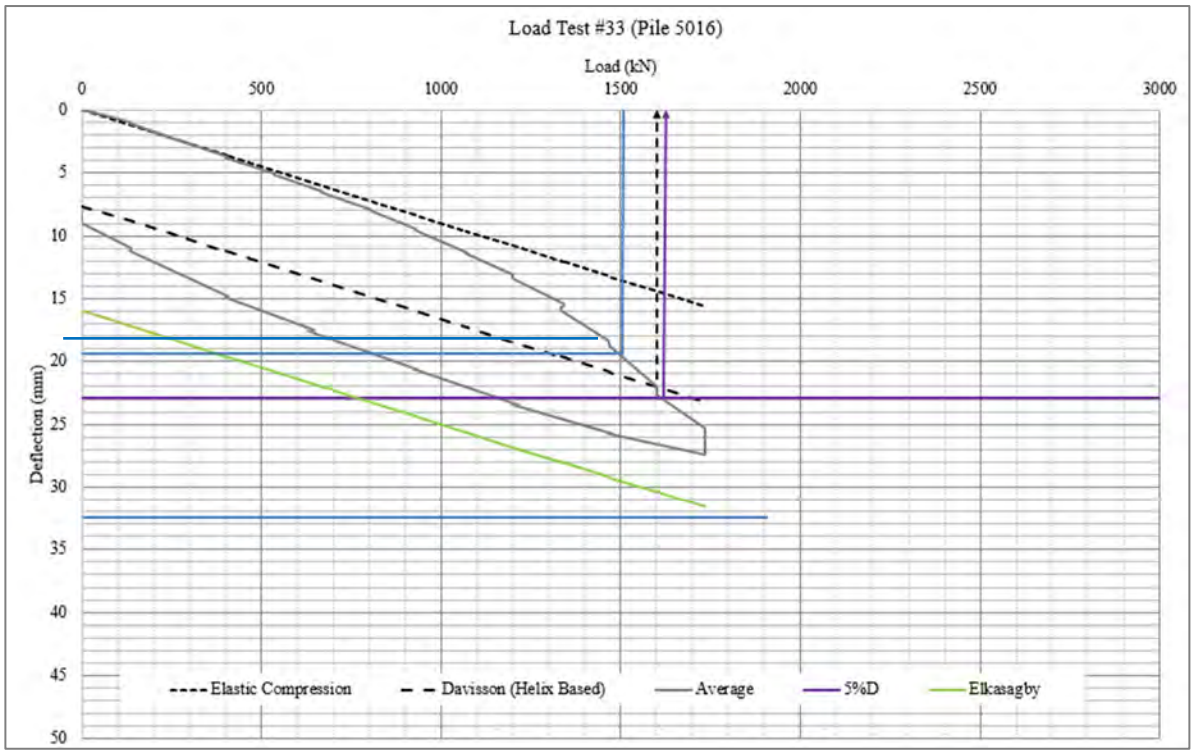


*Figure A20a. Load Test Interpretation*

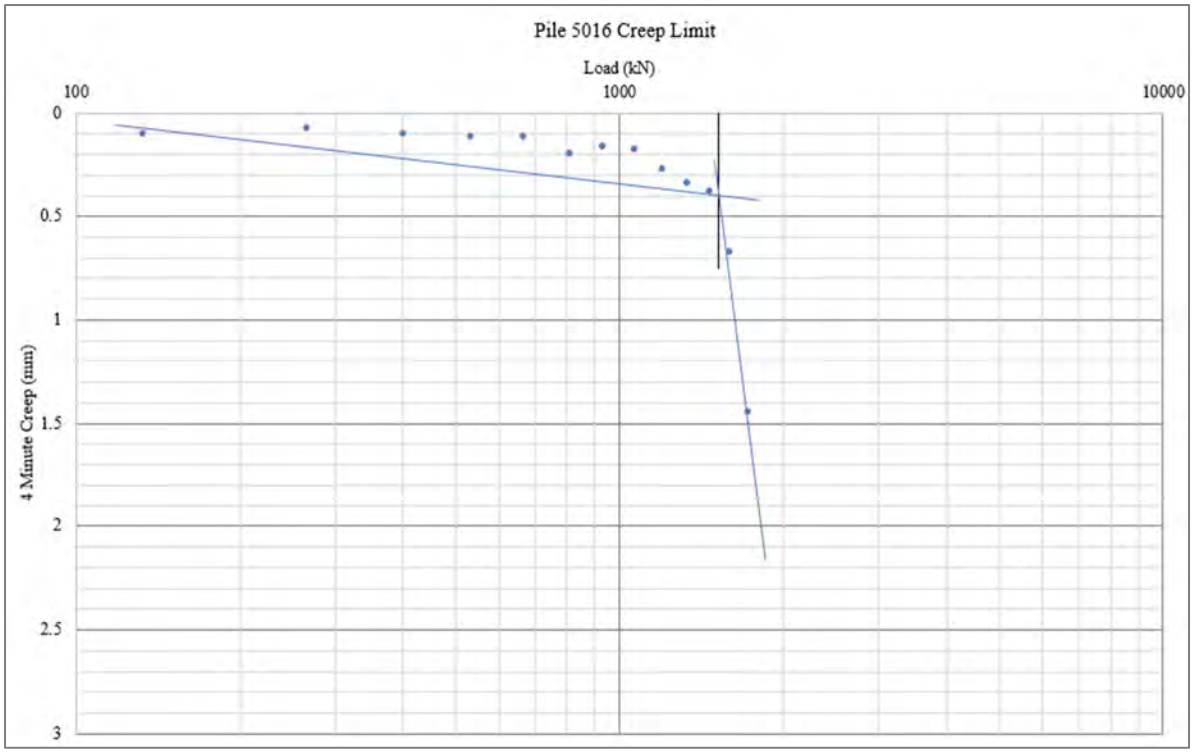


*Figure A20b. Creep Limit Interpretation. Creep limit=1510kN. Creep method did not cross curve.*

**Figure A21. Pile Load Test #34 – Pile 6112**

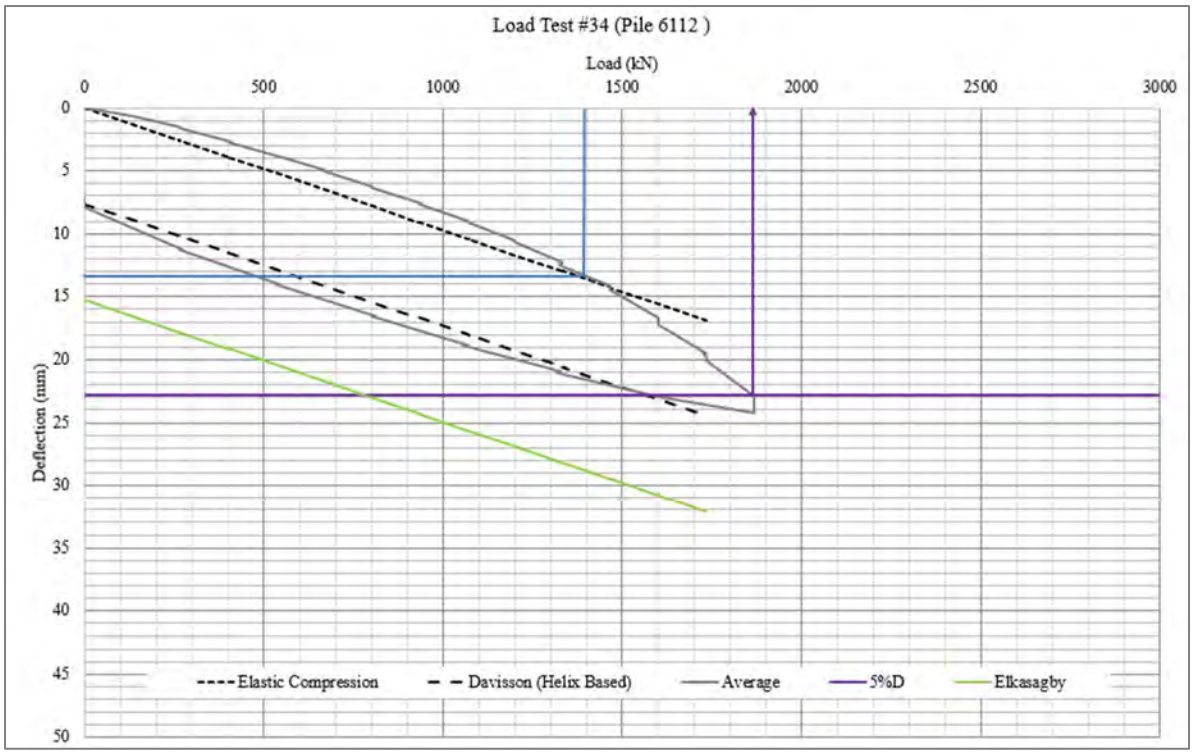


*Figure A21a. Load Test Interpretation*

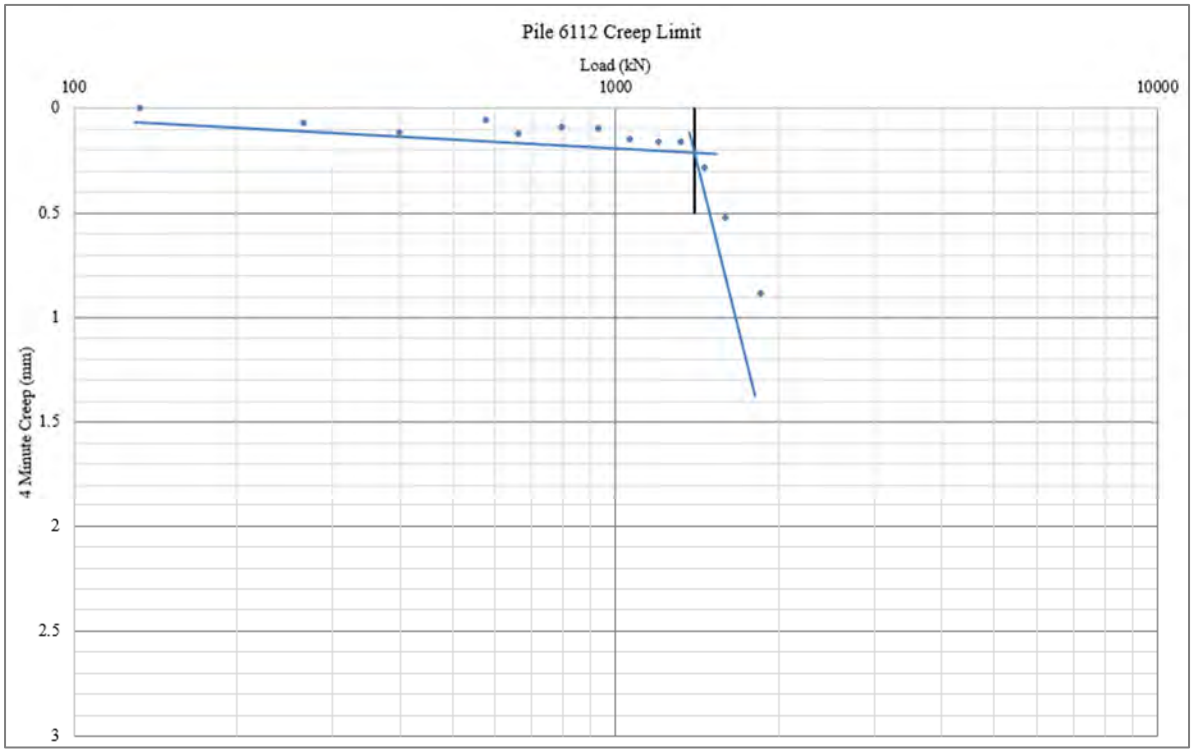


*Figure A21b. Creep Limit Interpretation. Creep limit=1400kN. Creep method did not cross load curve.*

**Figure A22. Pile Load Test #36 – Pile 5033**

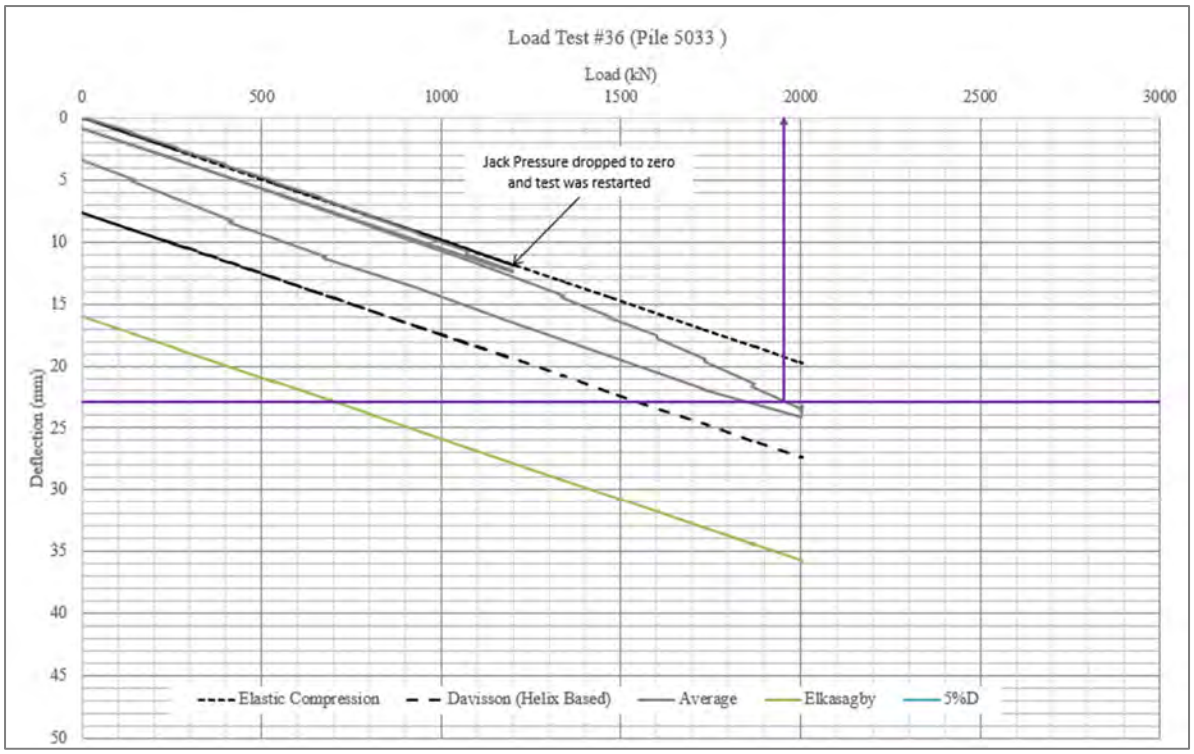


*Figure A22a. Load Test Interpretation*

Creep limit did not develop.

**Figure A23. Pile Load Test #38 – Pile 5014**

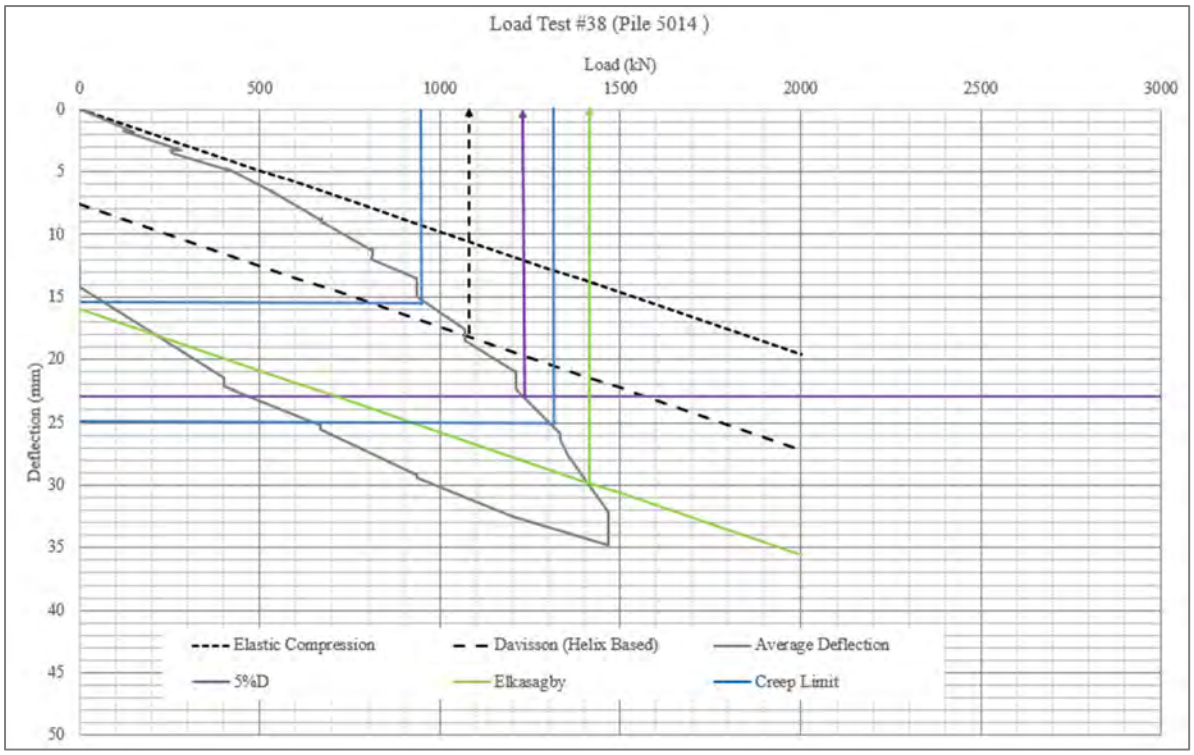


*Figure A23a. Load Test Interpretation*

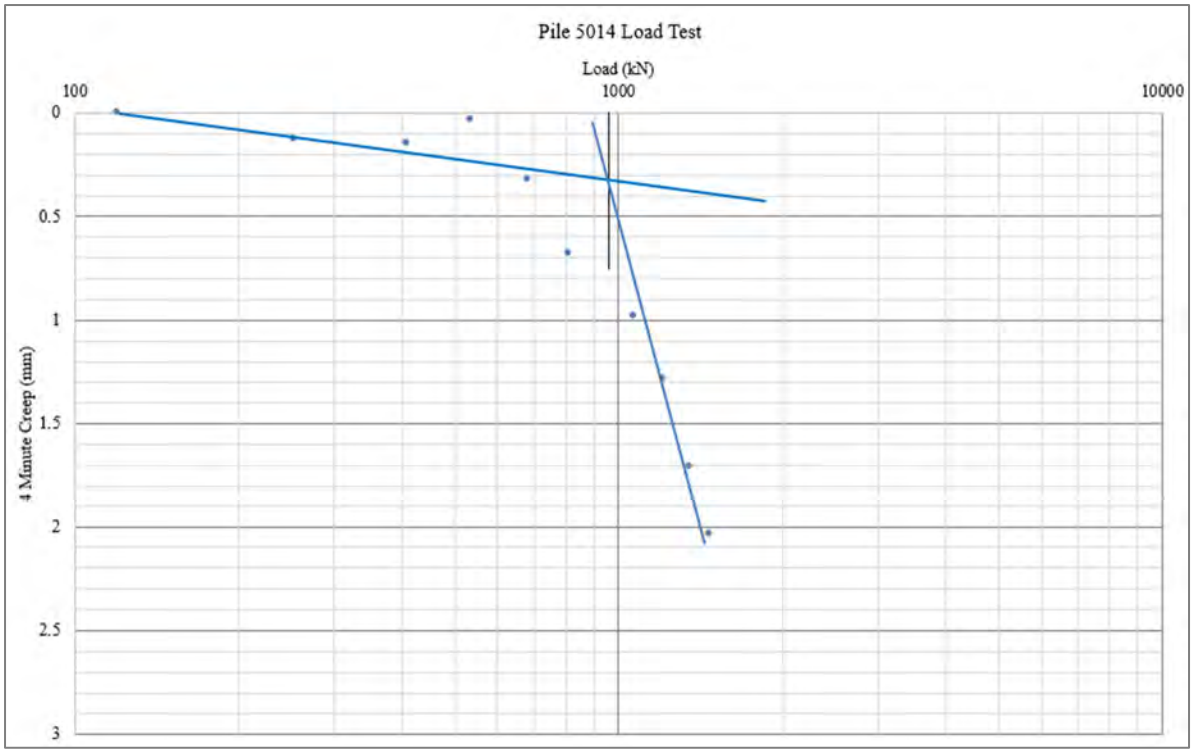


*Figure A23b. Creep Limit Interpretation. Creep limit=960kN*

**Figure A24. Pile Load Test #40 – Pile X730**

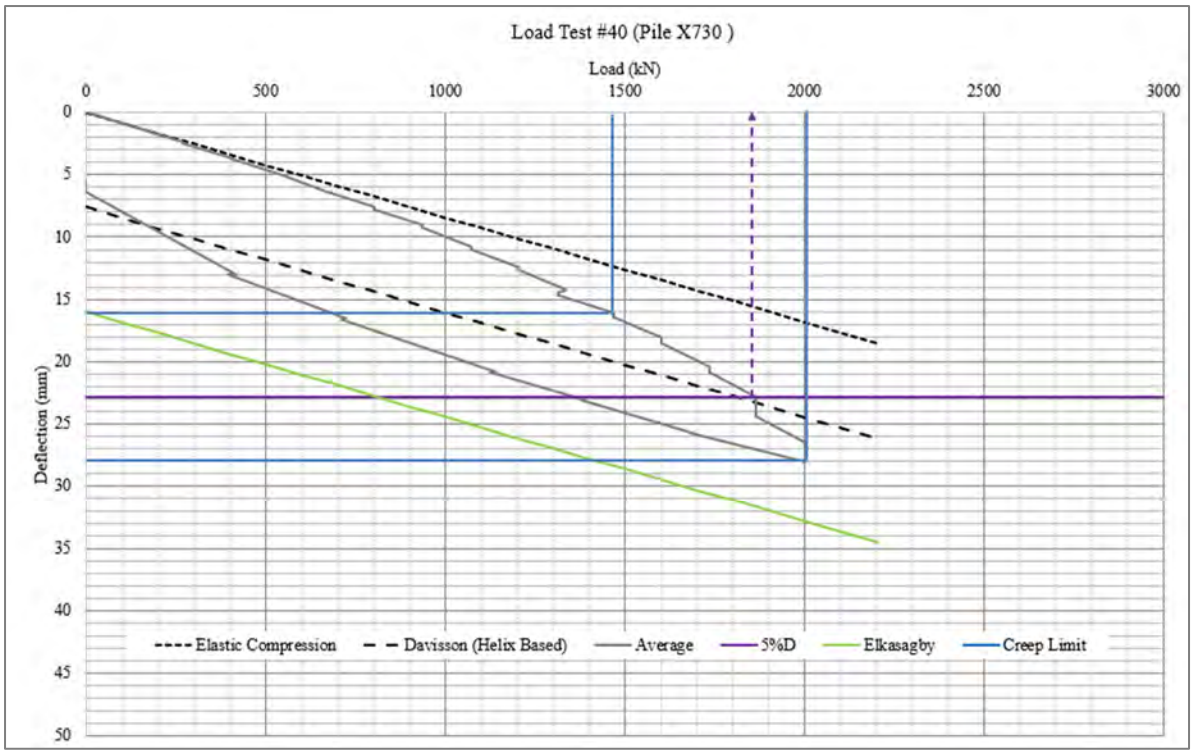


*Figure A24a. Load Test Interpretation*

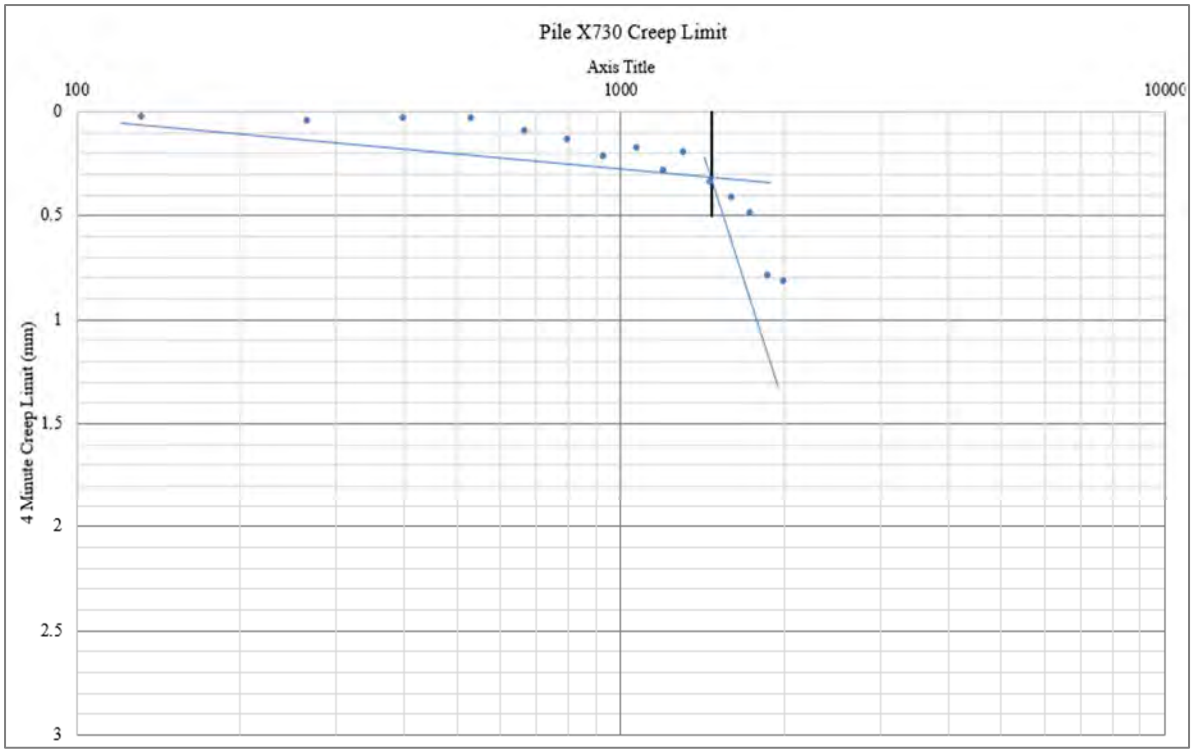


*Figure A24b. Creep Limit Interpretation.* Creep limit=1470kN

**Figure A25. Pile Load Test #42 – Pile X360**

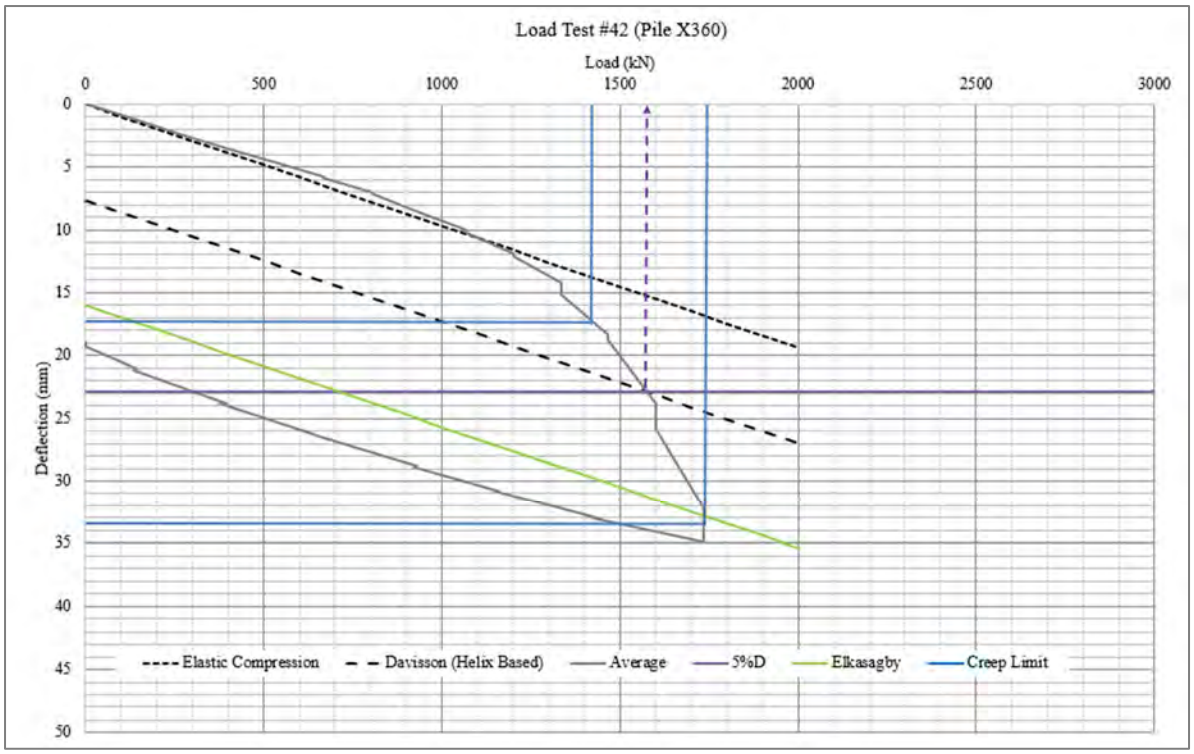


*Figure A25a. Load Test Interpretation*

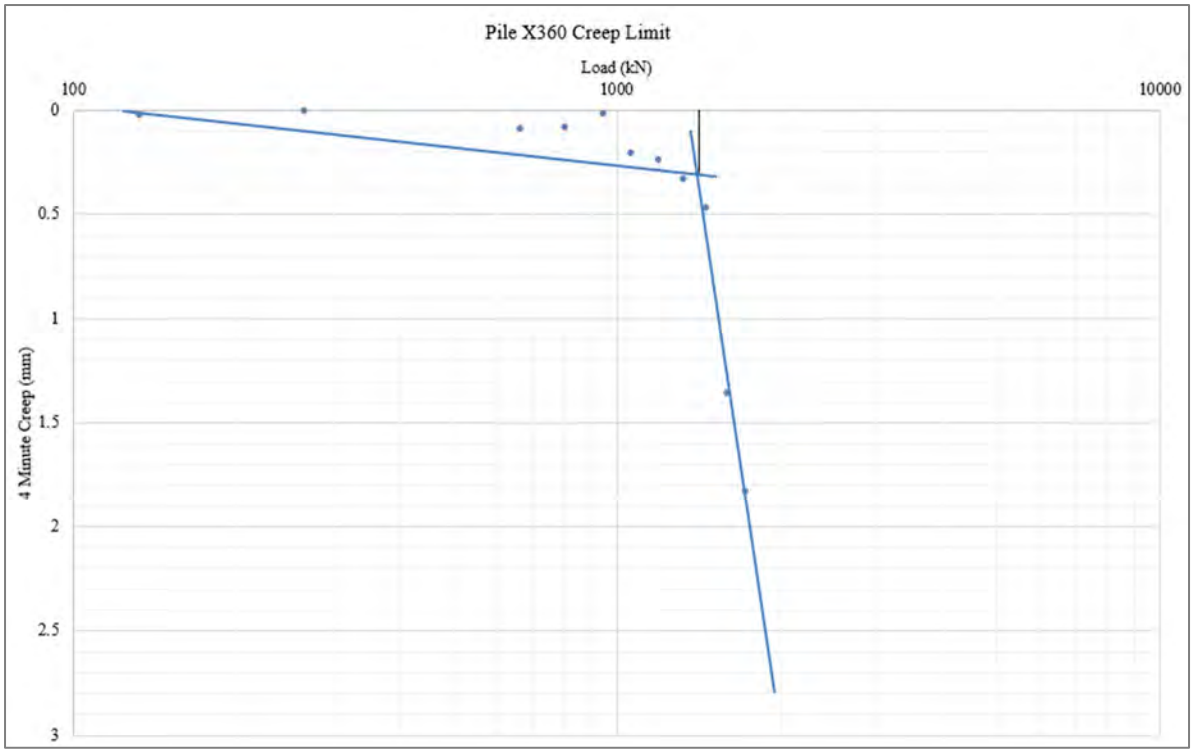


*Figure A25b. Creep Limit Interpretation. Creep limit=1420kN*

**Figure A26. Pile Load Test #43 – Pile X375**

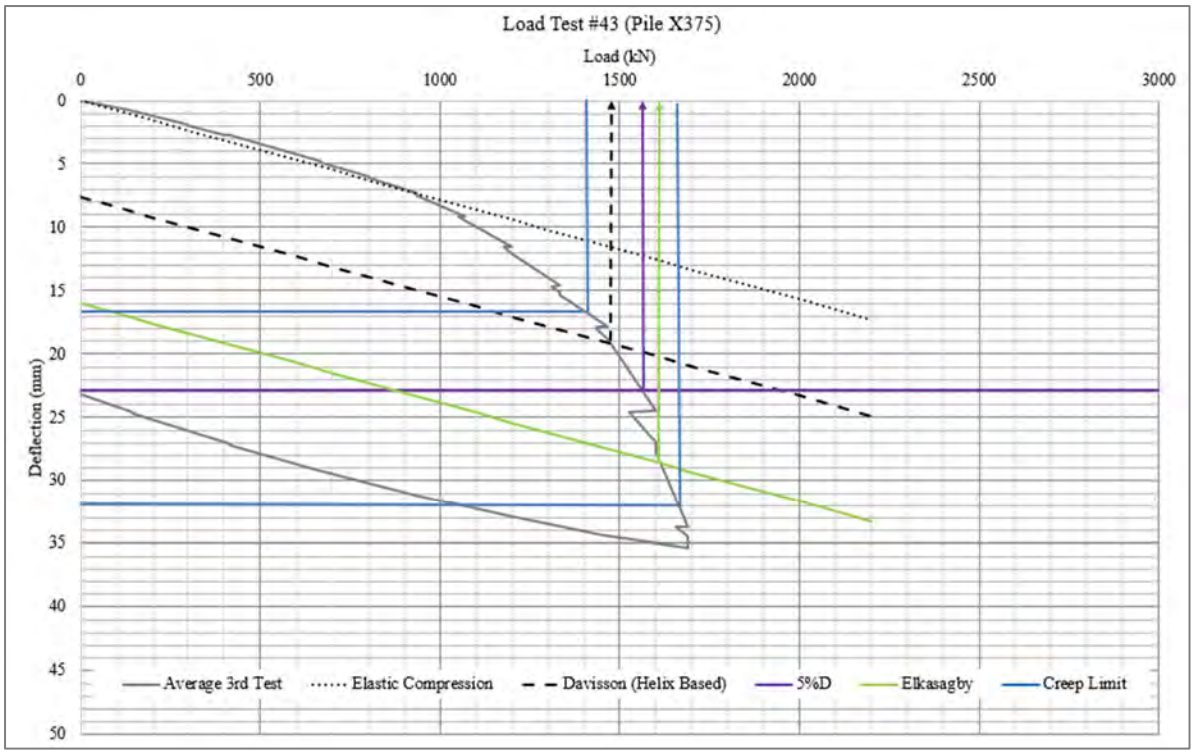


*Figure A26a. Load Test Interpretation*

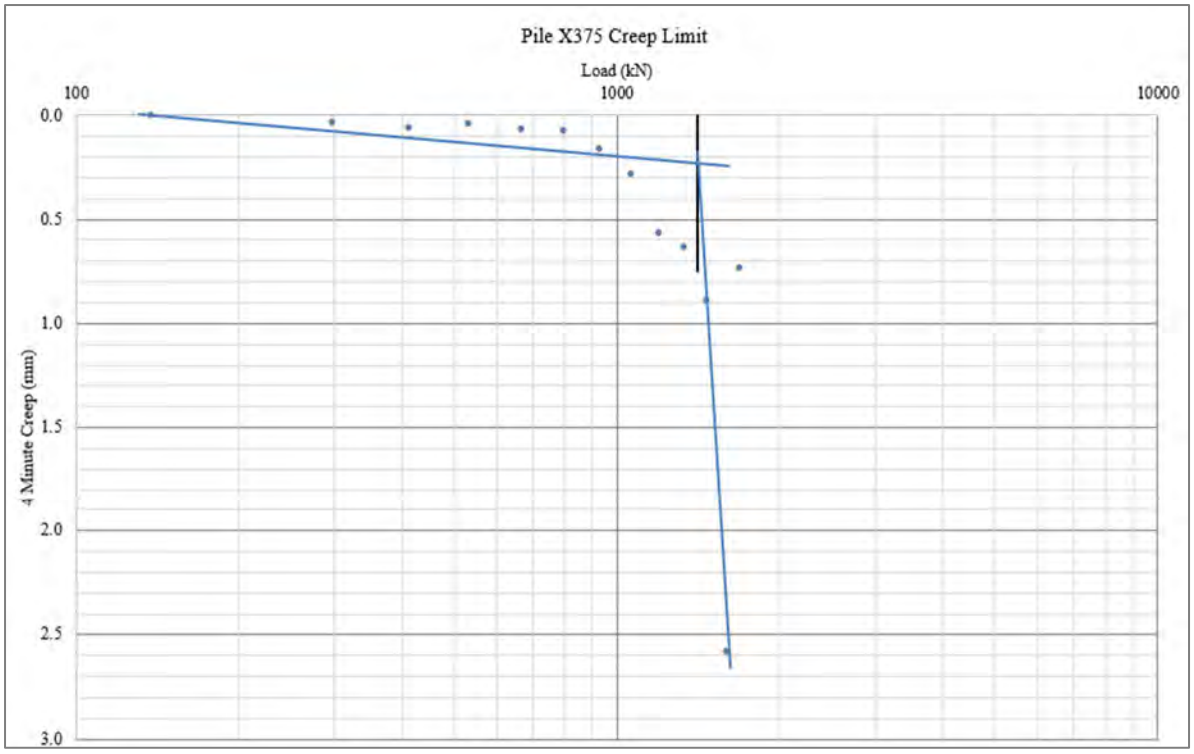


*Figure A26b. Creep Limit Interpretation. Creep limit=1410kN*

**Figure A27. Pile Load Test #49 – Pile X318**

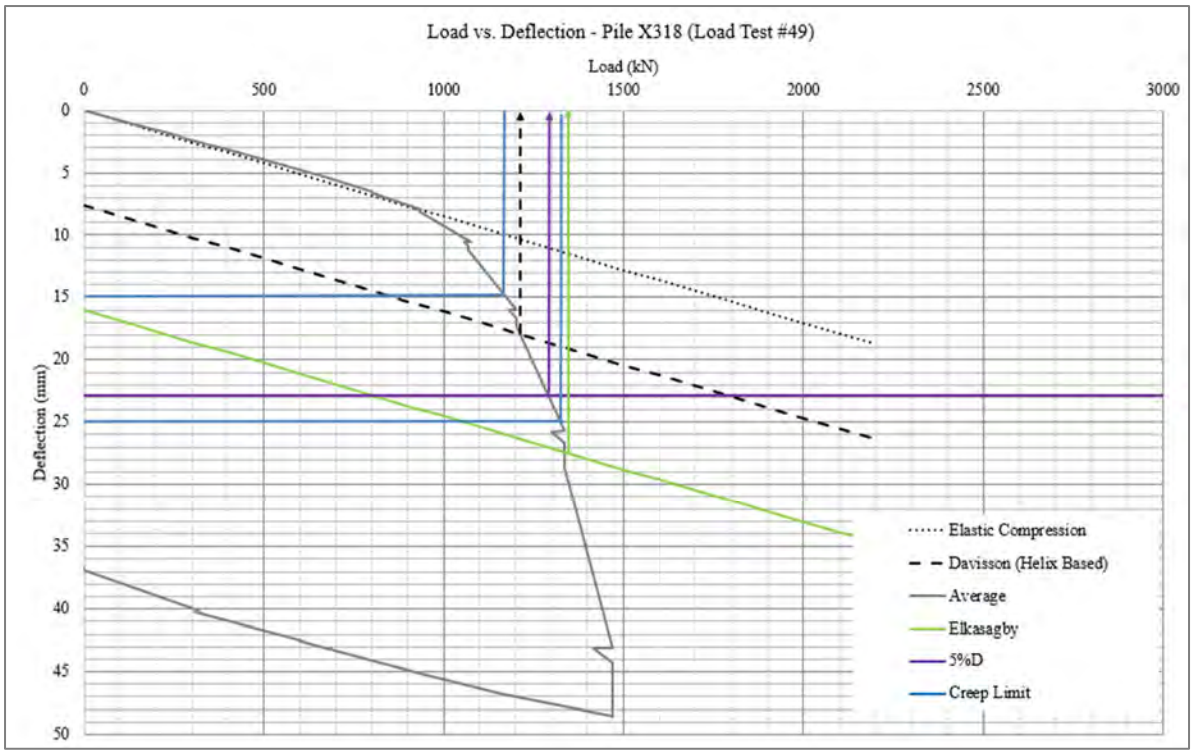


*Figure A27a. Load Test Interpretation*

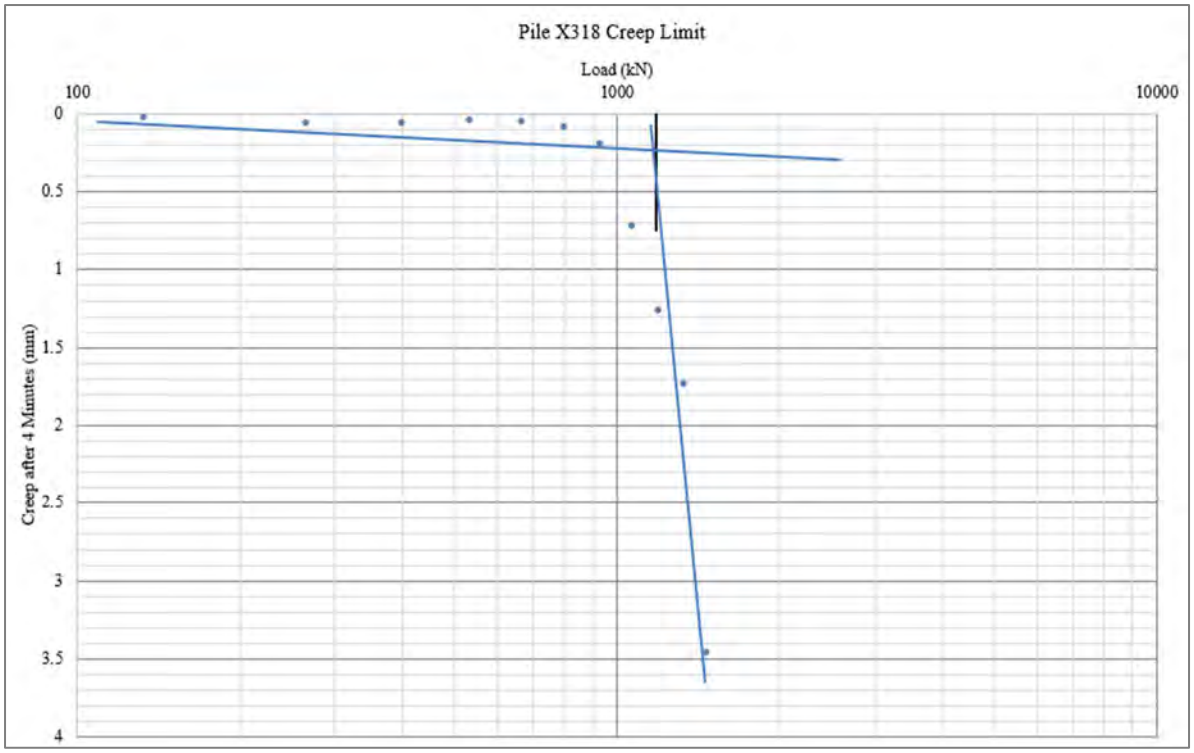


*Figure A27b. Creep Limit Interpretation. Creep limit=1180kN*

**Figure A28. Pile Load Test #50 – Pile X323**

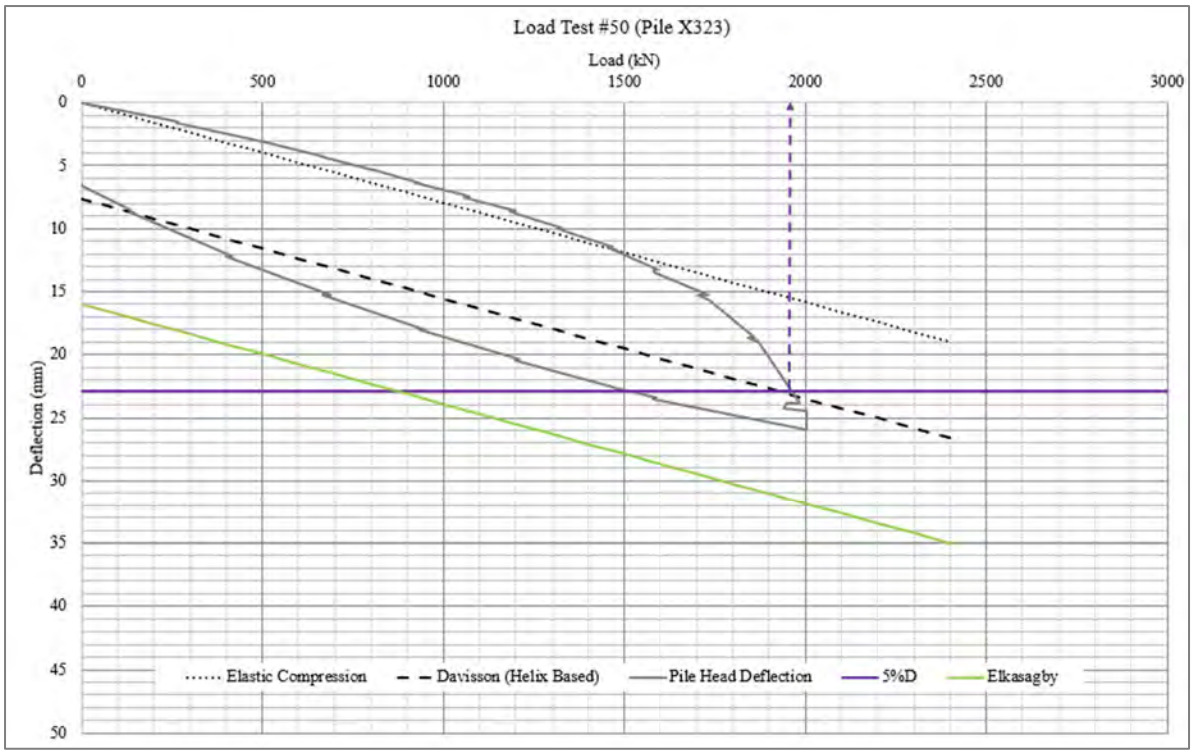


*Figure A28a. Load Test Interpretation*

Creep Limit not developed.

**Figure A29. Pile Load Test #52 – Pile X578**

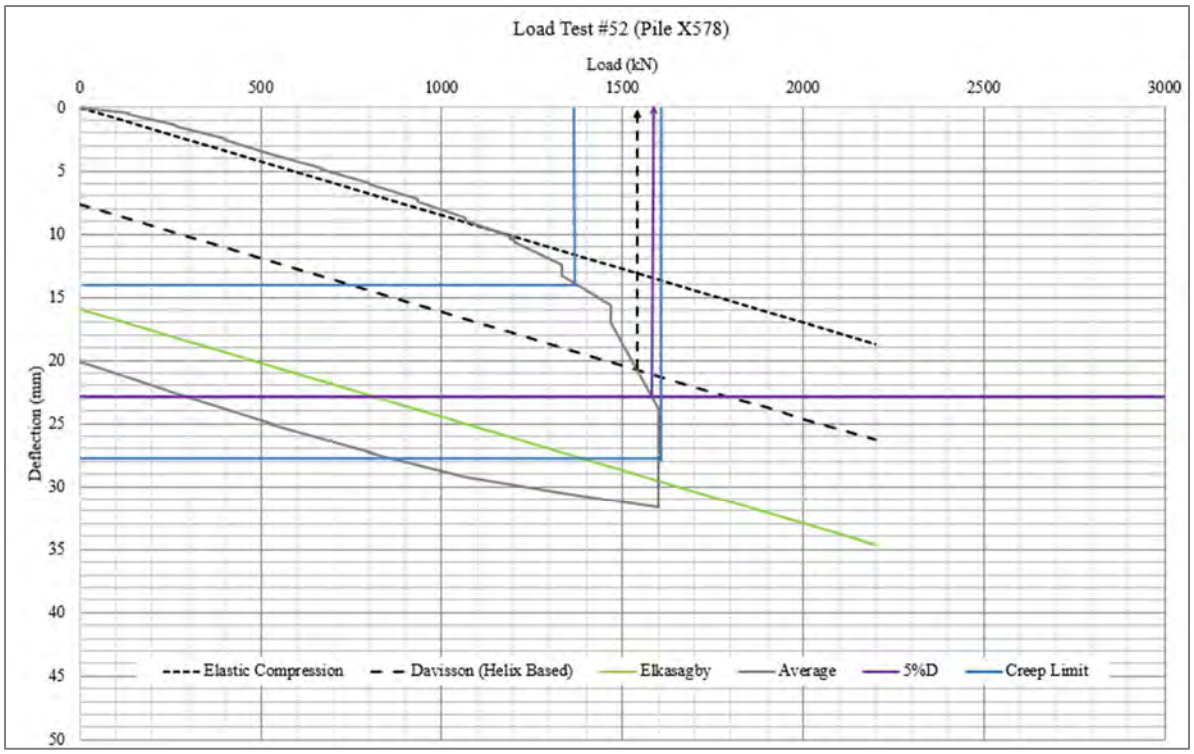


*Figure A29a. Load Test Interpretation*

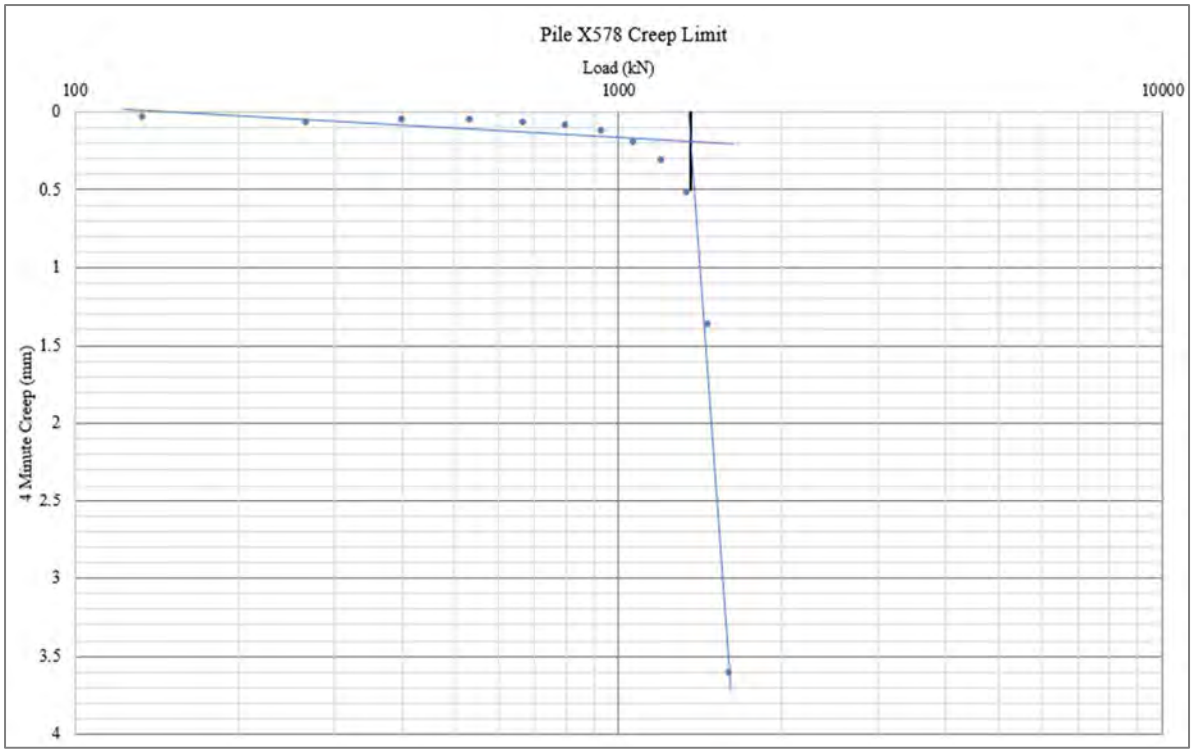


*Figure A29b. Creep Limit Interpretation. Creep Load =1380kN*

**Figure A30. Pile Load Test #53 – Pile X780**

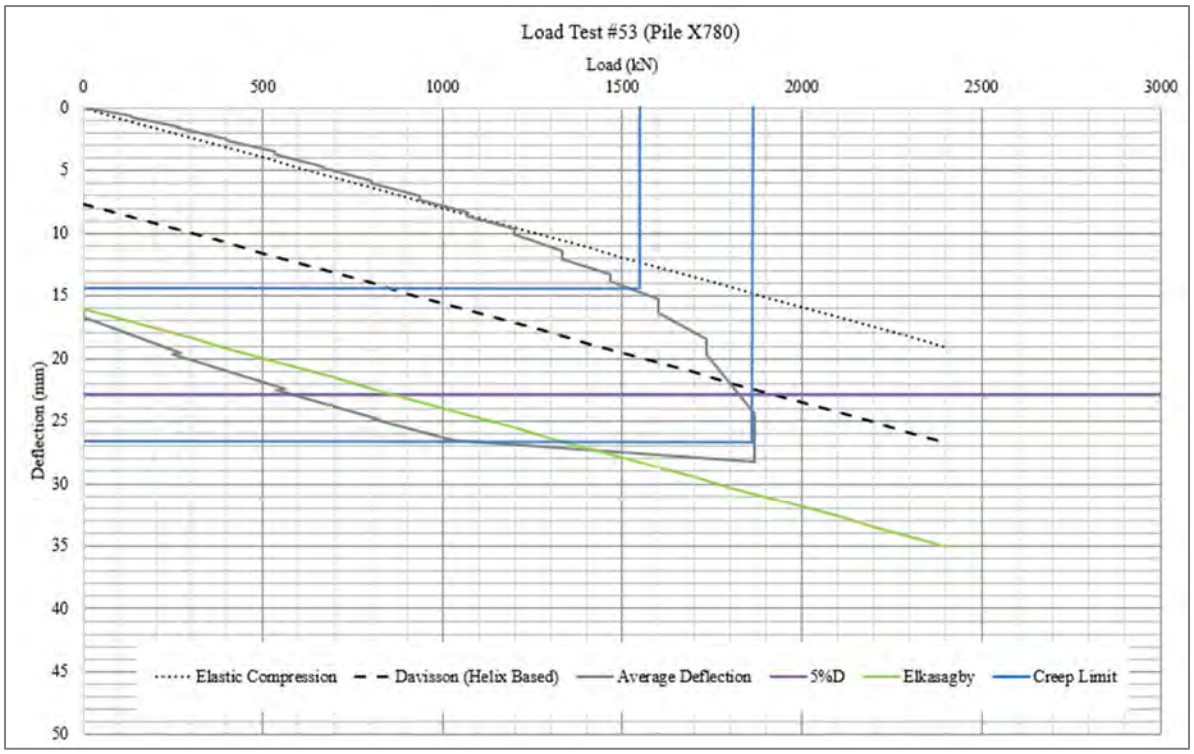


*Figure A30a. Load Test Interpretation*

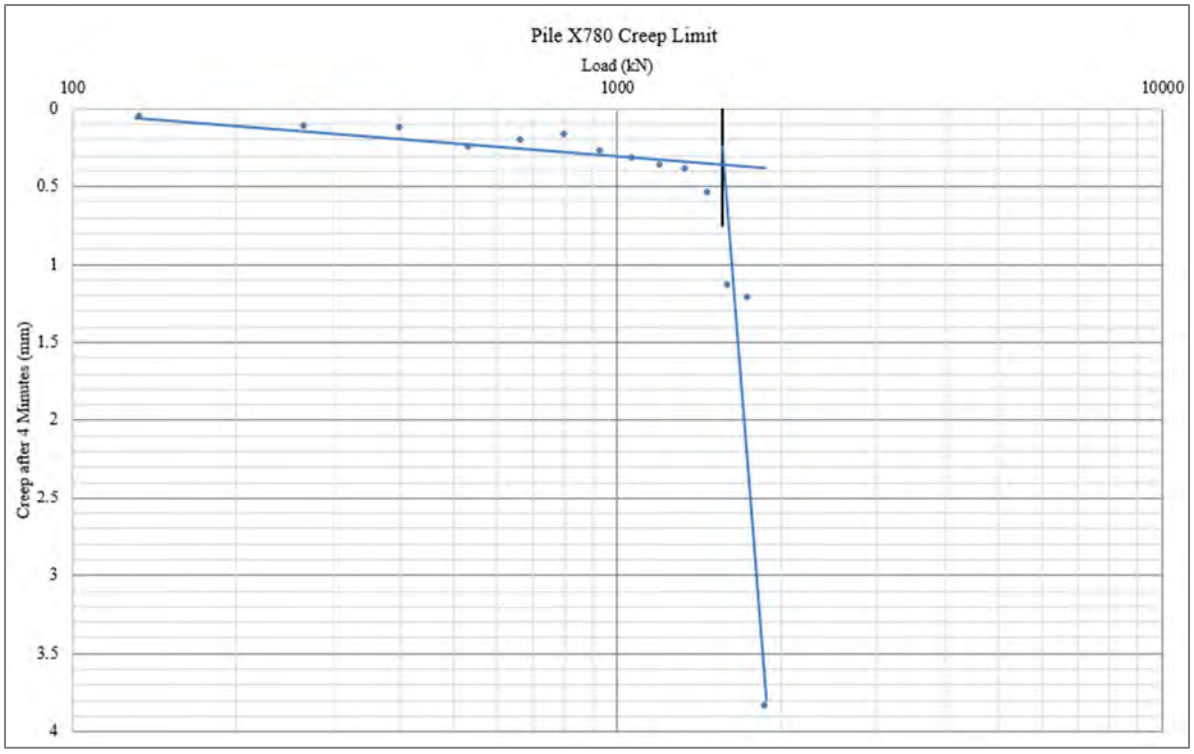


*Figure A30b. Creep Limit Interpretation. Creep Limit=1560kN.*

**Figure A31. Pile Load Test #59 – Pile X406**

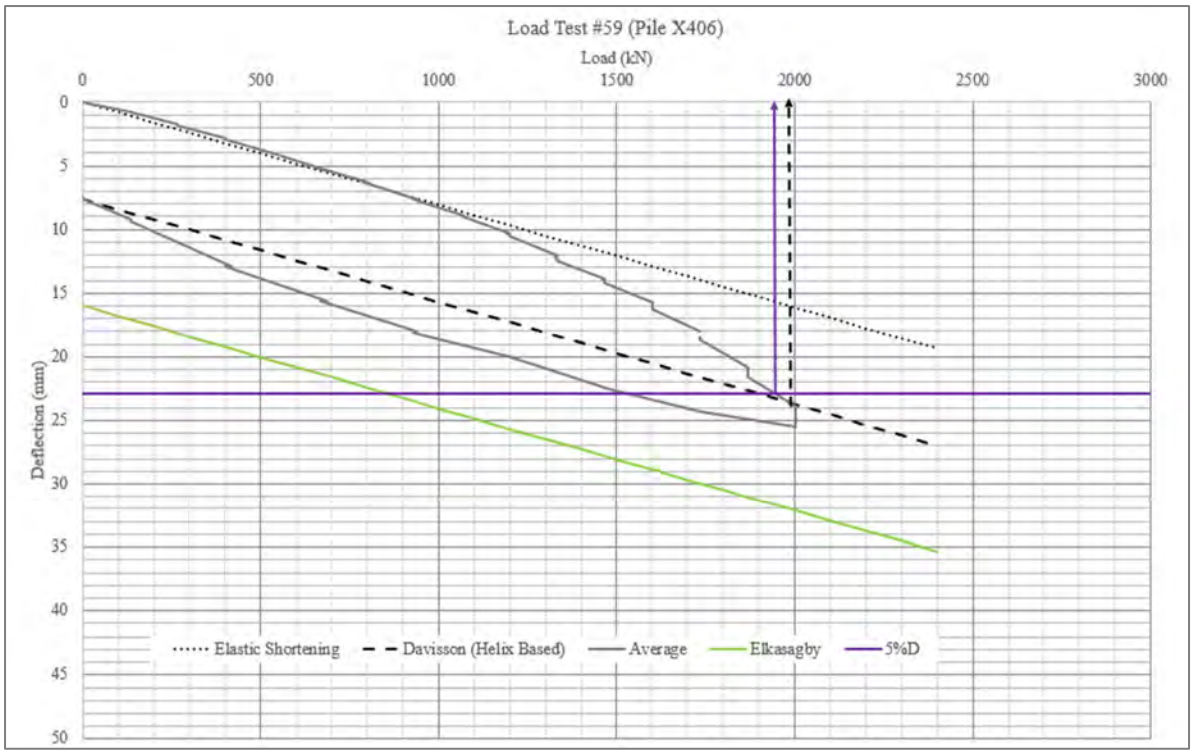


*Figure A31a. Load Test Interpretation*

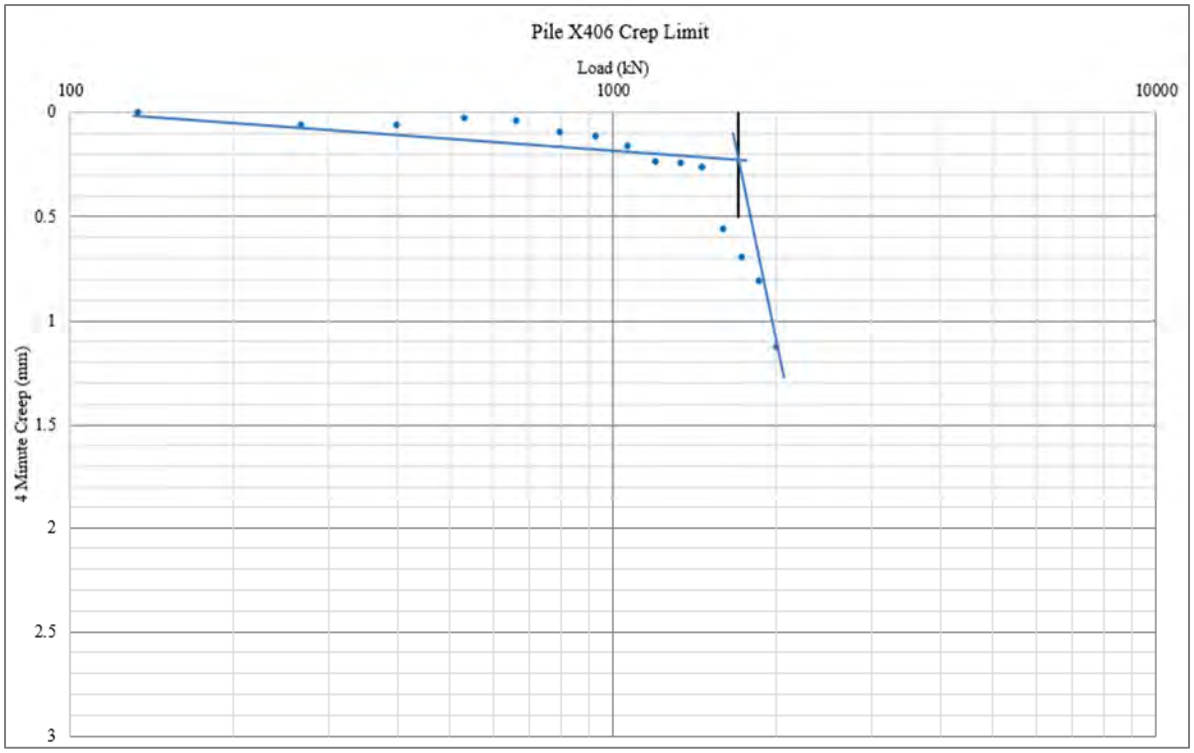


*Figure A31b. Creep Limit Interpretation. Creep limit=1700kN. Creep method did not cross load curve.*

**Figure A32. Pile Load Test #64 – Pile X515**

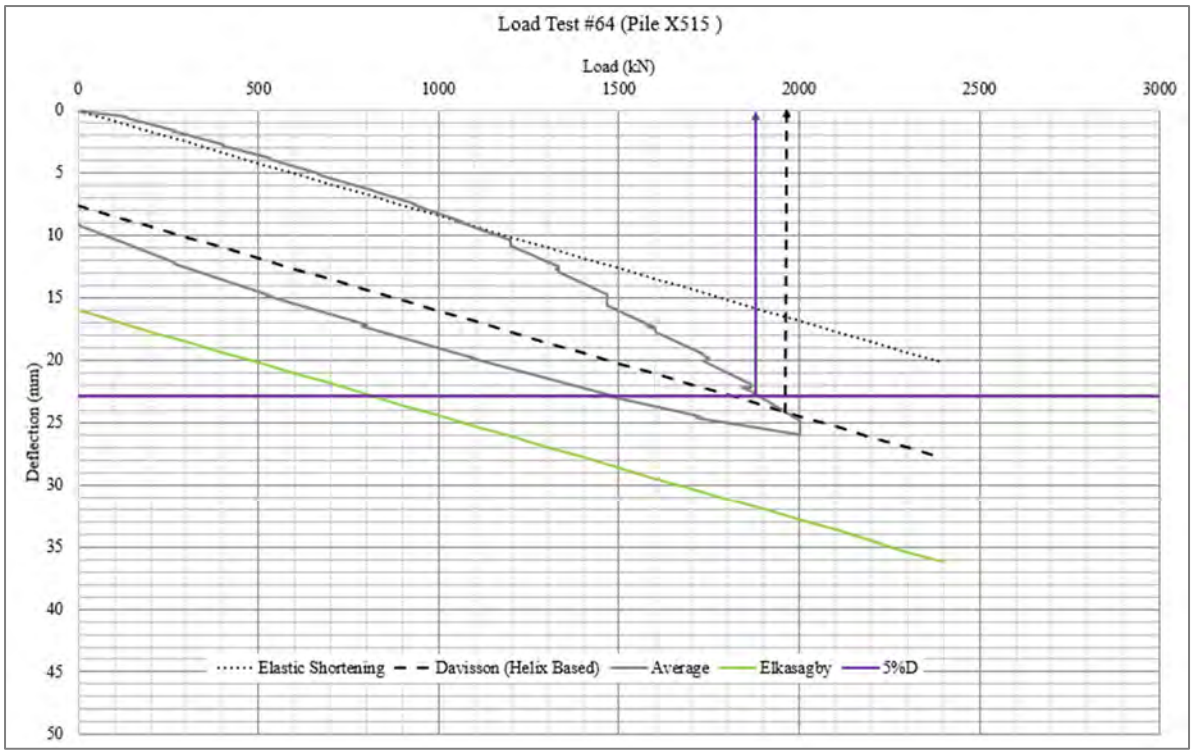


*Figure A32a. Load Test Interpretation*

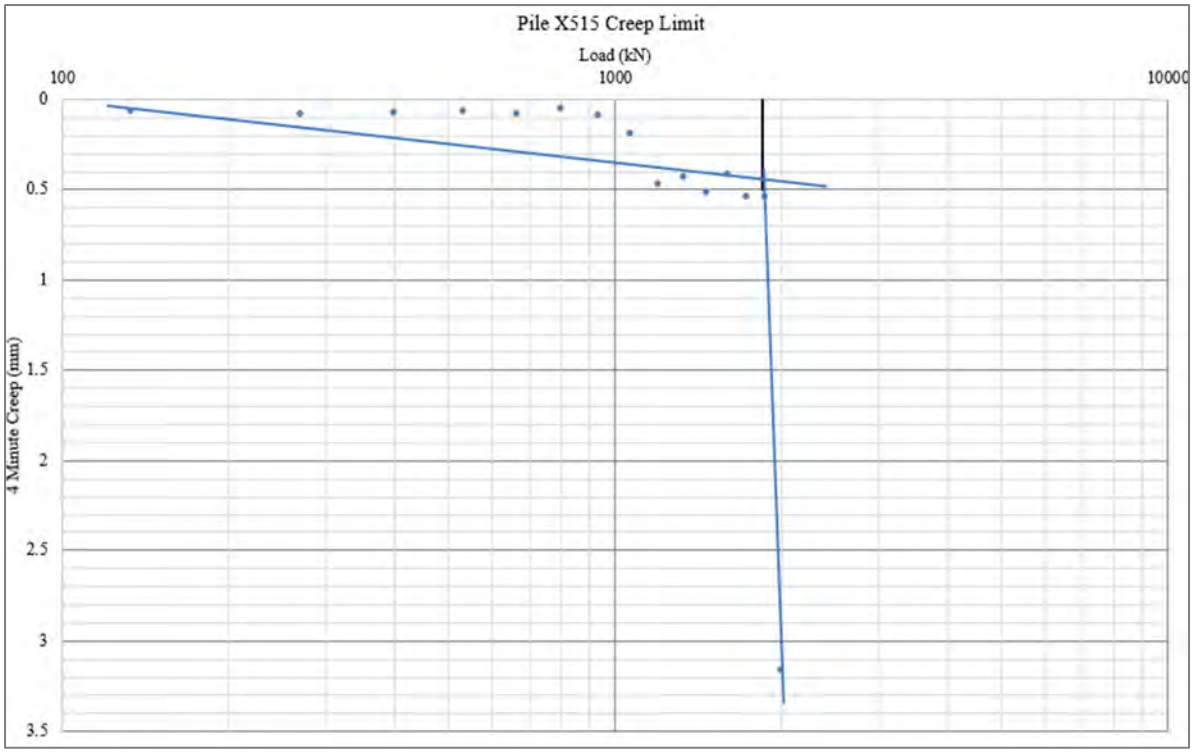


*Figure A32b. Creep Limit Interpretation. Creep limit=1850kN. Creep method did not cross load curve.*

**Figure A33. Pile Load Test #65 – Pile X550**

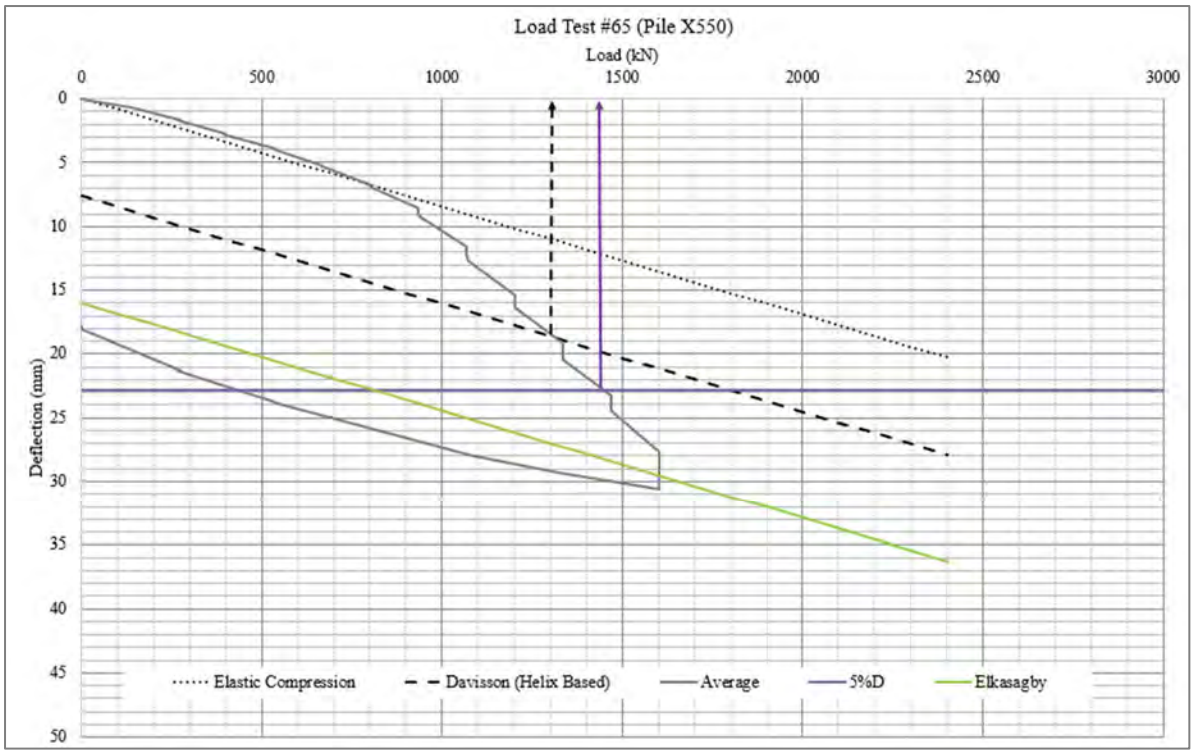


*Figure A33a. Load Test Interpretation*

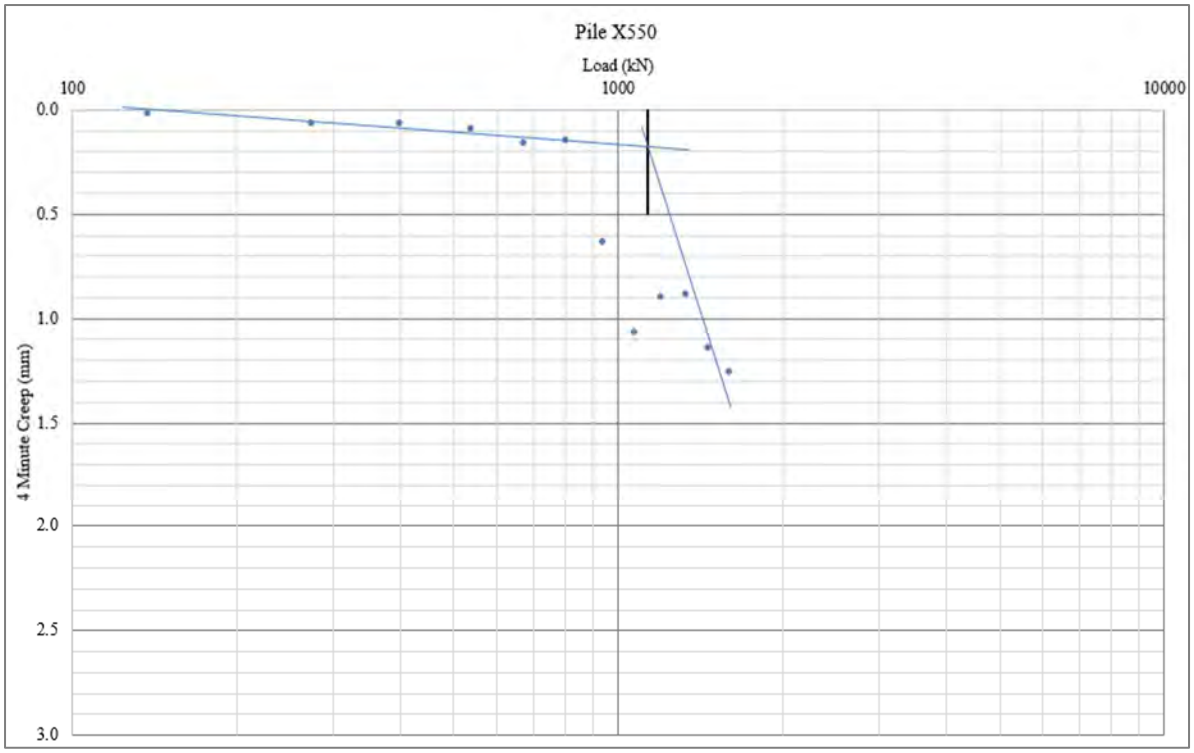


*Figure A33b. Creep Limit Interpretation Plunging failure not well developed and poor dial gauge readings resulted in noisy data and creep limit could not be interpreted. Results shown for discussion*.

**Figure A34. Pile Load Test #68 – Pile X734**

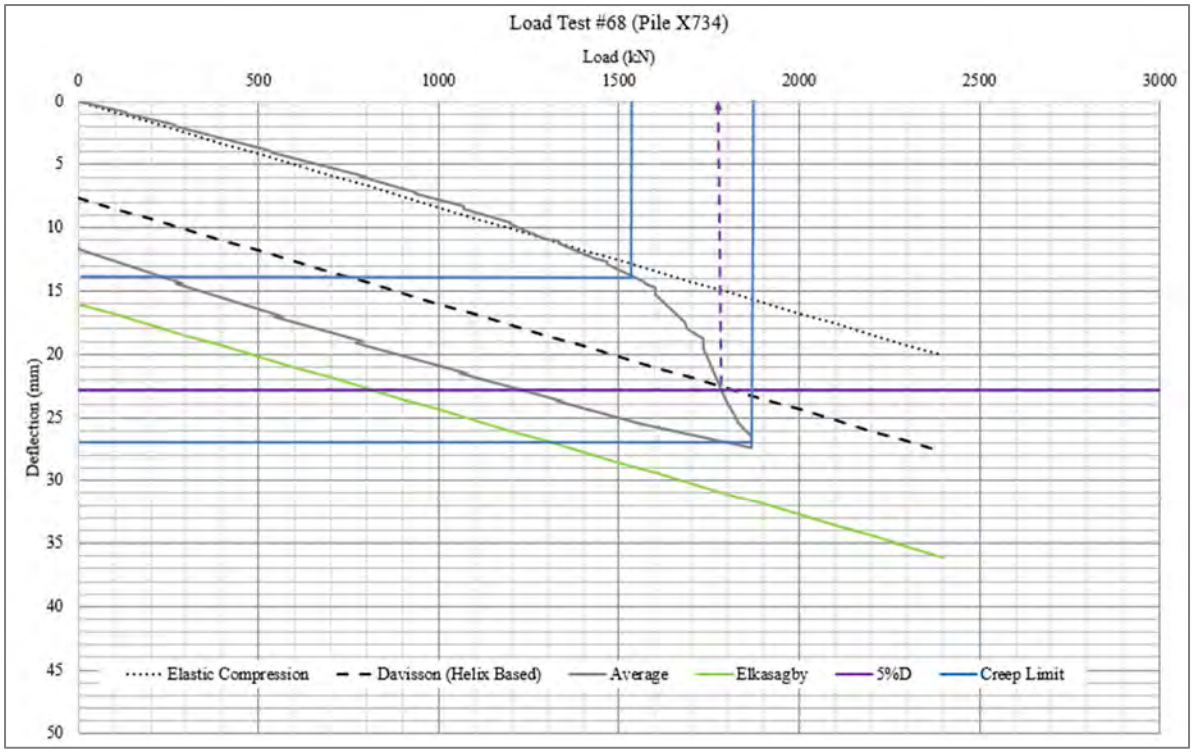


*Figure A34a. Load Test Interpretation*

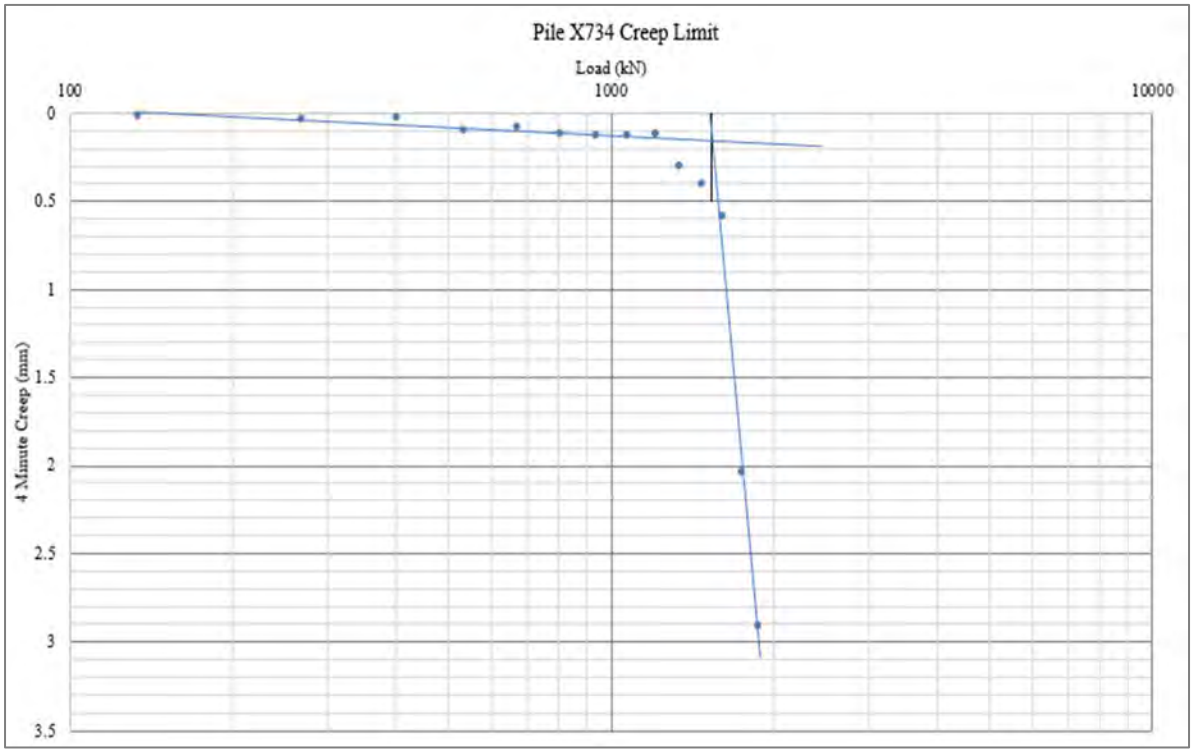


*Figure A34b. Creep Limit Interpretation. Creep limit=1530kN*